Journal of Medicinal Chemistry

Article

Discovery of 7-Oxo-2,4,5,7-tetrahydro-6H-pyrazolo[3,4-c]pyridine Derivatives as Potent, Orally Available, and Brain-penetrating Receptor Interacting Protein 1 (RIP1) Kinase Inhibitors; Analysis of Structure–Kinetic Relationships

Masato Yoshikawa, Morihisa Saitoh, Taisuke Katoh, Tomohiro Seki, Simone V. Bigi, Yuji Shimizu, Tsuyoshi Ishii, Takuro Okai, Masako Kuno, Harumi Hattori, Etsuro Watanabe, Kumar Singh Saikatendu, Hua Zou, Masanori Nakakariya, Takayuki Tatamiya, Yoshihisa Nakada, and Takatoshi Yogo

J. Med. Chem., **Just Accepted Manuscript** • DOI: 10.1021/acs.jmedchem.7b01647 • Publication Date (Web): 27 Feb 2018

Just Accepted

ACS Publications

Journal of Medicinal Chemistry is published by the American Chemical Society. 1155 Sixteenth Street N.W., Washington, DC 20036

Discovery of 7-Oxo-2,4,5,7-tetrahydro-6*H*-pyrazolo[3,4-*c*]pyridine Derivatives as Potent, Orally Available, and Brain-penetrating Receptor Interacting Protein 1 (RIP1) Kinase Inhibitors; Analysis of Structure–Kinetic Relationships

Masato Yoshikawa,[†] Morihisa Saitoh,[†] Taisuke Katoh,[†] Tomohiro Seki,[†] Simone V. Bigi,[‡] Yuji Shimizu,[†] Tsuyoshi Ishii,[†] Takuro Okai,[†] Masako Kuno,[†] Harumi Hattori,[†] Etsuro Watanabe,[†] Kumar S. Saikatendu,[‡] Hua Zou,[‡] Masanori Nakakariya,[†] Takayuki Tatamiya,[†] Yoshihisa Nakada,[†] Takatoshi Yogo[†]*

†Research, Takeda Pharmaceutical Company Limited, 26-1 Muraoka-Higashi 2-chome, Fujisawa, Kanagawa 251-8555, Japan

‡Takeda Pharmaceuticals, 10410 Science Center Drive, San Diego, CA 92121, USA

KEYWORDS

Receptor interacting protein 1, multiple sclerosis, experimental autoimmune encephalomyelitis, structure–kinetic relationship

Abstract

We report the discovery of 7-oxo-2,4,5,7-tetrahydro-6*H*-pyrazolo[3,4-*c*]pyridine derivatives as a novel class of receptor interacting protein 1 (RIP1) kinase inhibitors. Based on the overlay study between HTS hit **10** and GSK2982772 (**6**) in RIP1 kinase, we designed and synthesized a novel class of RIP1 kinase inhibitor **11**, possessing moderate RIP1 kinase inhibitory activity and P-gp mediated efflux. The optimization of the core structure, the exploration of appropriate substituents utilizing SBDD approach led to the discovery of **22**, a highly potent, orally available, and brain-penetrating RIP1 kinase inhibitor with excellent PK profiles. Compound **22** significantly suppressed necroptotic cell death both in mouse and human cells. Oral administration of **22** (10 mg/kg, bid) attenuated disease progression in the mouse experimental autoimmune encephalomyelitis (EAE) model of multiple sclerosis (MS). Moreover, analysis of structure–kinetic relationship (SKR) for our novel chemical series was also discussed.

INTRODUCTION

A process of programmed necrosis, termed necroptosis, has recently been recognized as an important physiological process that involves cell death, innate immunity, and inflammation.[1] Receptor interacting protein 1 (RIP1) kinase is a crucial upstream regulator of necroptosis, and association of RIP1 kinase with a variety of pathologies, such as ischemic injury, inflammatory diseases, and neurodegenerative diseases, has been investigated.[2,3]

Neurodegenerative diseases, such as multiple sclerosis (MS),[4] Parkinson's disease (PD),[5] and amyotrophic lateral sclerosis (ALS),[6, 7] have recently been intensively studied to understand their relationship with the necroptosis pathway. Ofengeim *et al*. showed the involvement of RIP1 kinase and necroptosis in mediating the deleterious process in MS by using both animal models and human tissues from MS patients.[4] RIP1-mediated axonal degradation has also been demonstrated in ALS. Thus, inhibitors of RIP1 kinase have the potential to provide new therapeutic opportunities to neurodegenerative diseases with significant unmet medical needs.

The first published RIP1 kinase inhibitor, Nec-1 (**1**),[8,9] was discovered by Degterev *et al.* in 2005, with a subsequent disclosure of an analog, Nec-1s (**2**),[10] with improved metabolic stability. Both have been widely used to elucidate the biology of the necroptosis pathway. Over the recent years, additional series of RIP1 kinase inhibitors have been identified as illustrated in Figure 1 such as a type-II[11] RIP1 kinase inhibitor **3**[12] and a hybrid-type RIP1 kinase inhibitor **4**[13] which was designed based on **2** and ponatinib.[14] Among them, benzo[*b*][1,4]oxazepin-4-one analogs,[15] represented by **5**,

comprise the most advanced series, with the optimized analog **6**[16] currently being evaluated in human clinical trials for inflammatory diseases such as ulcerative colitis, rheumatoid arthritis, and psoriasis. However, despite the attractiveness of RIP1 kinase inhibitors as a therapeutic option for neurodegenerative disorders, the chemical series reported so far are not suitable for clinical development to treat CNS related disorders because of either low oral bioavailability and/or low brain permeability. For example, the necrostatin series (**2**) has shown efficacy in animal models of MS or ALS by oral administration, but its low metabolic stability has likely hindered its clinical development. Compound **8**[17] has been detected in mouse brains but only after intravenous injection. The brain penetration or the *in vivo* efficacy of the other compounds (**3**-**7**)[18] in neurodegenerative diseases have not been reported to date. Thus, to develop RIP1 kinase inhibitors targeting CNS diseases, we focused on the development of a novel chemical series of RIP1 kinase inhibitors with good oral bioavailability and brain-penetrating properties for treatment of neurodegenerative diseases.

Herein, we report the discovery of (3*S*)-3-(2-benzyl-3-chloro-7-oxo-2,4,5,7-tetrahydro-6*H*-pyrazolo[3,4-*c*]pyridin-6-yl)-5-methyl-4-oxo-2,3,4,5-tetrahydro-1,5-benzoxazepine-8-carbonitrile (**22**) as a potent, orally bioavailable, and brain-penetrating RIP1 kinase inhibitor. The following strategies were used to identify **22**: (i) optimization of core structures for appropriate brain penetration in light of favorable physicochemical properties such as topological polar surface area (TPSA)[19] and the number of

hydrogen-bonding donors (HBDs); (ii) exploration of potent substituents in back pockets by utilizing structure-based drug design (SBDD); and (iii) introduction of substituents toward the solvent-accessible region to control the favorable ADMET profiles. Compound **22** exhibited potent cellular activity both in humans and mice and an excellent pharmacokinetic (PK) profile with brain exposure in mice after oral administration. Compound **22** was efficacious in experimental autoimmune encephalomyelitis (EAE),[20] which is a model of human inflammatory demyelinating disease such as MS. Moreover, in the course of optimization, kinetic profiles of all synthesized compounds were evaluated to analyze structure−kinetic relationships (SKRs). We also discuss the SKR of our novel chemical series of RIP1 kinase inhibitors later in this paper.

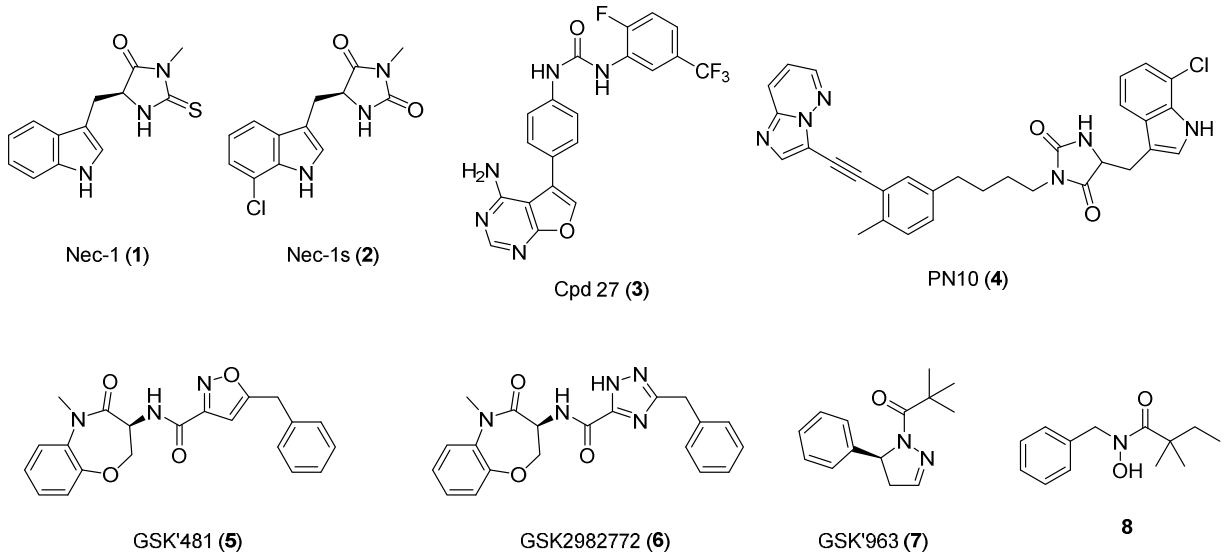

Figure 1. Chemical structures of reported RIP1 kinase inhibitors.

RESULTS AND DISCUSSION

Assay Development. The kinetics of the interaction between a ligand and its target has been recognized as an important factor for lead generation/optimization[21,22] and long drug-target residence time is often correlated with potent *in vivo* efficacy.[23–25] In the case of RIP1 kinase inhibitors, the benzoxazepinone-based compounds have a long drug-target residence time ($t_{1/2}$ = 112 min for **6**),[16] which could translate into prolonged efficacy in cellular assays and potentially *in vivo*. These results led us to analyze kinetic profiles including $t_{1/2}$ in the course of the optimization to identity potent and brain-penetrating RIP1 kinase inhibitors. Measurement of the binding affinity for RIP1 kinase and kinetic profiles was performed by using a time-resolved fluorescence resonance energy transfer (TR-FRET) assay and a novel fluorescent probe, 3-(3-((3-(4-amino-5-(4-(3-(2-fluoro-5-(trifluoromethyl)phenyl)ureido)phenyl)-7*H*-pyrrolo[2,3-*d*]pyrimidin-7-yl)propyl)amino)-3-oxopropyl)-5,5-difluoro-7,9-dimethyl-5*H*-dipyrrolo[1,2-*c*:2',1'-*f*][1,3,2]diazaborinin-4-ium-5-uide (**9**) described in Figure 2 (the synthesis of **9** is described in a supplementary information). By using the TR-FRET assay, a high-throughput assay format was achieved sufficiently to evaluate all synthesized compounds. The binding affinity (pK_i) was calculated as the sum of $logk_{on}$ and pk_{off}. The drug-target residence time ($t_{1/2}$) was defined as $ln2/k_{off}$. Regarding compounds that quickly dissociate from the target ($t_{1/2}$ < 5 min), the kinetic profiles could not be precisely evaluated because of the detection limit of this TR-FRET assay.

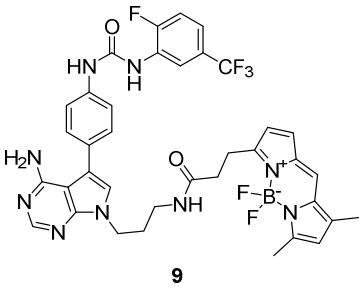

9

Figure 2. Structure of fluorescent probe **9**.

Lead Generation. To identify good starting points for lead optimization and subsequent development, we performed high-throughput screening (HTS) against RIP1 kinase by using our compound library and identified a benzimidazole derivative **10** (pK_i = 7.20) (Figure 3A). Reported RIP1 kinase inhibitors can be classified into three categories based on the binding modes; (i) type-II class[11] targeting "DFG-out (or DLG-out in the case of RIP1 kinase)" conformation of kinase (e.g., **3**), (ii) type-III (allosteric) class[11] (e.g., **1**, benzo[*b*][1,4]oxazepin-4-one series **5** and **6**), or (iii) hybrid type **4**[13] (Figure 1). To clarify the binding mode of **10**, an X-ray co-crystal structure of **10** with RIP1 kinase was obtained (Figure 3B). The X-ray co-crystal structure revealed that compound **10** had no hinge-binding interaction and occupied an allosteric lipophilic pocket at the back of the ATP binding site, making a hydrogen-bonding interaction with the amide NH of Asp156 at a distance of 2.8 Å, which indicated that the binding mode of compound **10** was type-III class similar to that of the Nec-1 and benzo[*b*][1,4]oxazepin-4-one series. The overlaid image of **10** and the benzo[*b*][1,4]oxazepin-4-one derivative **6** in RIP1 kinase showed that the compounds occupied the same space and that the benzyl group and the 5-membered heteroaromatic ring of compounds **6** and

10 were well-overlapped (Figure 3C). This result led us to design and synthesize a novel class of RIP1 kinase inhibitor **11**, possessing a 4-oxo-6,7-dihydro-1*H*-imidazo[4,5-*c*]pyridine moiety as a core structure (Figure 4). As a result, compound **11** showed moderate RIP1 kinase inhibitory activity (pK_i = 6.93). Parent compound **6** had potent RIP1 kinase inhibitory activity with excellent in vitro and *in vivo* profiles with highly favorable physicochemical and ADMET properties. However, **6** was reported to have low brain penetration,[16] presumably due to active extrusion of drug from the brain via the efflux drug transporter P-glycoprotein (P-gp). On the other hand, compound **11** showed a better P-gp–mediated efflux (ER = 1.9) than that of **6** (ER = 3.1), likely reflecting the decreased TPSA and HBD.[26,27] On the basis of this result, further 6,5-bicyclic core structures were investigated as replacements of the 4-oxo-6,7-dihydro-1*H*-imidazo[4,5-*c*]pyridine maintaining the favorable physicochemical parameters (TPSA < 90 Å^2, HBD = 0) for brain exposure[28,29] and enhancing RIP1 kinase inhibitory activity.

(A)

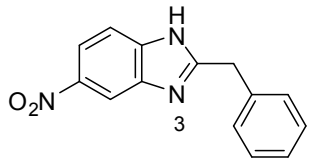

10: pK_i = 7.20

(B) (C)

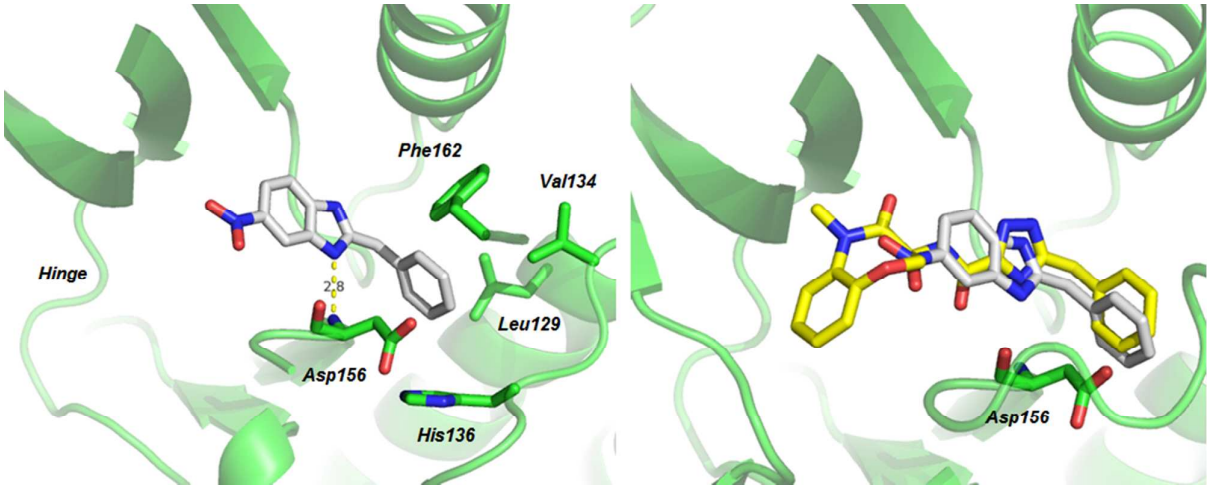

Figure 3. HTS hit compound **10**. (A) Structure of compound **10** and K_i for human RIP1 kinase. (B) Co-crystal structure of **10** with hRIP1 kinase. (C) Overlay study between compounds **6** (yellow) and **10** (white) in hRIP1 kinase.

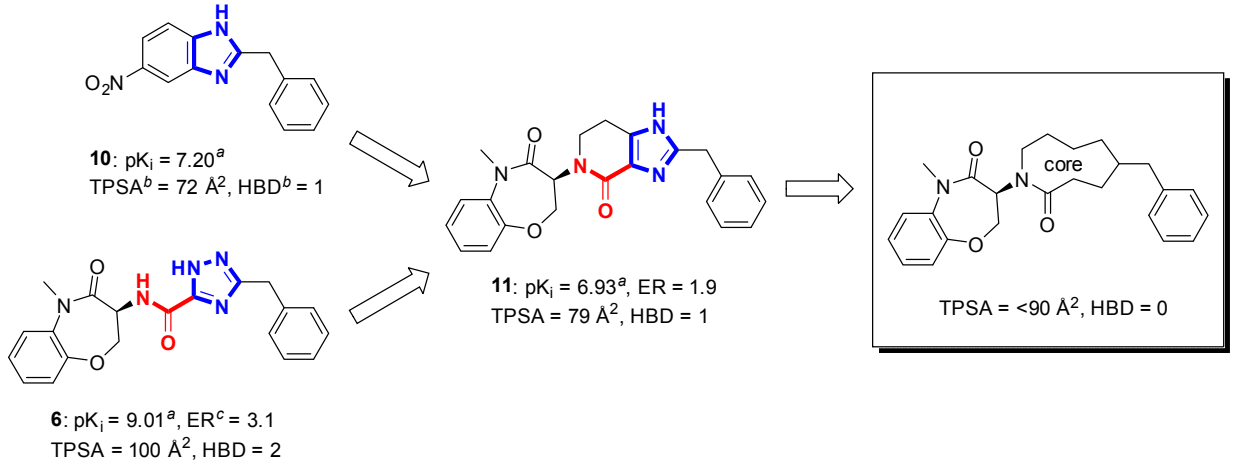

Figure 4. Design concept for a new class of brain-penetrating RIP1 kinase inhibitors. (a) Binding

affinity for human RIP1 kinase. (b) Calculated by Daylight. (c) Efflux ratio in P-gp–overexpressing cells at 1 μM.

The results of modification of the core structure are summarized in Table 1. Triazole derivative **12**, which was synthesized from **6** and removed HBD, showed dramatically decreased P-gp–mediated efflux and enhanced binding affinity (pK_i) compared to those of **11**. Although imidazole derivative **13**, which has a nitrogen atom on a bridgehead, maintained moderate potency, **13** exhibited a higher ER than that of **12** despite reducing TPSA, presumably due to the basicity of the imidazole moiety. Pyrazole derivatives **14** and **15** also had a lower ER. These results in Table 1 indicated that our design strategy of lowering TPSA and removing HBD was effective in reducing ER. Compound **14** showed the strongest binding affinity for RIP1 kinase and longest drug-target residence time. Accordingly, the 7-oxo-2,4,5,7-tetrahydro-6*H*-pyrazolo[3,4-*c*]pyridine moiety of **14** (pK_i = 8.41, $t_{1/2}$ = 59 min, ER = 0.7) was identified as the most suitable core structure for further optimization.

Table 1. Modification of Core Structure

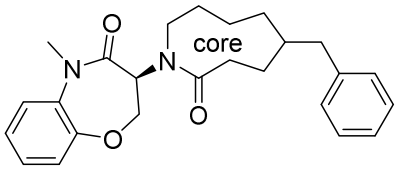

Compd	core	TPSA[a] (Å^2)	HBD	ER[b]	pK$_i$	logk$_{on}$[c]	pk$_{off}$[c]	t$_{1/2}$[c,d] (min)
12	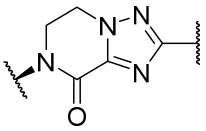	81	0	0.8	7.26	6.27 (6.04–6.43)	0.984 (0.803–1.30)	6.7 (4.4–14)
13	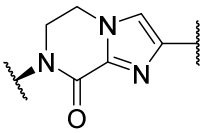	68	0	1.2	6.97	5.85 (5.55–6.02)	1.13 (0.909–1.58)	9.3 (5.6–26)
14	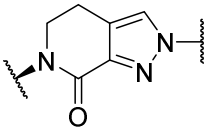	68	0	0.7	8.41	6.48 (6.39–6.55)	1.93 (1.83–2.06)	59 (46–80)
15	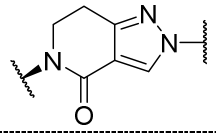	68	0	0.49	6.60	n.d.[e]	n.d.[e]	<5
11	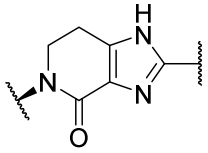	79	1	1.9	6.93	n.d.[e]	n.d.[e]	<5

[a]Calculated by Daylight. [b]Efflux ratios in P-gp–overexpressing cells at 1 μM. [c]95% confidence intervals (given in parentheses) determined in duplicate (n = 2). [d]$t_{1/2} = \ln 2/k_{off}$. [e]not determined.

Lead Optimization. A docking model of **14** with RIP1 kinase was developed to utilize SBDD for further optimization (Figure 5A). This model showed that the benzyl group deeply occupied the allosteric hydrophobic pocket (we refer to this pocket as deep pocket 1: DP1) at the back of the ATP

binding site. The DP1 was mainly constructed by the side chains of lipophilic amino acid residues such as Leu129 and Val134. According to the X-ray co-crystal structure of **2** with RIP1 kinase, a hydrogen-bonding interaction was observed between the OH of Ser161 and NH of the indole in **2** in DP1. As shown in Figure 5B, a small unoccupied pocket, which is defined by Met67 and Leu70, was found around the 3-position of the core structure (referred to as deep pocket 2: DP2). The docking model also suggested that the 7- and 8-positions of the benzoxazepinone ring were oriented toward the solvent-accessible region. On the basis of these analyses, optimization of **14** was continued by (i) investigation of favorable substituents in DP1 (R^1) in view of the lipophilicity, size, or hydrogen bonding with OH of Ser161, (ii) exploration of substituents in DP2 (R^2) that can efficiently occupy the small lipophilic pocket, and (iii) introduction of an appropriate substituent (R^3) into the 7- or 8-positions of the benzoxazepinone ring to control the favorable ADMET profiles (Figure 5C).

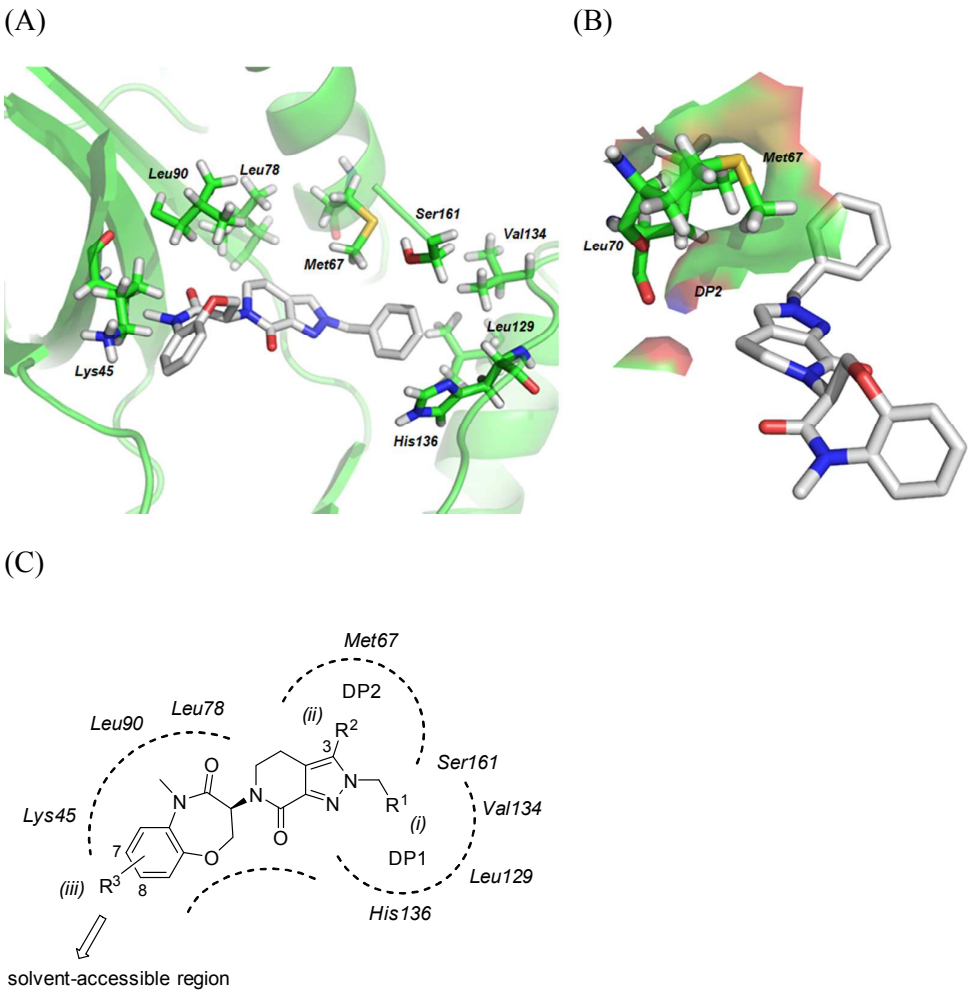

Figure 5. Synthetic strategy based on the docking model. (A) The docking study between **14** and RIP1 kinase. The DLG motif including Asp156 in the activation loop was omitted for simplicity. (B) Image of the protein surface around DP2. (C) Schematic illustration of **14** in RIP1 kinase.

First, modification of the substituent R^1 was conducted. The results are summarized in Table 2 (The detailed SKR analysis for all synthesized compounds will be discussed (*vide infra*)). Introduction of a fluoro group into the *o*-position resulted in enhanced binding affinity (compound **16a**), whereas introduction into the *m*- and *p*-positions (compounds **16b**,**c**) decreased the affinity compared to that of the non-substituted analog **14**. An additional fluoro group was introduced into the second *o*-position of **16a**, yielding compound **16d**, increasing the binding affinity. Replacement of the phenyl group with a cyclobutyl group resulted in reduced binding affinity. To direct a hydrogen-bonding interaction toward the OH of Ser161, substituents possessing a hydrogen-bonding acceptor (HBA), such as heteroaromatic rings and sulfone groups, were introduced. Pyridine analogs **16f** and **16g** exhibited 10-fold lower K_i values than that of **14**, whereas introduction of sulfone groups (**16h** and **16i**) dramatically decreased the binding affinity. Among all compounds with modification of substituents for R^1, the 2-fluorophenyl analog **16a** and 2,6-difluorophenyl analog **16d** showed more potent binding affinities and longer drug-target residence times. Therefore, 2-fluorophenyl and 2,6-difluorophenyl groups were selected as favorable substituents for R^1 for further optimization.

Table 2. Modification of Substituent R^1

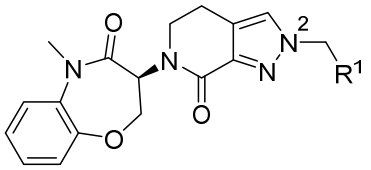

Compd	R^1	pK_i	$logk_{on}$ [a]	pk_{off} [a]	$t_{1/2}$ [a,b] (min)
16a		8.76	6.54 (6.49–6.59)	2.21 (2.14–2.30)	110 (96–140)
16b		8.29	6.48 (6.40–6.54)	1.82 (1.73–1.94)	46 (37–60)
16c		8.10	6.65 (6.52–6.75)	1.45 (1.32–1.65)	20 (14–31)
16d		8.94	6.58 (6.54–6.61)	2.36 (2.31–2.43)	160 (140–180)
16e		7.86	6.49 (6.33–6.60)	1.37 (1.22–1.61)	16 (11–29)
16f		7.47	5.90 (5.77–6.00)	1.58 (1.45–1.76)	26 (19–40)
16g		7.42	5.98 (5.81–6.10)	1.44 (1.28–1.69)	19 (13–34)
16h		5.16	n.d.[c]	n.d.[c]	<5
16i		5.37	n.d.[c]	n.d.[c]	<5
14		8.41	6.48 (6.39–6.55)	1.93 (1.83–2.06)	59 (46–80)

[a]95% confidence intervals (given in parentheses) determined in duplicate (n = 2). [b]$t_{1/2} = \ln 2/k_{off}$. [c]not determined.

Second, the results of introduction of the substituent R^2 are summarized in Table 3. The methyl analog **17** showed slightly enhanced pK_i compared to that of the non-substituted derivative **14**.

Introduction of a chloro group (**18**) significantly boosted the binding affinity and resulted in marked prolongation of $t_{1/2}$ ($t_{1/2}$ = 210 min). Compounds **19** and **20**, which had polar substituents such as cyano and carboxamide groups, also enhanced their binding affinity. These results demonstrated that filling the DP2 with not only lipophilic groups but also polar groups, was remarkably effective to enhance the binding affinity. Accordingly, a chloro group was identified as the most potent and slow-dissociating substituent (pK_i = 9.39, $t_{1/2}$ = 210 min).

Table 3. Effect of Introducing a Substituent into the 3-Position of the Core Structure

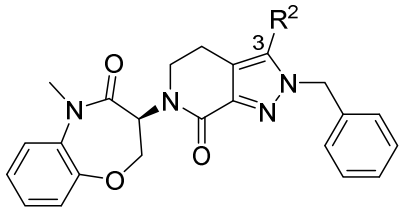

Compd	R^2	pK_i	$logk_{on}$ [a]	pk_{off} [a]	$t_{1/2}$ [a,b] (min)
17	Me	8.59	6.30 (6.25–6.35)	2.29 (2.21–2.39)	130 (110–170)
18	Cl	9.39	6.91 (6.87–6.95)	2.48 (2.41–2.57)	210 (180–260)
19	CN	8.94	6.52 (6.46–6.57)	2.42 (2.33–2.55)	180 (150–240)
20	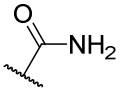	8.60	6.27 (6.21–6.32)	2.33 (2.24–2.44)	150 (120–190)
14	H	8.41	6.48 (6.39–6.55)	1.93 (1.83–2.06)	59 (46–80)

[a]95% confidence intervals (given in parentheses) determined in duplicate (n = 2). [b]$t_{1/2} = \ln 2/k_{off}$.

We identified the favorable substituents for R^1 and R^2 to show potent binding affinity and slow dissociation (i.e., 2,6-difluorophenyl and 2-fluorophenyl groups for R^1 and chloro group for R^2), so further optimization of the scaffold was continued to control the favorable ADMET profiles by using substituent R^3 toward the solvent-accessible region. Compounds **16a**, **16d**, and **18** bearing these optimal substituents showed potent pK_i and long $t_{1/2}$ value, but they had an issue of poor metabolic stabilities (data for **18** in Table 4, and data for **16a** and **16d** in a supplementary information). We assumed the benzene ring of the benzoxazepinone would be metabolically labile due to the high electron density. Therefore, electron-withdrawing and polar substituents such as cyano and amide groups were introduced as R^3 into the 7- and 8-positions of the benzoxazepinone ring to block the assumed metabolic site, reduce the electron density of the benzoxazepinone, and decrease the total lipophilicity of the molecule. The results of introduction of the substituent R^3 and the combination between R^1 and R^2 are summarized in Table 4. Introduction of cyano groups into the 7- and 8-positions improved the metabolic stabilities while maintaining potent binding affinity. In particular, the 8-cyano analog **22** showed better metabolic stability than that of the 7-cyano analog **21**. This result suggests that a metabolic soft spot could be the 8-position of the benzoxazepinone. Amide groups were introduced into the 8-position instead of the cyano group of **22**. The amide analogs **23** and **24** showed high P-gp–mediated efflux (ER = 17 and 15, respectively) despite maintaining moderate to potent binding affinity and satisfactory metabolic stability. Compounds **25** and **26** possessing 2-fluorophenyl or 2,6-difluorophenyl groups were synthesized. Compounds **25** and **26**

had moderate potency and good metabolic stability in addition to improved P-gp–mediated efflux (ER = 1.1 and 1.3, respectively). On the basis of these results, we selected compound **22** for further evaluation considering the balance between potency, metabolic stability, and P-gp ER. We also evaluated the selectivity of compound **22** for RIP1 kinase by using Reaction Biology Corp kinase panel and Eurofins Panlabs panel. As a result, compound **22** represented excellent specificity for RIP1 kinase over 406 kinases including RIP3 kinase (%inhibition: <50% at 10 μM) other than LIMK2 (>50% at 10 μM) in Reaction Biology Corp kinase panel. Compound **22** also showed excellent selectivity against 106 targets in Eurofins Panlabs panel. The results of Reaction Biology Corp kinase panel and Eurofins Panlabs panel are listed in supporting information (Supplemental Tables 4 and 5).

Table 4. Optimization of Substituents R^1, R^2, and R^3

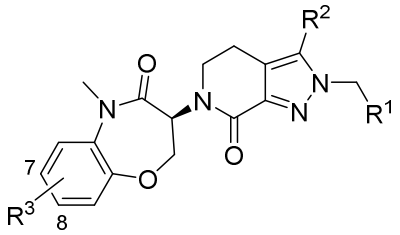

Compd	R^1	R^2	R^3	pK_i	$logk_{on}$ [a]	pk_{off} [a]	$t_{1/2}$ [a,b] (min)	HLM/MLM [c] (μL/min/mg)	ER [d]
21		Cl	7-CN	9.07	6.58 (6.55–6.61)	2.49 (2.43–2.55)	210 (190–250)	27/38	0.7
22		Cl	8-CN	9.04	6.55 (6.51–6.59)	2.49 (2.41–2.58)	210 (180–260)	<1/<1	0.6
23		Cl	8-CONHMe	9.04	6.52 (6.49–6.54)	2.52 (2.47–2.57)	230 (200–260)	13/<1	17
24		Cl	8-$CONMe_2$	8.46	6.13 (6.09–6.17)	2.32 (2.27–2.39)	150 (130–170)	19/7.0	15
25		H	8-CN	8.53	6.19 (6.15–6.24)	2.33 (2.26–2.42)	150 (130–180)	<1/<1	1.1
26	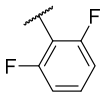	H	8-CN	8.75	6.29 (6.23–6.33)	2.47 (2.38–2.58)	200 (170–260)	<1/11	1.3
18		Cl	H	9.39	6.91 (6.87–6.95)	2.48 (2.41–2.57)	210 (180–260)	101/100	NT [e]

[a]95% confidence intervals (given in parentheses) determined in duplicate (n = 2). [b]$t_{1/2} = \ln 2/k_{off}$. [c]Metabolic stability in human and mouse liver microsomes. [d]Efflux ratios in P-gp–overexpressing cells at 1 μM. [e]Not tested.

Crystal Structure of Compound 22. An X-ray co-crystal structure of **22** bound to RIP1 kinase is shown in Figure 6. As we expected, the type III binding mode was observed. The core structure formed a hydrogen-bonding network with Asp156 among the nitrogen atom at the 1-position and the carbonyl group at the 7-position. The benzyl group fit into the allosteric hydrophobic DP1 at the back of the ATP binding site. The chloro group effectively occupied the small DP2, presumably interacting with the carbonyl group of Met67 at a distance of 3.5 Å.[30,31] This chloro-oxygen interaction might result in extremely high affinity of **18** compared to that of the methyl analog **17**. The cyano group on the benzoxazepinone ring was exposed toward the solvent-accessible region. No interaction was observed between **22** and Ser161 which is an autophosphorylation site. Reflecting this type III binding mode, compound **22** represented excellent selectivity against 406 kinases including RIP3 kinase (%inhibition: <50% at 10 μM) other than LIMK2 (>50% at 10 μM). These results demonstrated that compound **22** would be an excellent tool compound for *in vitro* and *in vivo* experiments.

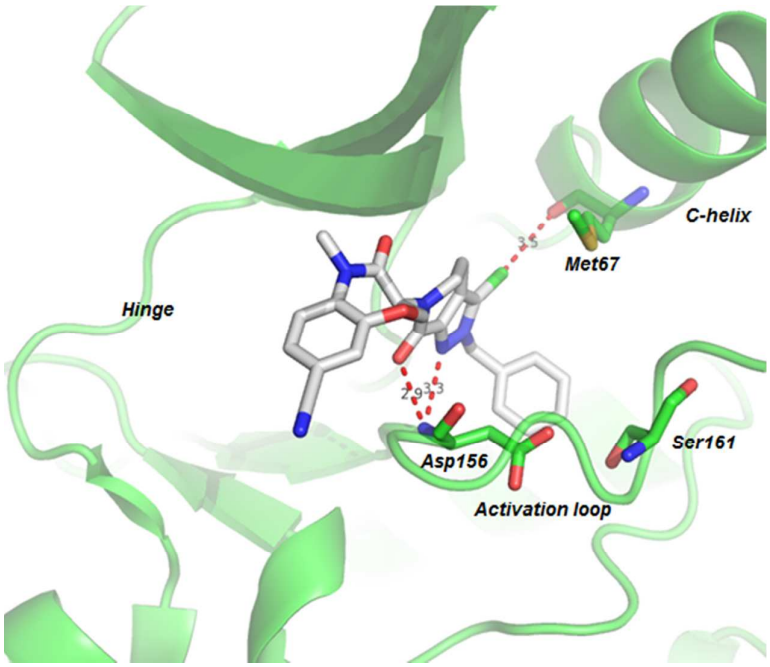

Figure 6. X-ray crystal structure of compound **22** (white).

In Vitro and In Vivo Profiling of Selected Candidate. Compound **22** was tested further in an *in vitro* binding assay for human and mouse RIP1 kinase proteins (Table 5). Compound **22** had approximately 90 times more potent affinity for human RIP1 kinase than that for mouse RIP1 kinase in TR-FRET assay. Cellular assays were also performed by using human colorectal adenocarcinoma HT-29 cells and mouse L-cells NCTC 929 (L929). L929 necroptosis assay has been generally used to examine the necroptosis pathways in mouse cells and regarded as well-established cellular model.[32] Compound **22** strongly suppressed necroptotic cell death and phosphorylation of MLKL (pMLKL), which was one of the hallmark mediators of necroptosis, in HT-29 cells (Table 5) (nectoptosis; IC_{50} = 2.0 nM, pMLKL; IC_{50} = 1.3 nM) as well as L929 cells (nectoptosis; IC_{50} = 15 nM, pMLKL; IC_{50} = 2.7 nM). The high correlation was observed between TR-FRET and cellular assays in human,

whereas there was a discrepancy between TR-FRET and cellular assays in mouse compared to human. It was not clear why there was a bigger discrepancy between TR-FRET and cellular assay of compound **22** in mouse than that in human, however the similar trend was observed between human and mouse in the other 7-oxo-2,4,5,7-tetrahydro-6*H*-pyrazolo[3,4-*c*]pyridine derivatives[33] and compound **6**.[16] In the cellular conditions, endogenous full-length enzyme of RIP1 kinase is expressed and forms a complex with a variety of proteins.[34–36] On the other hand, RIP1 kinase in the TR-FRET assay was composed of the catalytic domain of RIP1 kinase without any associated proteins. Although there is no information about the structural difference between the truncated catalytic domain of RIP1 kinase and the intracellular intact RIP1 kinase, the structural difference between truncated enzymes of human and mouse RIP1 kinase might explain the discrepancy between TR-FRET and cellular assays in mouse compared to human. Furthermore, in the case of L929 cells, TNF-α prominently causes necrosis instead of apoptosis, and this response is different from the other cell lines.[37] In fact, HT-29 cells require TNF-α, cIAP inhibitor, and a pan-caspase inhibitor to induce necroptosis.[32] Therefore, the necroptosis-inducible conditions are highly dependent on the kind of cell line. The L929 cells might be sensitive to necroptosis inducer and not require full target occupation of endogenous RIP1 kinase. Considering the excellent specificity for RIP1 kinase of **22** and the result of *in vivo* target engagement in mouse using cellular thermal shift assay (CETSA)[33], it is indicated that cellular activities of **22** should be caused by the inhibition of RIP1 kinase. Compound **22** was progressed to an *in vivo* study to evaluate its efficacy through inhibition of

non-primate RIP1 kinase.

Table 5. Cellular activities in HT-29 and L929 cells

Compd	pK_i		Necroptosis IC_{50} (nM)		pMLKL IC_{50} (nM)	
	human	mouse[a]	human[a,b]	mouse[a,c]	human[a,b]	mouse[a,c]
22	9.04	7.09 (6.96–7.23)	2.0 (1.5–2.7)	15 (14–17)	1.3 (0.3–5.5)	2.7 (1.9–3.7)

[a]95% confidence intervals (given in parentheses) determined in duplicate (n = 2). [b]HT-29 cells. [c]L929 cells.

PK study of compound **22** was conducted and the results are shown in Table 6. Compound **22** was administered to mice, and the plasma concentration was determined after oral (po, 1 mg/kg) and intravenous (iv, 0.1 mg/kg) administration. Compound **22** exhibited a desirable PK profile including high plasma exposure (AUC = 658 ng·h/mL) and a moderate plasma duration (MRT = 3.1 h).

Table 6. PK Parameters of Compound **22** in Mice[a]

Compd	PK parameters in mouse				
	CL* (mL/h/kg)	C_{max}** (ng/mL)	MRT** (h)	$AUC_{0\text{-}8h}$** (ng·h/mL)	F (%)
22	794	140.1	3.1	658	52.2

[a]The values are shown as means of three determinations (0.1 mg/kg, iv*, and 1.0 mg/kg, po**).

Moreover, compound **22** showed satisfactory brain exposure (Cb,u = 0.0230 μg/g), which was equivalent to 50 nM, and a brain-to-plasma ratio (Kp,uu = 0.3) 1 hour after oral administration (po,

10 mg/kg) in mice (Table 7). We have also confirmed the target association of **22** in the mouse brain tissues by using CETSA at 1 hour after oral administration of **22**.[33] On the basis of these results, compound **22** was selected for further evaluation in the EAE models of MS.

Table 7. Concentrations in Plasma and Brain of Compound **22** in Mice[a]

Compd	time (h)	Conc. (μg/mL or μg/g) Cp[b]	Cb[c]	Cp,u[d]	Cb,u[e]	Kp[f]	Kp,uu[g]
22	1	1.479	1.038	0.089	0.0230	0.7	0.3

[a]Administered orally at 10 mg/kg (n = 3). [b]Total plasma concentration. [c]Total brain concentration. [d]Unbound plasma concentration. [e]Unbound brain concentration. [f]Kp = Cb/Cp. [g]Kp,uu = Cb,u/Cp,u.

Compound **22** was orally administered from day 0 to day 26 and progression of clinical signs of EAE was daily monitored. Clinical signs of EAE in vehicle-treated mice were observed from day 12, and peaked at around day 21. On the other hand, the orally administered RIP1 kinase inhibitor **22** at doses of 10 mg/kg twice a day (20 mg/kg/day) attenuated the development of clinical symptoms of EAE (Figure 7A). Cumulative score of EAE was significantly lower than that of the vehicle-treated group (Figure 7B). These results indicated that compound **22** protected against disease progression in the EAE model. Ofengeim *et al.* also reported that Nec-1s (7N-1, compound **2** in this paper) blocks the disease progression in the EAE model.[4] Although it is difficult to compare the efficacy between **22** and **2** without head-to-head comparison in the same condition, compound **22** would be a novel class of an orally available and brain-penetrating *in vivo* tool for RIP1 kinase.

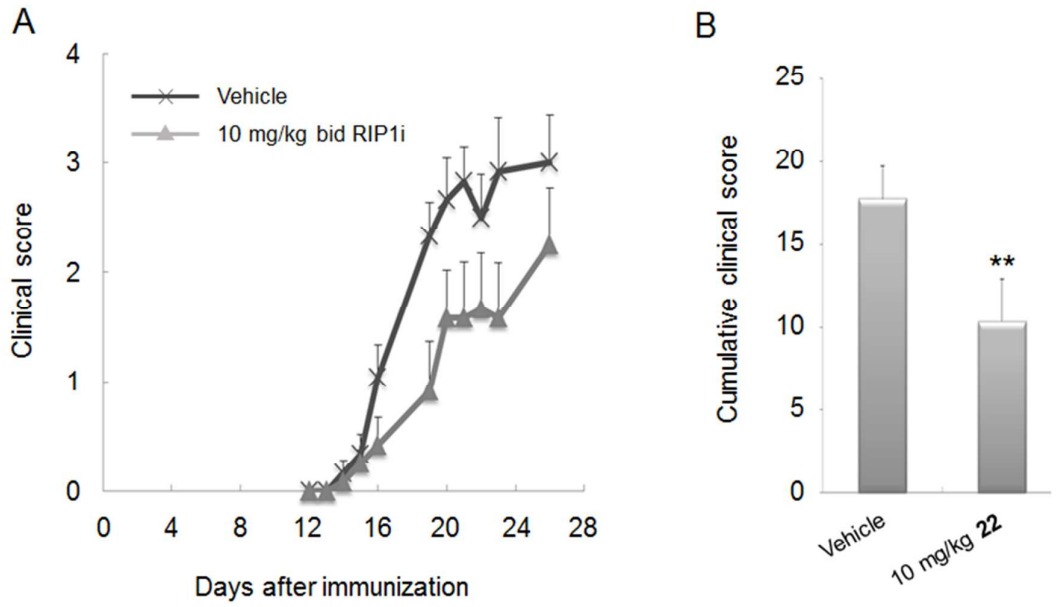

Figure 7. Assessment of compound **22** in the EAE model.

RIP1 kinase inhibitor **22** (10 mg/kg) or vehicle (0.5% methylcellulose) was orally administered to mice twice a day for 26 days. (A–B) The EAE clinical score of (A) the time course and (B) the cumulative clinical score from day 0 to day 26 are shown. Data are presented as the mean ± S.E. (n = 12). **$p < 0.05$ compared to the naïve group (Dunn's test).

Structure−kinetic relationship.

Several properties of ligands, including molecular weight, lipophilicity, and rotatable bond count, have been reported to affect kinetic parameters.[38] During the optimization of 7-oxo-2,4,5,7-tetrahydro-6*H*-pyrazolo[3,4-*c*]pyridine derivatives, molecular weight and rotatable bond count were not changed greatly and lipophilicity was the main parameter to optimize profiles such as binding activity and metabolic stability. Therefore, the SKR at R^1–R^3 substituents were analyzed in relation with lipophilicity. We also investigated the relationship between k_{on} and k_{off} to know the value of SKR analysis compared to that of conventional SAR.

In the modification of the substituent for R^1, relationships between kinetic profiles ($logk_{on}$: blue dots, pk_{off}: red dots) and lipophilicity are summarized in Figure 8 (the detailed kinetic parameters are listed in a supplementary information). Introduction of a fluoro group into the benzene ring in DP1 affected the pk_{off} more than the $logk_{on}$ (**14** and **16a**–**d**). Replacement of phenyl group with cyclobutyl group maintained the $logk_{on}$ value and resulted in a 4-fold decrease in the k_{off} value (**14** and **16e**). This finding suggested that the decreased k_{off} value of **16e** caused the decreased binding affinity. The pyridine analogs **16f** and **16g** exhibited slightly lower $logk_{on}$ and pk_{off} values than that of **14**, whereas introduction of sulfone groups (**16h** and **16i**) dramatically decreased both $logk_{on}$ and pk_{off} values. Overall, the $logk_{on}$ and pk_{off} values were mostly raised depending on the degree of increase in the clog P, and a particularly good correlation was observed between the $logk_{on}$ and clog P.

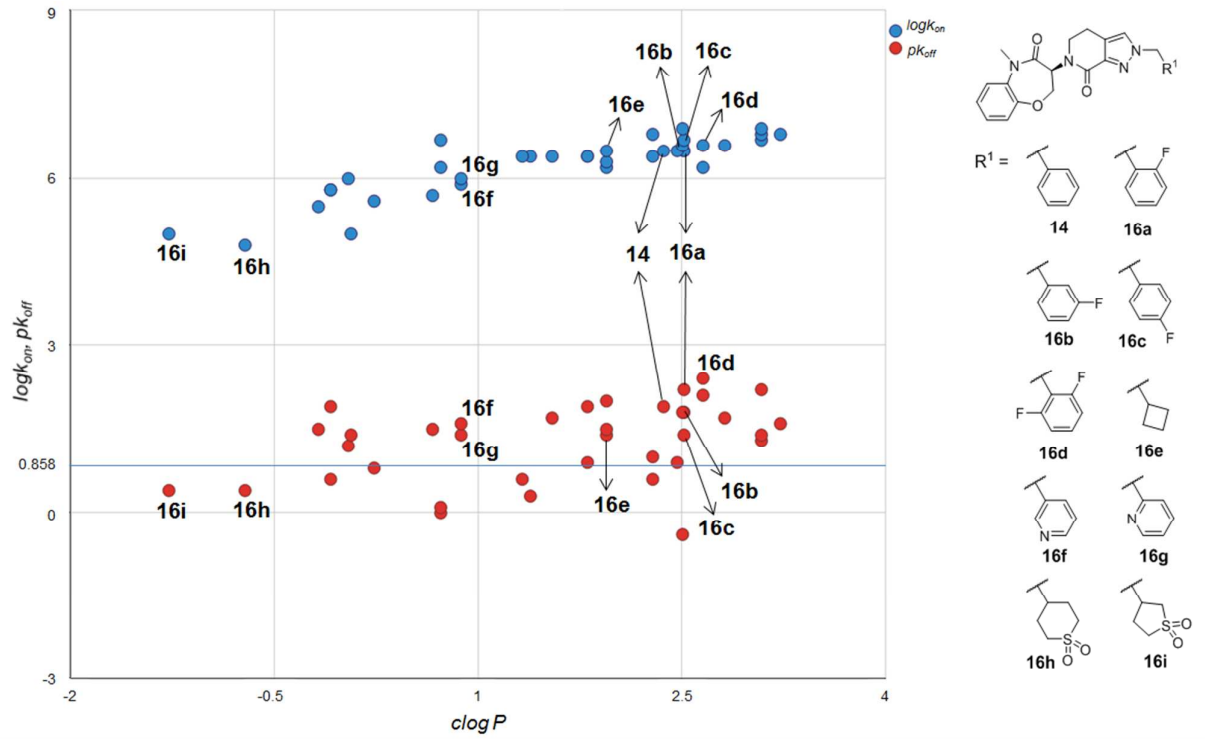

Figure 8. SKR and relationships between kinetic profiles and lipophilicity in the modification of R^1.

Relationship between the $logk_{on}$ and pk_{off} in modification of the substituent at R^1 is displayed in Figure 9. No apparent correlation was observed between the $logk_{on}$ and pk_{off}. Interestingly, it was revealed that the k_{on} and k_{off} changed independently although both the $logk_{on}$ and pk_{off} values roughly correlated with clog P. These results suggested that k_{on} and k_{off} can be optimized independently by measuring SKR, which would provide another medicinal chemistry strategy to obtain more potent compounds by combining the best k_{on} moiety with the best k_{off} moiety.

Regarding the substituents at R^2 and R^3, introduction of the appropriate R^2 substituent resulted in a longer drug-target residence time, but no notable effect on kinetic profiles was observed for substituent R^3 (Tables 3 and 4).

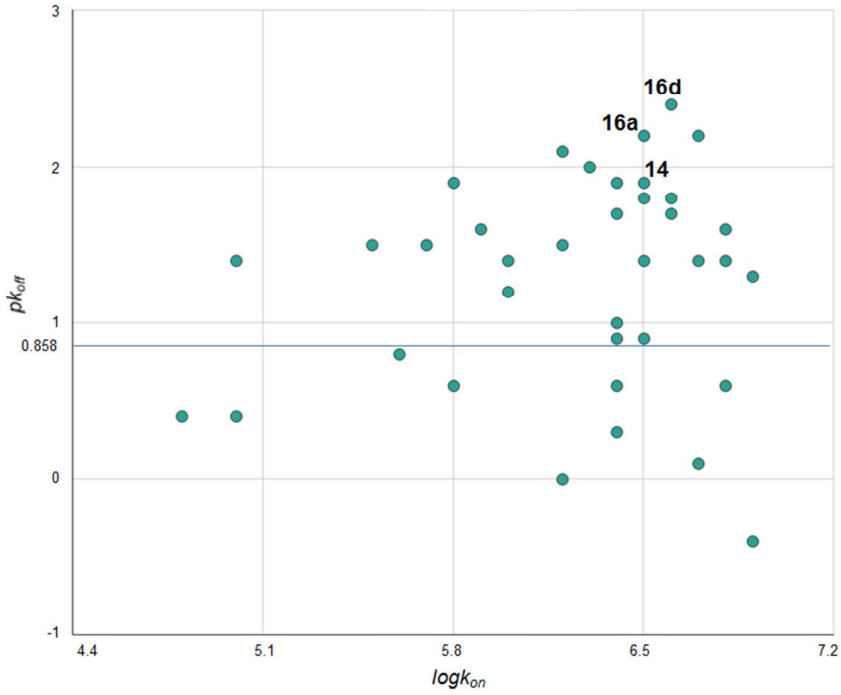

Figure 9. Relationships between $logk_{on}$ and pk_{off} in modification of R[1].

The cellular activity and binding parameters are summarized in Table 7. Based on the cocrystal structure of **22**, compounds **14** and **22** should be type III inhibitors and would also be ATP competitive inhibitors as **3** and **6**.[16] In comparison between four ATP competitive inhibitors in Table 7, slower dissociating compounds exhibited more potent cellular activity. The residence time ($t_{1/2}$) was more correlated with the cellular activity than the affinity (pK_i). It suggested that in the case of RIP1 kinase inhibitors, the residence time would be more important for achieving optimal cellular activity than affinity. However, further study is needed to conclude which is more critical for the cellular activity, the affinity or the residence time, because the sample size is small in this study. By

analyzing kinetic profiles as well as thermodynamic profiles, we succeeded to identify a favorable RIP1 kinase inhibitor that showed the potent cellular activity.

Table 7. Impact of $t_{1/2}$ on cellular activity

Compd	pK_i	HT29 Necroptosis IC_{50} (nM)[a,b]	$logk_{on}$[b]	pk_{off}[b]	$t_{1/2}$[b,c] (min)
3	8.69	300 (160–580)	7.63 (7.56–7.69)	1.06 (0.99–1.15)	8.0 (6.8–9.9)
14	8.41	18 (14–23)	6.48 (6.39–6.55)	1.93 (1.83–2.06)	59 (46–80)
6	9.01	4.1 (2.7–6.1)	6.79 (6.74–6.84)	2.22 (2.14–2.31)	115 (97–143)
22	9.04	2.0 (1.5–2.7)	6.55 (6.51–6.59)	2.49 (2.41–2.58)	210 (180–260)

[a]HT-29 cells. [b]95% confidence intervals (given in parentheses) determined in duplicate (n = 2). [c]$t_{1/2} = \ln 2/k_{off}$.

CONCLUSION

7-Oxo-2,4,5,7-tetrahydro-6*H*-pyrazolo[3,4-*c*]pyridine derivatives were discovered as potent and brain-penetrating RIP1 kinase inhibitors. Optimization of the core structure and exploration of appropriate substituents for DP1, DP2, and solvent-accessible region by utilizing the SBDD approach led to the discovery of (3*S*)-3-(2-benzyl-3-chloro-7-oxo-2,4,5,7-tetrahydro-6*H*-pyrazolo[3,4-*c*]pyridin-6-yl)-5-methyl-4-oxo-2,3,4,5-tetrahydro-1,5-benzoxazepine-8-carbonitrile (**22**), a highly potent, orally active, and brain-penetrating RIP1 kinase inhibitor with an excellent PK profile. Compound **22** significantly

suppressed necroptotic cell death and phosphorylation of MLKL in cellular assays using mouse cells in addition to human cells, which enabled evaluation of a RIP1 kinase inhibitor in a mouse neurodegenerative model. Oral administration of **22** at 10 mg/kg, bid attenuated disease progression in a mouse EAE model of MS. Although confirmation of the target binding of compound **22** with CETSA in the mouse brain tissues demonstrates that our novel chemical series target RIP1 kinase signaling pathway in CNS, further studies are needed to strengthen the evidence for the target engagement in animal brain tissues. Further evaluation of compound **22** is ongoing for neurodegenerative disorders. Compound **22** is also a good CNS tool compound for RIP1 kinase to investigate therapeutic opportunities for neurodegenerative disorders, such as MS, PD, and ALS, with significant unmet medical needs.

CHEMISTRY

Modifications of the core structure were performed according to Schemes 1–5. Synthesis of 4-oxo-1,4,6,7-tetrahydro-5*H*-imidazo[4,5-*c*]pyridine derivative **11** is described in Scheme 1. Commercially available **27** was reacted with methyl propiolate to afford imidazole **28**. After bromination and protection with a *p*-methoxybenzyl group (PMB), Sizuki-Miyaura coupling yielded **31**. The ethoxyvinyl group of **31** was converted to a formylmethyl group, followed by reductive amination with (*S*)-3-amino-5-methyl-2,3-dihydrobenzo[*b*][1,4]oxazepin-4(5*H*)-one hydrochloride[15,16] to give **33**. Cyclization using $AlMe_3$ and subsequent de-protection of the PMB group afforded 4-oxo-1,4,6,7-tetrahydro-5*H*-imidazo[4,5-*c*]pyridine derivative **11**.

Scheme 1[a]

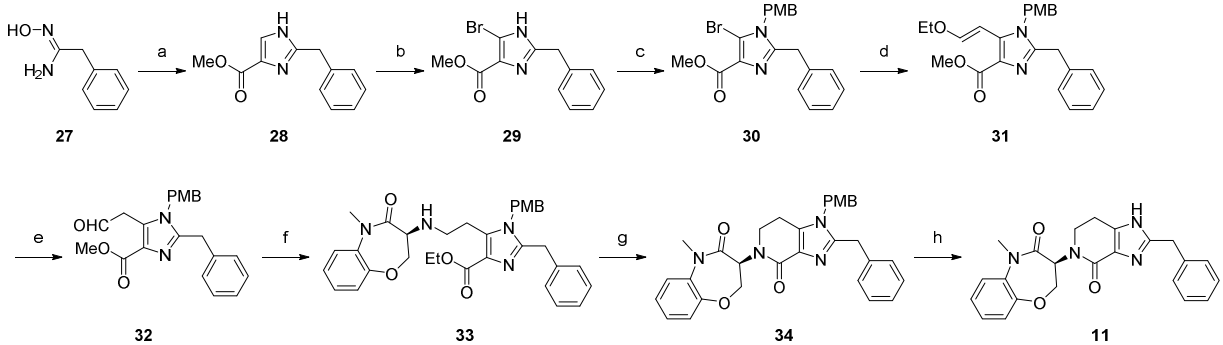

[a]Reagents and conditions: (a) methyl propiolate, diphenyl ether, microwave, 200 °C, 35%; (2) bromine, K_2CO_3, DMF, rt, 56%; (c) 4-methoxybenzyl chloride, K_2CO_3, DMF, 50 °C, 21%; (d) (*E*)-2-(2-ethoxyvinyl)-4,4,5,5-tetramethyl-1,3,2-dioxaborolane, $Pd(dppf)Cl_2 \cdot CH_2Cl_2$, Cs_2CO_3, DME/water, 90 °C, 75%; (e) 6 M HCl aq./THF, rt–60 °C, 98%; (f) (*S*)-3-amino-5-methyl-2,3-dihydrobenzo[*b*][1,4]oxazepin-4(5*H*)-one hydrochloride, 2-picoline boran, acetic acid, MeOH, rt, 65%; (g) $AlMe_3$, toluene, 120 °C, under Ar, 50%; (h) $Pd(OH)_2$, MeOH, 50 °C, under H_2, 66%.

8-Oxo-5,6-dihydro[1,2,4]triazolo[1,5-*a*]pyrazine derivative **12** was synthesized by cyclization of **6** with 1,2-dibromoethane (Scheme 2).

Scheme 2[a]

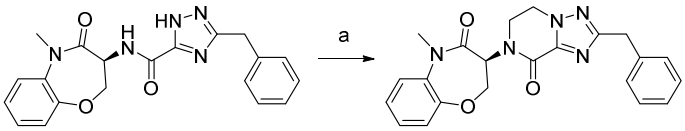

[a]Reagents and conditions: (a) NaH, 1,2-dibromoethane, DMF, 60 °C, 22%.

Treatment of commercially available **36** with ethyl 2-ethoxy-2-iminoacetate formed imidazole derivative **37**. After hydrolysis of the ester group and amidation, 8-oxo-5,6-dihydroimidazo[1,2-*a*]pyrazine derivative **13** was obtained by similar cyclization with **12** (Scheme 3).

Scheme 3[a]

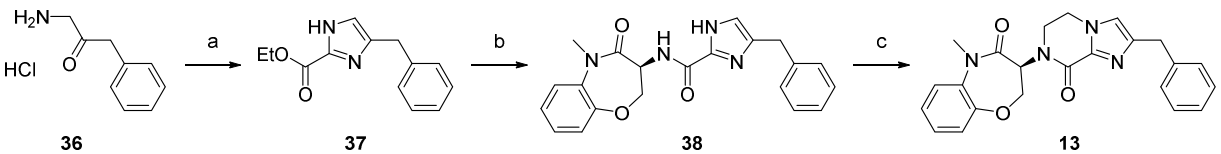

[a]Reagents and conditions: (a) ethyl 2-ethoxy-2-iminoacetate, NaOAc, AcOH, 110°C, 9.1%; (b) (1) 2 M NaOH aq., EtOH, 100 °C, (2) (*S*)-3-Amino-5-methyl-2,3-dihydrobenzo[*b*][1,4]oxazepin-4(5*H*)-one hydrochloride, HATU, DIPEA, DMF, rt, 59%; (c) Cs_2CO_3, 1,2-dibromoethane, DMF, 100 °C, 3.2%.

Preparation of 7-oxo-2,4,5,7-tetrahydro-6*H*-pyrazolo[3,4-*c*]pyridine derivative **14** was conducted in a manner similar to that for **11** (Scheme 4). Modification of the substituent for R^1 was conducted by iterative synthesis or combinatorial chemistry using de-benzylated compound **45**. Alkylation of **45** with the corresponding alkyl halide afforded compounds **16a**–**aj**, respectively.

Scheme 4[a]

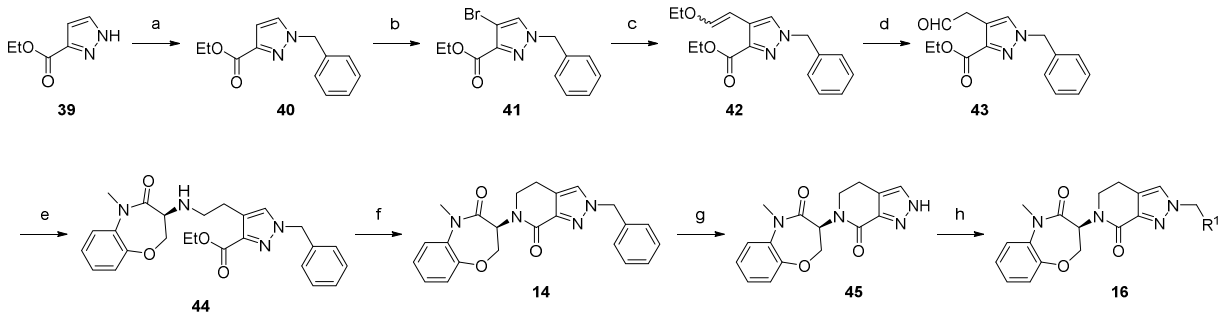

[a]Reagents and conditions: (a) K_2CO_3, benzyl bromide, DMF, rt, 64%; (b) bromine, MeCN, rt, 98%; (c) (*E*)-2-(2-ethoxyvinyl)-4,4,5,5-tetramethyl-1,3,2-dioxaborolane, $Pd(dppf)Cl_2 \cdot CH_2Cl_2$, Cs_2CO_3, DME/water, 90 °C, 94%; (d) 6 M HCl aq./THF, 60 °C, 94%; (e) (*S*)-3-amino-5-methyl-2,3-dihydrobenzo[*b*][1,4]oxazepin-4(5*H*)-one hydrochloride, 2-picoline boran, acetic acid, MeOH, rt, 94%; (f) $AlMe_3$, toluene, 120 °C, under Ar, 41%; (g) Pd/C, 1 M HCl aq., MeOH, rt, under H_2, 82%; (h) R^1CH_2Br, K_2CO_3, DMF or DMA, rt–80 °C, 1.4–65%.

Synthesis of 4-oxo-2,4,6,7-tetrahydro-5*H*-pyrazolo[4,3-*c*]pyridine derivative **15** was performed along with Scheme 5. Commercially available **46** was treated with hydrazine monohydrate to give pyrazole derivative **47**. After benzylation, de-protection and oxidation, aldehyde **50** was synthesized. Aldehyde **50** was reacted with (methoxymethyl)triphenylphosphonium chloride in a presence of

potassium *tert*-butoxide (^{t}BuOK), followed by hydrolysis, reductive amination and cyclization to give compound **15**.

Scheme 5[a]

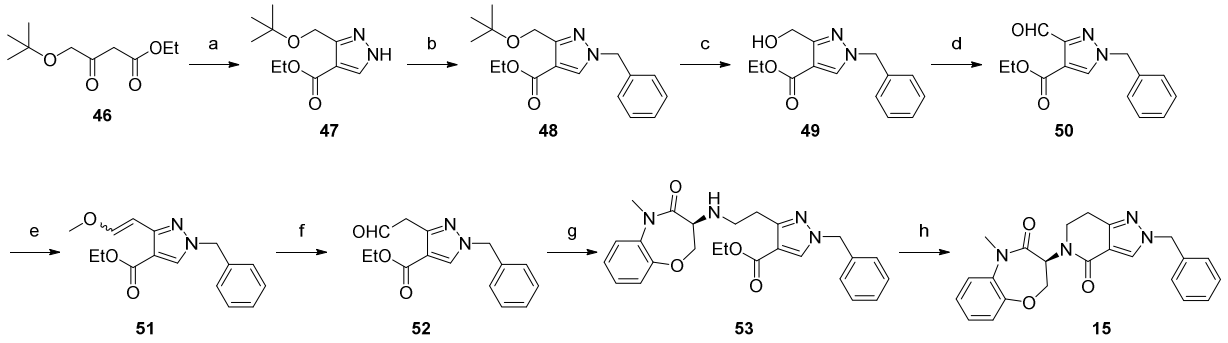

[a]Reagents and conditions: (a) (1) DMFDMA, toluene, 65 °C, (2) $NH_2NH_2 \cdot H_2O$, AcOH, rt, 52% in 2 steps; (b) benzyl chloride, K_2CO_3, MeCN, rt, 64%; (c) TFA, DCM, rt, 86%; (d) MnO_2, DCM, 40 °C, 59%; (e) (methoxymethyl)triphenylphosphonium chloride, ^{t}BuOK, THF, rt, 53%; (f) (1) 6 M HCl aq./THF, rt, (2) (*S*)-3-amino-5-methyl-2,3-dihydrobenzo[*b*][1,4]oxazepin-4(5*H*)-one hydrochloride, 2-picoline boran, acetic acid, MeOH, rt; (h) $AlMe_3$, toluene, 100 °C, 6% in 3 steps.

3-Substituted 7-oxo-2,4,5,7-tetrahydro-6*H*-pyrazolo[3,4-*c*]pyridine derivatives **17**–**20** were synthesized as shown in Scheme 6. Treatment of commercially available **54** with benzylhydrazine hydrochloride yielded **55**, followed by conversion to compounds **56a,b** by using phosphoryl bromide or phosphoryl chloride. Compounds **18** and **60** were prepared in a similar way with **15**. Sizuki-Miyaura coupling of **60** provided methyl analog **17**. The cyanation of **60** using dicyanozinc formed compound **19**, followed by hydrolysis to give **20**.

Scheme 6[a]

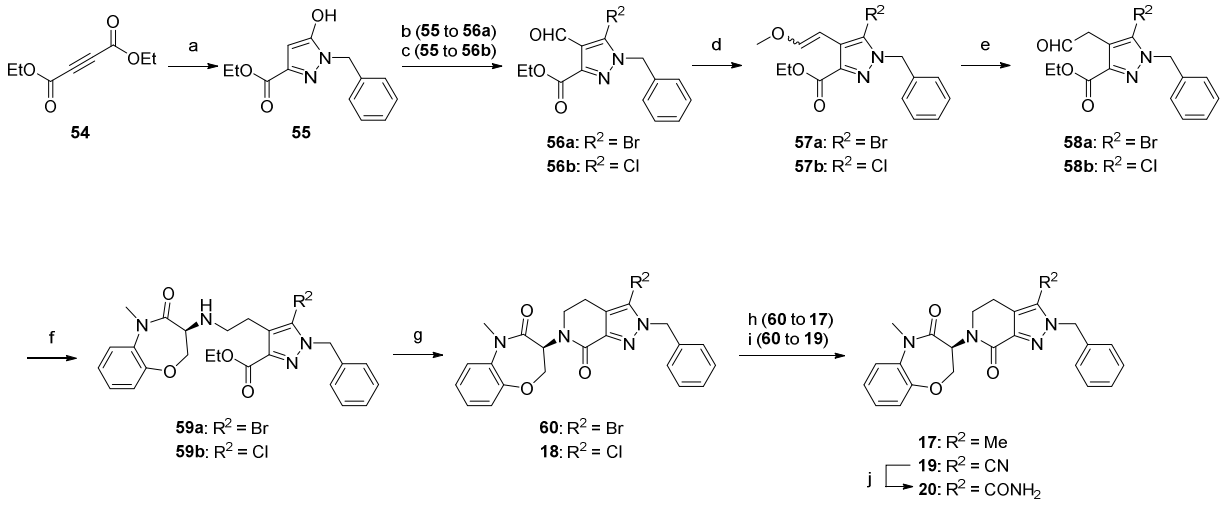

[a]Reagents and conditions: (a) benzylhydrazine hydrochloride, K_2CO_3, EtOH, 90 °C, 36%; (b) phosphoryl bromide, DMF, 1,2-dichloroethane, 90 °C, 48%; (c) phosphoryl chloride, DMF, 90 °C, 36%; (d) (methoxymethyl)triphenylphosphonium chloride, ^{t}BuOK, THF, rt, 30–42%; (e) 6 M HCl aq/THF, rt; (f) (*S*)-3-amino-5-methyl-2,3-dihydrobenzo[*b*][1,4]oxazepin-4(5*H*)-one hydrochloride, 2-picoline boran, acetic acid, MeOH, rt, 67–94% in 2 steps; (g) $AlMe_3$, toluene, 100 °C, 23–82%; (h) $Pd(PPh_3)_4$, 2,4,6-trimethyl-1,3,5,2,4,6-trioxatriborinane, KOH, THF, 100 °C, under Ar, 9%; (i) dicyanozinc, $Pd(PPh_3)_4$, DMF, 100 °C, under Ar, 90%; (j) K_2CO_3, H_2O_2, DMSO, rt, 60%.

Synthesis of key intermediates **64a,b** and **70a**–**d** are described in Schemes 7 and 8, respectively. Compounds **64a,b** were synthesized in a manner similar to that described for **43** in Scheme 4. Substituted fluoronitrobenzenes **65a**–**c** were reacted with (*S*)-2-((*tert*-butoxycarbonyl)amino)-3-hydroxypropanoic acid in a presence of sodium hydride, followed by reduction of the nitro group, intramolecular amidation and *N*-methylation to give Boc-protected **69a**–**c**. Compound **69c** was converted to compounds **69e**,**f** via de-protection of the benzyl group and amidation. (*S*)-3-Amino-5-methyl-2,3-dihydrobenzo[*b*][1,4]oxazepin-4(5*H*)-one **70a**–**d** were obtained by de-protection of the corresponding intermediate.

Scheme 7[a]

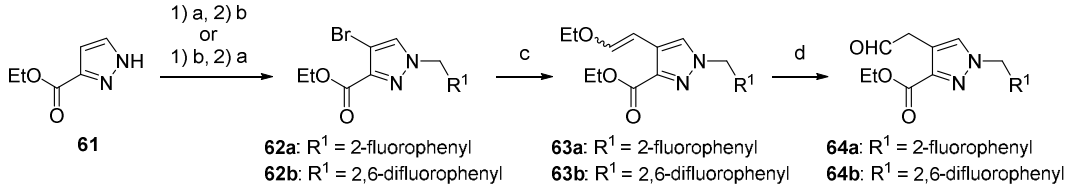

[a]Reagents and conditions: (a) R^1CH_2Br, NaH, THF, rt, 95–97%; (b) bromine, MeCN, rt, 88–98%; (c) (*E*)-2-(2-ethoxyvinyl)-4,4,5,5-tetramethyl-1,3,2-dioxaborolane, $Pd(dppf)Cl_2 \cdot CH_2Cl_2$, Cs_2CO_3, DME/water, 90 °C, under Ar, 84–87%; (d) 6 M HCl aq./THF, rt, 68%–quant.

Scheme 8[a]

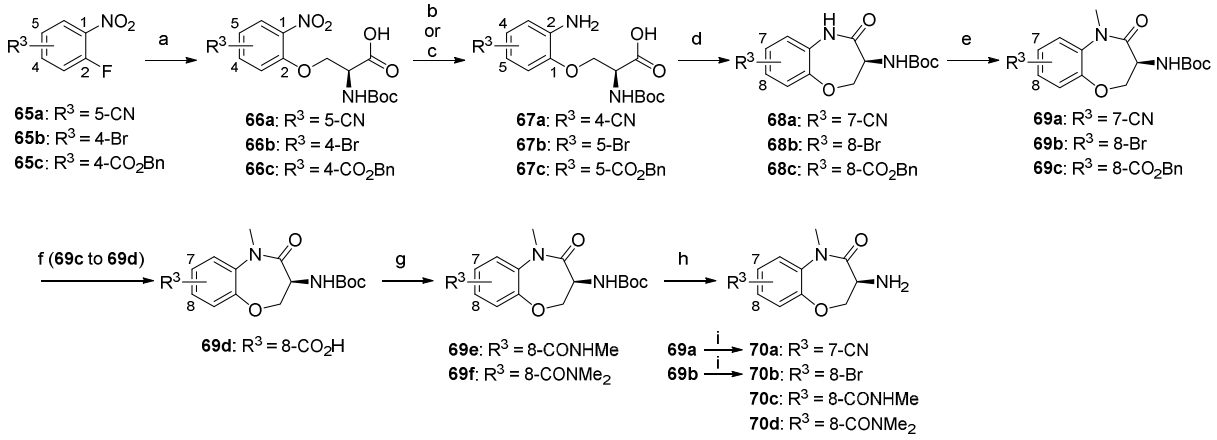

[a]Reagents and conditions: (a) (*S*)-2-((tert-butoxycarbonyl)amino)-3-hydroxypropanoic acid, NaH, DMF, rt, 22–74 %; (b) Fe, NH_4Cl, EtOH/water, 80 °C; (c) Zn, AcOH, 0 °C; (d) HATU, TEA, DMSO, rt, 3–26% in 2 steps; (e) MeI, Cs_2CO_3, DMF, rt, 45–75%; (f) Pd/C, THF, rt, under H_2, 99%; (g) methylamine or dimethylamine, HATU, TEA, DMF, rt, 85–100%; (h) 4 M HCl in EtOAc, THF, rt, 60–98%.

Modifications of the substituent for R^3 were performed according to Scheme 9. Reductive amination of aldehydes **58b** and **64a**,**b** with the corresponding amines **70a**–**d** gave compounds **71a**–**f**, respectively. After cyclization and cyanation if needed, compounds **21**–**26** were finally synthesized.

Scheme 9[a]

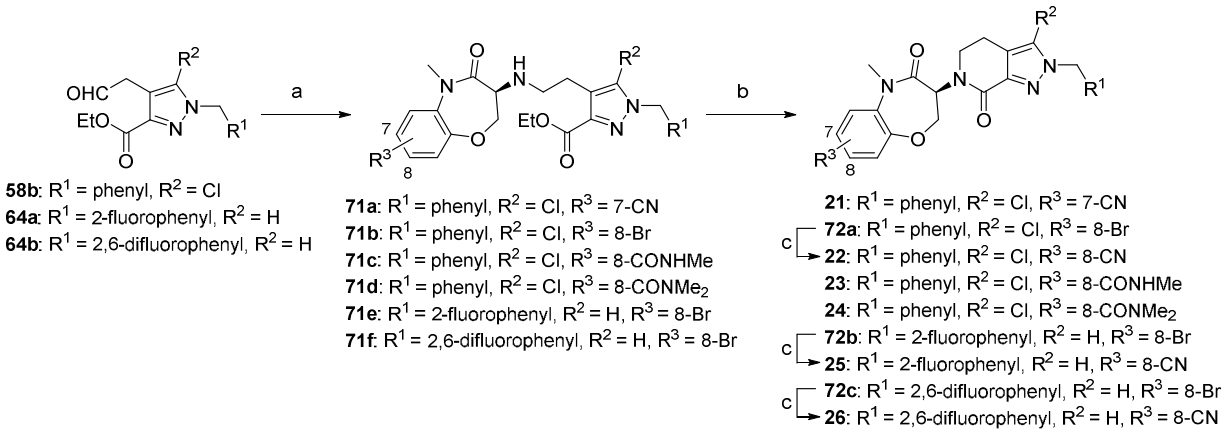

[a]Reagents and conditions: (a) **70a**–**d**, 2-picoline boran, acetic acid, MeOH, rt, 48–100%; (b) $AlMe_3$, toluene, 100 °C, 29–89%; (c) dicyanozinc, $Pd(PPh_3)_4$, DMF, 100 °C, under Ar, 62–85%.

EXPERIMENTAL SECTION

General Chemistry Information. All commercially available solvents and reagents were used without further purification. Yields were not optimized. ^{1}H NMR spectra were recorded on Bruker DPX300 (300 MHz) or DPX400 (400 MHz) instruments. Chemical shifts are reported as δ values (ppm) downfield from internal TMS of the indicated organic solution. Peak multiplicities are expressed as follows: s, singlet; d, doublet; t, triplet; q, quartet; dd, doublet of doublets; td, triplet of doublets; ddd, doublet of doublet of doublets; brs, broad singlet; m, multiplet. Coupling constants (*J* values) are given in hertz (Hz). LC-MS was performed on a Waters liquid chromatography-mass spectrometer system, using a CAPCELL PAK UG-120 ODS column (2.0 mm i.d. × 50 mm, Shiseido Co., Ltd.) with a 5–95% gradient of MeCN in water containing 0.04% TFA and an HP-1100 (Agilent Technologies) apparatus for monitoring at 220 nm. All microwave reactions were performed in a Biotage Initiator 2.0 or 2.5 microwave synthesizer. Preparative HPLC was performed on an automated Gilson HPLC system using a YMC C-18 column (S-5 μm, 50 mm × 20 mm i.d.) with a 5–95% gradient of MeCN in water containing 0.1% TFA. Reaction progress was determined by TLC analysis on Merck Kieselgel 60 F254 plates or Fuji Silysia NH plates. Column chromatography was performed using silica gel (Merck Kieselgel 60, 70–230 mesh), basic silica gel (Chromatorex NH-DM 1020, 100-200 mesh, Fuji Silysia Chemical, Ltd.), or Purif-Pack (SI ϕ 60 μM or NH ϕ 60 μM, Fuji Silysia Chemical, Ltd.). Unless otherwise stated, the purities of synthesized compounds for biological testing were > 95% determined by analytical HPLC. (The purities of **11**, **13**, **16b**, **16h** and

16t were 89.6%, 86.8%, 94.7%, 94.4% and 93.9%, respectively.) Analytical HPLC was performed with Corona Charged Aerosol Detector (CAD), Nano quantity analyte detector (NQAD), or photo diode array detector. The column was a Capcell Pak C18AQ (50 mm × 3.0 mm I.D., Shiseido, Japan) or L-column 2 ODS (30 mm × 2.0 mm I.D., CERI, Japan) with a temperature of 50 °C and a flow rate of 0.5 mL/min. Mobile phase A and B under a neutral condition were a mixture of 50 mmol/L ammonium acetate, water, and acetonitrile (1:8:1, v/v/v) and a mixture of 50 mmol/L ammonium acetate and acetonitrile (1:9, v/v), respectively. The ratio of mobile phase B was increased linearly from 5% to 95% over 3 min, 95% over the next 1 min. Mobile phase A and B under acidic conditions were a mixture of 0.2% formic acid in 10 mmol/L ammonium formate and 0.2% formic acid in acetonitrile, respectively. The ratio of mobile phase B was increased linearly from 14% to 86% over 3 min, 86% over the next 1 min. Abbreviations of solvents are used as follows: $CDCl_3$, deuterated chloroform; DMSO-d_6, dimethyl sulfoxide-d_6; dichloromethane, DCM; EtOAc, ethyl acetate; DMF, *N*,*N*-dimethylformamide; MeOH, methanol; THF, tetrahydrofuran; EtOH, ethanol; DMSO, dimethyl sulfoxide; DMA, *N*,*N*-dimethylactamide; AcOH, acetic acid; DMFDMA, *N*,*N*-dimethylformamide dimethylacetal; MeCN, acetonitrile; DIPEA, *N*,*N*-diisopropylethylamine; TEA, triethylamine; IPE, diisopropyl ether.

(3*S*)-3-(2-Benzyl-4-oxo-1,4,6,7-tetrahydro-5*H*-imidazo[4,5-*c*]pyridin-5-yl)-5-methyl-2,3-dihydro-1,5-benzoxazepin-4(5*H*)-one trifluoroacetic acid (11). Two batches of the reaction were conducted and worked up together after the reaction. A mixture of **34** (10 mg, 0.02 mmol) and 10%

$Pd(OH)_2$ on carbon (2.4 mg, 1.71 μmol) in MeOH (5 mL) was hydrogenated under balloon pressure at room temperature overnight. $Pd(OH)_2$ (7 mg) and 6 M HCl aq (1 mL) were added. After stirring at rt under H_2 atmosphere for 2 h, the mixture was heated to 50 °C and stirred at 30 min. The catalyst was removed by filtration and the filtrate was concentrated under reduced pressure.

A mixture of **34** (22 mg, 0.04 mmol) and 10% $Pd(OH)_2$ on carbon (16 mg, 0.01 mmol) in MeOH (5 ml) and 6 M HCl aq (1.000 mL) was hydrogenated under balloon pressure at 50 °C for 2.5 h. The catalyst was removed by filtration and the filtrate was concentrated under reduced pressure.

The residues were combined and diluted with MeOH. The solution of the mixture in MeOH was purified by preparative HPLC (L-Column 2 ODS, eluted with H_2O in acetonitrile containing 0.1% TFA). The desired fractions were concentrated under reduced pressure to give **11** (21 mg, 66%) as a light brown amorphous powder. ^{1}H NMR (300 MHz, $CDCl_3$) δ 3.01-3.17 (1H, m), 3.20-3.39 (4H, m), 3.63-3.79 (1H, m), 3.89-4.13 (2H, m), 4.29-4.46 (2H, m), 4.74 (1H, dd, *J* = 11.7, 10.2 Hz), 5.64 (1H, dd, *J* = 11.9, 7.7 Hz), 6.77-6.89 (1H, m), 6.95-7.21 (5H, m), 7.28-7.35 (3H, m). LC-MS (APCI) *m*/*z* 403.2 $[M + H]^+$. Analytical HPLC 89.6% purity.

(3*S*)-3-(2-Benzyl-8-oxo-5,6-dihydro[1,2,4]triazolo[1,5-*a*]pyrazin-7(8*H*)-yl)-5-methyl-2,3-dihydro-1,5-benzoxazepin-4(5*H*)-one (12). To a solution of **6** (47 mg, 0.12 mmol) and sodium hydride (10.96 mg, 0.27 mmol) in DMF (1 mL) was added 1,2-dibromoethane (0.013 mL, 0.15 mmol) at room temperature, and the mixture was stirred 24 h at 60 °C. The reaction mixture was fileterd through a short pad of silica gel eluted by EtOAc/MeOH (1/1) and concentrated under reduced

pressure. The residue was purified by column chromatography (silica gel, eluted with 80% - 100% EtOAc in hexane) to give **12** (11.10 mg, 22%) as a white amorphous solid. ^{1}H NMR (300 MHz, $CDCl_3$) δ 3.38 (3H, s), 3.82 (1H, ddd, *J* = 12.4, 11.0, 4.2 Hz), 4.06-4.18 (2H, m), 4.34-4.80 (5H, m), 5.82 (1H, dd, *J* = 11.7, 8.3 Hz), 7.14-7.40 (9H, m). LC-MS (APCI) *m*/*z* 404.3 $[M + H]^+$. Analytical HPLC 100% purity.

(3*S*)-3-(2-Benzyl-8-oxo-5,6-dihydroimidazo[1,2-*a*]pyrazin-7(8*H*)-yl)-5-methyl-2,3-dihydro-1,5-benzoxazepin-4(5*H*)-one (13). To a solution of **38** (89 mg, 0.24 mmol) and 1,2-dibromoethane (commercially available, 0.072 mL, 0.83 mmol) in DMF (2 mL, 25.83 mmol) was added cesium carbonate (308 mg, 0.95 mmol) at room temperature, and the mixture was stirred for 2 h at 100 °C. To the reaction mixture was added water and extracted with EtOAc. The organic layer was washed twice with water and once with brine, dried over Na_2SO_4, filtered and concentrated under reduced pressure. The residue was purified by column chromatography (silica gel, eluted with 17% - 43% MeOH in EtOAc). The residue was purified by preparative HPLC (L-Column 2 ODS, eluted with H_2O in acetonitrile containing 0.1% TFA). The desired fraction was neutralized with saturated $NaHCO_3$ aq. and extracted with EtOAc. The organic layer was separated, dried over Na_2SO_4 and concentrated under reduced pressure to give **13** (3.0 mg, 3.2%) as a white solid. ^{1}H NMR (300 MHz, $CDCl_3$) δ3.37 (3H, s), 3.74 (1H, td, *J* = 11.6, 4.0 Hz), 3.99 (2H, s), 4.06 (1H, dt, *J* = 12.6, 3.9 Hz), 4.28-4.66 (4H, m), 5.89 (1H, dd, *J* = 11.7, 8.3 Hz), 6.56 (1H, s), 7.15-7.34 (9H, m). LC-MS (APCI) *m*/*z* 403.2 $[M + H]^+$. Analytical HPLC 86.8% purity.

(3*S*)-3-(2-Benzyl-7-oxo-2,4,5,7-tetrahydro-6*H*-pyrazolo[3,4-*c*]pyridin-6-yl)-5-methyl-2,3-dihydro-1,5-benzoxazepin-4(5*H*)-one (14). Compound **14** was obtained (41%) as a white amorphous solid in a manner similar to that described for the synthesis of **34**. ^{1}H NMR (300 MHz, $CDCl_3$) δ 2.70 (1H, dt, *J* = 15.5, 4.7 Hz), 3.10 (1H, ddd, *J* = 15.6, 10.7, 4.7 Hz), 3.38 (3H, s), 3.54 (1H, td, *J* = 11.2, 4.3 Hz), 4.22 (1H, dt, *J* = 11.9, 5.0 Hz), 4.42 (1H, dd, *J* = 9.8, 8.3 Hz), 4.62 (1H, dd, *J* = 11.7, 10.2 Hz), 5.34 (2H, s), 5.96 (1H, dd, *J* = 11.7, 8.3 Hz), 7.11-7.26 (7H, m), 7.29-7.39 (3H, m). LC-MS (APCI) *m*/*z* 403.3 $[M + H]^+$. ^{13}C NMR (75 MHz, $CDCl_3$) δ 20.6, 35.6, 45.8, 51.2, 56.8, 74.8, 121.3, 122.6, 123.3, 125.7, 125.9, 127.2, 128.0, 128.3, 128.9, 135.8, 136.8, 142.7, 150.0, 161.4, 169.6. Anal. Calcd for $C_{23}H_{22}FN_4O_3$ + 0.4 H_2O: C, 67.43; H, 5.61; N, 13.68. Found: C, 67.54; H, 5.63; N, 13.48. Analytical HPLC 99.9% purity.

(3*S*)-3-(2-Benzyl-4-oxo-2,4,6,7-tetrahydro-5*H*-pyrazolo[4,3-*c*]pyridin-5-yl)-5-methyl-2,3-dihydro-1,5-benzoxazepin-4(5*H*)-one (15). To a solution of **51** (200 mg, 0.699 mmol) in THF (5 mL) was added 6 M HCl aq. (0.47 mL, 2.80 mmol). After stirring at 25–30 °C for 14 h, the micture was diluted with water, neutralized with saturated $NaHCO_3$ aq. till pH = 7, and extracted with EtOAc (twice). The combined organic layer was washed with brine, dried over Na_2SO_4, filtered and concentrated under reduced pressure to give **52** as a colorless oil. To a solution of the crude of **52** and (*S*)-3-amino-5-methyl-2,3-dihydrobenzo[*b*][1,4]oxazepin-4(5*H*)-one hydrochloride (75 mg, 0.33 mmol) in MeOH (2 mL) and AcOH (0.2 mL) was added 2-picoline boran (53 mg, 0.50 mmol) at 0 °C, the mixture was stirred at 0 °C for 0.5 hr. The reaction was quenched with water (20 mL) and

to the mixture was added saturated $NaHCO_3$ aq. till pH = 7, then it was extracted with EtOAc (30 mL X2). The combined organic layer was washed with brine (50 mL) and dried over Na_2SO_4. The organic layer was concentrated under reduced pressure. The residue was purified by column chromatography (silica gel, eluted with petroleum ether/EtOAc (1:1)) to give **53** as an off-white solid (LC-MS (APCI) *m/z* 449.3 $[M + H]^+$). To a solution of the crude of **53** in toluene (2 mL) was added $AlMe_3$ (2 M in toluene, 0.25 mL,0.51 mmol) at 25 °C. The mixture was stirred at 100 °C under N_2 for 1 hr. After cooling to 20 °C, the reaction mixture was quenched with water (30 mL) and it was extracted with EtOAc (30 mL X3). The combined organic layer was washed with brine (50 mL) and dried over Na_2SO_4. The organic layer was concentrated under reduced pressure to give crude product. It was purified by prep-HPLC (0.1% $NH_3 \cdot H_2O$ as additive), and most of MeCN was removed under reduced pressure to give the residue, and it was lyophilized to give **15** (18 mg, 6% in 3 steps) as an off-white solid.

LC-MS (Mobile phase: from 90% [water + 0.04% TFA] and 10% [MeCN +0.02 % TFA] to 20% [water + 0.04% TFA] and 80% [MeCN + 0.02% TFA] in 1.35 min, then under this conditionfor 0.9 min, finally changed to 90% [water + 0.04% TFA] and 10% [MeCN + 0.02% TFA] and under this condition for 0.75 min.) purity is > 99%, Rt = 1.615 min; MS Calcd.: 402.2; MS Found: 403.1 $[M + H]^+$. ^1H NMR (400 MHz, $CDCl_3$) δ 2.75-2.85 (1H, m), 3.10-3.20 (1H, m), 3.31 (3H, s), 3.45-3.55 (1H, m), 4.15-4.25 (1H, m), 4.31 (1H, dd, *J* = 10.0, 8.4 Hz), 4.60 (1H, dd, *J* = 11.6, 10.0 Hz), 5.18 (2H, s), 5.75 (1H, dd, *J* = 11.6, 8.0 Hz), 7.05-7.20 (6H, m), 7.25-7.35 (3H, m, overlap with $CDCl_3$

signal), 7.66 (1H, s). ^{13}C NMR (75 MHz, $CDCl_3$) δ23.3, 35.5, 45.1, 50.9, 56.4, 74.9, 113.8, 122.6, 123.1, 125.8, 127.1, 127.9, 128.4, 129.0, 130.7, 135.4, 136.9, 149.9, 152.4, 162.6, 169.7. Anal. Calcd for $C_{23}H_{22}FN_4O_3$ + 0.5 H_2O: C, 67.14; H, 5.63; N, 13.62. Found: C, 67.09; H, 5.61; N, 13.44. Analytical HPLC 98.5% purity.

(3*S*)-3-(2-(2-Fluorobenzyl)-7-oxo-2,4,5,7-tetrahydro-6*H*-pyrazolo[3,4-*c*]pyridin-6-yl)-5-methyl-2,3-dihydro-1,5-benzoxazepin-4(5*H*)-one (16a). 2-Fluorobenzyl bromide (commercially available, 12 µl, 0.10 mmol) was added to a solution of **45** (26 mg, 0.08 mmol) and potassium carbonate (34.5 mg, 0.25 mmol) in DMF (1.0 mL) at room temperature. The mixture was stirred at room temperature overnight. The mixture was partitioned between EtOAc and water. The organic layer was separated, washed with brine, dried over Na_2SO_4 and concentrated under reduced pressure. The residue was purified by column chromatography (silica gel, eluted with 80% - 100% EtOAc in hexane) to give **16a** (17.6 mg, 0.042 mmol, 50%) as a white solid. LC-MS (APCI) *m*/*z* 421.2 $[M + H]^+$. ^{1}H NMR (300 MHz, $CDCl_3$) δ 2.77 (1H, dt, *J* = 15.9, 5.3 Hz), 3.12 (1H, ddd, *J* = 15.7, 10.4, 4.9 Hz), 3.38 (3H, s), 3.59 (1H, ddd, *J* = 12.1, 10.2, 4.5 Hz), 4.18-4.31 (1H, m), 4.40 (1H, dd, *J* = 9.8, 7.9 Hz), 4.67 (1H, dd, *J* = 11.9, 10.0 Hz), 5.66-5.88 (3H, m), 6.88-6.96 (1H, m), 6.97-7.06 (2H, m), 7.12-7.25 (5H, m), 7.42 (1H, s). ^{13}C NMR (75 MHz, $CDCl_3$) δ 20.5, 35.6, 45.8, 50.1 (d, *J* = 4.4 Hz), 51.2, 74.8, 115.5 (d, *J* = 20.9 Hz), 121.3, 122.6, 123.0 (d, *J* = 14.9 Hz), 123.3, 124.7 (d, *J* = 3.9 Hz), 125.9, 126.0 (d, *J* = 1.7 Hz), 127.2, 130.4 (d, *J* = 8.3 Hz), 130.6 (d, *J* = 3.9 Hz), 136.8, 142.9, 150.0, 160.4 (d, *J* = 247 Hz), 161.3, 169.6. Anal. Calcd for $C_{23}H_{21}FN_4O_3$ + 0.7 H_2O: C, 63.79; H, 5.21; N, 12.94. Found: C,

63.92; H, 5.16; N, 12.68. Analytical HPLC 96.3% purity.

(3*S*)-3-(2-(3-Fluorobenzyl)-7-oxo-2,4,5,7-tetrahydro-6*H*-pyrazolo[3,4-*c*]pyridin-6-yl)-5-methyl-2,3-dihydro-1,5-benzoxazepin-4(5*H*)-one (16b). Compound **16b** was obtained (2% in 4 steps) as a white solid in a manner similar to that described for the synthesis of **14**. LC-MS (APCI) *m*/*z* 421.2 $[M + H]^+$. ^{1}H NMR (400 MHz, DMSO-d_6) δ 2.65-2.80 (1H, m), 2.80-2.95 (1H, m), 3.29 (3H, s, overlap with water signal), 3.50-3.65 (1H, m), 3.90-4.05 (1H, m), 4.32 (1H, dd, *J* = 10.0, 8.0 Hz), 4.75-4.90 (1H, m), 5.38 (2H, s), 5.56 (1H, dd, *J* = 12.0, 7.6 Hz), 7.04-7.09 (2H, m), 7.10-7.20 (1H, m), 7.25-7.45 (4H, m), 7.45-7.55 (1H, m), 7.78 (1H, s). Analytical HPLC 94.7% purity.

(3*S*)-3-(2-(4-Fluorobenzyl)-7-oxo-2,4,5,7-tetrahydro-6*H*-pyrazolo[3,4-*c*]pyridin-6-yl)-5-methyl-2,3-dihydro-1,5-benzoxazepin-4(5*H*)-one (16c). Compound **16c** was obtained (23%) as a white solid in a manner similar to that described for the synthesis of **14**. LC-MS (APCI) *m*/*z* 421.2 $[M + H]^+$. ^{1}H NMR (400 MHz, DMSO-d_6) δ 2.61-2.73 (1H, m), 2.75-2.90 (1H, m), 3.29 (3H, s, overlap with water signal), 3.50-3.62 (1H, m), 3.92-4.01 (1H, m), 4.25-4.35 (1H, m), 4.75-4.85 (1H, m), 5.34 (2H, s), 5.56 (1H, dd, *J* = 15.6, 8.0 Hz), 7.12-7.37 (7H, m), 7.45-7.53 (1H, m), 7.75 (1H, s). ^{13}C NMR (75 MHz, $CDCl_3$) δ 20.5, 35.6, 45.8, 51.2, 56.0, 74.8, 115.8 (d, *J* = 21.5 Hz), 121.4, 122.6, 123.3, 125.6, 125.9, 127.2, 129.8 (d, *J* = 8.3 Hz), 131.6 (d, *J* = 3.3 Hz), 136.8, 142.9, 150.0, 161.3, 162.6 (d, *J* = 248 Hz), 169.5. Anal. Calcd for $C_{23}H_{21}FN_4O_3$ + 0.1 H_2O: C, 65.42; H, 5.06; N, 13.27. Found: C, 65.14; H, 5.10; N, 13.03. Analytical HPLC 98.2% purity.

(3*S*)-3-(2-(2,6-Difluorobenzyl)-7-oxo-2,4,5,7-tetrahydro-6*H*-pyrazolo[3,4-*c*]pyridin-6-yl)-5-meth

yl-2,3-dihydro-1,5-benzoxazepin-4(5*H*)-one (16d). Compound **45** (25.0 mg, 80 μmol), potassium carbonate (22.3 mg, 160 μmol), 2,6-difluorobenzyl bromide (commercially available, 160 μmol), and DMA (1 mL) were charged to 16.5 mL test tube. After the mixture was stirred at 80 ℃ for 1.5 h, the salt was removed by filtration and washed with MeOH. The filtrate was purified by directly injecting into the Gilson Preparative-HPLC under neutral conditions. The obtained fraction was dried by blowing away with the air at 60 °C to give **16d** (17.9 mg, 51%). LC-MS (APCI) m/z 439.1 $[M + H]^+$. Analytical HPLC 99.7% purity.

(3*S*)-3-(2-(Cyclobutylmethyl)-7-oxo-2,4,5,7-tetrahydro-6*H*-pyrazolo[3,4-*c*]pyridin-6-yl)-5-meth yl-2,3-dihydro-1,5-benzoxazepin-4(5*H*)-one (16e). Compound **16e** was obtained (22%) in a manner similar to that described for the synthesis of **16d**. LC-MS (APCI) *m*/*z* 381.1 $[M + H]^+$. Analytical HPLC 100% purity.

(3*S*)-5-Methyl-3-(7-oxo-2-(pyridin-3-ylmethyl)-2,4,5,7-tetrahydro-6*H*-pyrazolo[3,4-*c*]pyridin-6-yl)-2,3-dihydro-1,5-benzoxazepin-4(5*H*)-one (16f). Compound **16f** was obtained (9.3%) as a white solid in a manner similar to that described for the synthesis of **16a**. LC-MS (APCI) *m*/*z* 404.3 $[M + H]^+$. ^{1}H NMR (300 MHz, $CDCl_3$) δ 2.72 (1H, dt, *J* = 15.49, 4.72 Hz), 3.12 (1H, tdd, *J* = 10.39, 10.39, 5.29, 4.15 Hz), 3.38 (3H, s), 3.55 (1H, ddd, *J* = 11.99, 10.67, 4.15 Hz), 4.23 (1H, dt, *J* = 11.99, 5.15 Hz), 4.42 (1H, dd, *J* = 10.01, 8.12 Hz), 4.63 (1H, dd, *J* = 11.71, 9.82 Hz), 5.36 (2H, d, *J* = 0.76 Hz), 5.94 (1H, dd, *J* = 11.71, 8.31 Hz), 7.13-7.32 (5H, m), 7.57 (1H, dq, *J* = 7.93, 1.26 Hz), 8.56 (2H, td, *J* = 4.63, 1.70 Hz). Analytical HPLC 98.7% purity.

(3*S*)-5-Methyl-3-(7-oxo-2-(pyridin-2-ylmethyl)-2,4,5,7-tetrahydro-6*H*-pyrazolo[3,4-*c*]pyridin-6-yl)-2,3-dihydro-1,5-benzoxazepin-4(5*H*)-one (16g). Compound **16g** was obtained (11%) in a manner similar to that described for the synthesis of **16d**. LC-MS (APCI) *m*/*z* 404.1 $[M + H]^+$. Analytical HPLC 96.5% purity.

(3*S*)-3-(2-((1,1-Dioxidotetrahydro-2H-thiopyran-4-yl)methyl)-7-oxo-2,4,5,7-tetrahydro-6*H*-pyrazolo[3,4-*c*]pyridin-6-yl)-5-methyl-2,3-dihydro-1,5-benzoxazepin-4(5*H*)-one (16h). Compound **16h** was obtained (9.5%) as a white solid in a manner similar to that described for the synthesis of **16a**. LC-MS (APCI) *m*/*z* 459.2 $[M + H]^+$. ^{1}H NMR (300 MHz, $CDCl_3$) δ 1.80-2.01 (4H, m), 2.24-2.42 (1H, m), 2.75 (1H, dt, *J* = 15.6, 4.8 Hz), 2.85-3.19 (5H, m), 3.38 (3H, s), 3.50-3.62 (1H, m), 4.05 (2H, d, *J* = 7.4 Hz), 4.24 (1H, dt, *J* = 12.0, 5.2 Hz), 4.43 (1H, dd, *J* = 9.9, 8.2 Hz), 4.64 (1H, dd, *J* = 11.5, 10.0 Hz), 5.93 (1H, dd, *J* = 11.7, 8.3 Hz), 7.10-7.34 (5H, m). Analytical HPLC 94.4% purity.

(3*S*)-3-(2-((1,1-Dioxidotetrahydrothiophen-3-yl)methyl)-7-oxo-2,4,5,7-tetrahydro-6*H*-pyrazolo[3,4-*c*]pyridin-6-yl)-5-methyl-2,3-dihydro-1,5-benzoxazepin-4(5*H*)-one (16i). Compound **16i** was obtained (1.4%) as a white solid in a manner similar to that described for the synthesis of **16a**. LC-MS (APCI) *m*/*z* 445.2 $[M + H]^+$. ^{1}H NMR (300 MHz, $CDCl_3$) δ 1.86-2.02 (1H, m), 2.22-2.38 (1H, m), 2.69-2.86 (2H, m), 2.99-3.27 (5H, m), 3.39 (3H, s), 3.56 (1H, td, *J* = 11.1, 4.5 Hz), 4.19-4.34 (3H, m), 4.43 (1H, dd, *J* = 9.6, 8.5 Hz), 4.65 (1H, dd, *J* = 11.7, 9.8 Hz), 5.93 (1H, dd, *J* = 11.7, 8.3 Hz), 7.13-7.30 (5H, m). Analytical HPLC 67.8% purity.

(3*S*)-3-(2-(4-Chloro-2-fluorobenzyl)-7-oxo-2,4,5,7-tetrahydro-6*H*-pyrazolo[3,4-*c*]pyridin-6-yl)-5-methyl-2,3-dihydro-1,5-benzoxazepin-4(5*H*)-one (16j). Compound **16j** was obtained (51%) as a white solid in a manner similar to that described for the synthesis of **16a**. LC-MS (APCI) *m*/*z* 455.2 $[M + H]^+$. ^{1}H NMR (300 MHz, $CDCl_3$) δ 2.72 (1H, dt, *J* = 15.39, 4.77 Hz), 3.11 (1H, tdd, *J* = 10.34, 10.34, 5.38, 4.15 Hz), 3.38 (3H, s), 3.54 (1H, ddd, *J* = 11.80, 10.67, 4.34 Hz), 4.22 (1H, dt, *J* = 11.80, 5.24 Hz), 4.41 (1H, dd, *J* = 10.01, 8.12 Hz), 4.62 (1H, dd, *J* = 11.71, 10.20 Hz), 5.35 (2H, s), 5.93 (1H, dd, *J* = 11.71, 8.31 Hz), 7.05-7.30 (8H, m), 11.35-11.35 (1H, m). ^{13}C NMR (75 MHz, $CDCl_3$) δ 20.5, 35.6, 45.8, 49.5 (d, *J* = 3.9 Hz), 51.2, 74.8, 116.4 (d, *J* = 24.8 Hz), 121.4, 121.8 (d, *J* = 14.9 Hz), 122.6, 123.3, 125.1 (d, *J* = 3.3 Hz), 125.9, 126.0 (d, *J* = 1.1 Hz), 127.2, 131.3 (d, *J* = 4.4 Hz), 135.4 (d, *J* = 9.9 Hz), 136.8, 143.2, 150.0, 160.1 (d, *J* = 250 Hz), 161.2, 169.5. Anal. Calcd for $C_{23}H_{20}ClFN_4O_3$: C, 60.73; H, 4.43; N, 12.32. Found: C, 60.82; H, 4.49; N, 12.20. Analytical HPLC 99.3% purity.

(3*S*)-5-Methyl-3-(2-(2-methylbenzyl)-7-oxo-2,4,5,7-tetrahydro-6*H*-pyrazolo[3,4-*c*]pyridin-6-yl)-2,3-dihydro-1,5-benzoxazepin-4(5*H*)-one (16k). Compound **16k** was obtained (44%) in a manner similar to that described for the synthesis of **16d**. LC-MS (APCI) *m*/*z* 417.1 $[M + H]^+$. Analytical HPLC 98.8% purity.

(3*S*)-3-(2-(2-Chlorobenzyl)-7-oxo-2,4,5,7-tetrahydro-6*H*-pyrazolo[3,4-*c*]pyridin-6-yl)-5-methyl-2,3-dihydro-1,5-benzoxazepin-4(5*H*)-one (16l). Compound **16l** was obtained (46%) in a manner similar to that described for the synthesis of **16d**. LC-MS (APCI) *m*/*z* 437.1 $[M + H]^+$. ^{1}H NMR (400

MHz, DMSO-d_6) δ 2.65-2.78 (1H, m), 2.80-2.92 (1H, m), 3.30 (3H, s), 3.52-3.63 (1H, m), 3.93-4.04 (1H, m), 4.32 (1H, dd, J = 10.0, 7.8 Hz), 4.83 (1H, dd, J = 12.0, 10.3 Hz), 5.47 (2H, s), 5.57 (1H, dd, J = 11.9, 7.9 Hz), 6.99-7.07 (1H, m), 7.21-7.40 (5H, m), 7.45-7.54 (2H, m), 7.75 (1H, s). Analytical HPLC 100% purity.

(3*S*)-3-(2-(3-Chlorobenzyl)-7-oxo-2,4,5,7-tetrahydro-6*H*-pyrazolo[3,4-*c*]pyridin-6-yl)-5-methyl-2,3-dihydro-1,5-benzoxazepin-4(5*H*)-one (16m). Compound **16m** was obtained (29%) in a manner similar to that described for the synthesis of **16d**. LC-MS (APCI) *m*/*z* 437.1 $[M + H]^+$. Analytical HPLC 100% purity.

(3*S*)-3-(2-(4-Chlorobenzyl)-7-oxo-2,4,5,7-tetrahydro-6*H*-pyrazolo[3,4-*c*]pyridin-6-yl)-5-methyl-2,3-dihydro-1,5-benzoxazepin-4(5*H*)-one (16n). Compound **16n** was obtained (7%) as a white solid in a manner similar to that described for the synthesis of **14**. LC-MS (APCI) *m*/*z* 437.2 $[M + H]^+$. ^{1}H NMR (400 MHz, DMSO-d_6) δ 2.65-2.75 (1H, m), 2.80-2.90 (1H, m), 3.30 (3H, s, overlap with water signal), 3.54-3.65 (1H, m), 3.90-4.00 (1H, m), 4.26-4.36 (1H, m), 4.76-4.86 (1H, m), 5.36 (2H, s), 5.52-5.62 (1H, m), 7.20-7.35 (5H, m), 7.41 (2H, d, J = 8.4 Hz), 7.47-7.54 (1H, m), 7.77 (1H, s). ^{13}C NMR (75 MHz, $CDCl_3$) δ 20.5, 35.6, 45.8, 51.2, 56.0, 74.8, 121.4, 122.6, 123.3, 125.7, 125.9, 127.2, 129.1, 129.2, 134.3, 136.7, 143.0, 150.0, 161.3, 169.5. Anal. Calcd for $C_{23}H_{21}ClN_4O_3$: C, 63.23; H, 4.84; N, 12.82. Found: C, 62.83; H, 4.84; N, 12.52. Analytical HPLC 99.6% purity.

(3*S*)-5-Methyl-3-(2-(4-(methylsulfonyl)benzyl)-7-oxo-2,4,5,7-tetrahydro-6*H*-pyrazolo[3,4-*c*]pyridin-6-yl)-2,3-dihydro-1,5-benzoxazepin-4(5*H*)-one (16o). Compound **16o** was obtained (10%) as a

white solid in a manner similar to that described for the synthesis of **16a**. LC-MS (APCI) *m*/*z* 481.2 $[M + H]^+$. ^1H NMR (300 MHz, $CDCl_3$) δ 2.75 (1H, dt, *J* = 15.5, 4.7 Hz), 3.00-3.07 (3H, m), 3.14 (1H, ddd, *J* = 15.4, 10.7, 4.5 Hz), 3.39 (3H, s), 3.57 (1H, td, *J* = 11.2, 4.3 Hz), 4.25 (1H, dt, *J* = 12.0, 5.1 Hz), 4.43 (1H, dd, *J* = 9.8, 8.3 Hz), 4.64 (1H, dd, *J* = 11.7, 10.2 Hz), 5.43 (2H, s), 5.94 (1H, dd, *J* = 11.5, 8.1 Hz), 7.14-7.30 (5H, m), 7.38 (2H, d, *J* = 8.3 Hz), 7.90 (2H, d, *J* = 8.3 Hz). Analytical HPLC 99.3% purity.

(3*S*)-5-Methyl-3-(2-(3-(methylsulfonyl)benzyl)-7-oxo-2,4,5,7-tetrahydro-6*H*-pyrazolo[3,4-*c*]pyridin-6-yl)-2,3-dihydro-1,5-benzoxazepin-4(5*H*)-one (16p). Compound **16p** was obtained (34%) as a white solid in a manner similar to that described for the synthesis of **16a**. LC-MS (APCI) *m*/*z* 481.2 $[M + H]^+$. ^1H NMR (300 MHz, $CDCl_3$) δ 2.75 (1H, dt, *J* = 15.7, 4.6 Hz), 3.04 (3H, s), 3.08-3.23 (1H, m), 3.39 (3H, s), 3.58 (1H, td, *J* = 11.3, 4.2 Hz), 4.25 (1H, dt, *J* = 12.1, 5.3 Hz), 4.44 (1H, dd, *J* = 10.0, 8.1 Hz), 4.64 (1H, dd, *J* = 11.7, 10.2 Hz), 5.43 (2H, d, *J* = 1.9 Hz), 5.94 (1H, dd, *J* = 11.7, 7.9 Hz), 7.13-7.30 (5H, m), 7.45-7.63 (2H, m), 7.80 (1H, s), 7.85-7.92 (1H, m). ^{13}C NMR (75 MHz, $CDCl_3$) δ 20.5, 35.6, 44.5, 45.7, 51.3, 55.8, 74.8, 121.6, 122.6, 123.2, 125.9, 126.2, 126.3, 127.2, 130.1, 132.9, 136.7, 137.8, 141.2, 143.5, 149.9, 159.7, 161.2, 169.5. Analytical HPLC 99.1% purity.

4-((6-((3*S*)-5-Methyl-4-oxo-2,3,4,5-tetrahydro-1,5-benzoxazepin-3-yl)-7-oxo-4,5,6,7-tetrahydro-2*H*-pyrazolo[3,4-*c*]pyridin-2-yl)methyl)benzonitrile (16q). Compound **16q** was obtained (17%) in a manner similar to that described for the synthesis of **16d**. LC-MS (APCI) *m*/*z* 428.1 $[M + H]^+$. Analytical HPLC 100% purity.

2-((6-((3*S*)-5-Methyl-4-oxo-2,3,4,5-tetrahydro-1,5-benzoxazepin-3-yl)-7-oxo-4,5,6,7-tetrahydro-2*H*-pyrazolo[3,4-*c*]pyridin-2-yl)methyl)benzonitrile (16r). Compound **16r** was obtained (37%) in a manner similar to that described for the synthesis of **16d**. LC-MS (APCI) *m*/*z* 428.1 $[M + H]^+$. Analytical HPLC 100% purity.

3-((6-((3*S*)-5-Methyl-4-oxo-2,3,4,5-tetrahydro-1,5-benzoxazepin-3-yl)-7-oxo-4,5,6,7-tetrahydro-2*H*-pyrazolo[3,4-*c*]pyridin-2-yl)methyl)benzonitrile (16s). Compound **16s** was obtained (21%) in a manner similar to that described for the synthesis of **16d**. LC-MS (APCI) *m*/*z* 428.1 $[M + H]^+$. Analytical HPLC 100% purity.

3-Chloro-2-((6-((3*S*)-5-methyl-4-oxo-2,3,4,5-tetrahydro-1,5-benzoxazepin-3-yl)-7-oxo-4,5,6,7-tetrahydro-2*H*-pyrazolo[3,4-*c*]pyridin-2-yl)methyl)benzonitrile (16t). Compound **16t** was obtained (41%) as a white solid in a manner similar to that described for the synthesis of **16a**. LC-MS (APCI) *m*/*z* 462.2 $[M + H]^+$. ^{1}H NMR (300 MHz, $CDCl_3$) δ 2.71 (1H, dt, *J* = 15.5, 4.7 Hz), 3.10 (1H, ddd, *J* = 15.6, 10.7, 4.7 Hz), 3.37 (3H, s), 3.53 (1H, td, *J* = 11.2, 4.3 Hz), 4.21 (1H, dt, *J* = 11.7, 5.3 Hz), 4.39 (1H, dd, *J* = 9.8, 8.3 Hz), 4.62 (1H, dd, *J* = 11.7, 9.8 Hz), 5.67 (2H, s), 5.92 (1H, dd, *J* = 11.7, 8.3 Hz), 7.12-7.26 (5H, m), 7.40-7.49 (1H, m), 7.62-7.71 (2H, m). ^{13}C NMR (75 MHz, $CDCl_3$) δ 20.5, 35.6, 45.7, 51.1, 52.2, 74.8, 115.9, 116.5, 121.0, 122.6, 123.2, 125.8, 126.1, 127.2, 130.6, 131.9, 134.9, 135.7, 136.8, 137.1, 143.3, 149.9, 161.1, 169.5. Analytical HPLC 93.9% purity.

3-Fluoro-4-((6-((3*S*)-5-methyl-4-oxo-2,3,4,5-tetrahydro-1,5-benzoxazepin-3-yl)-7-oxo-4,5,6,7-tetrahydro-2*H*-pyrazolo[3,4-*c*]pyridin-2-yl)methyl)benzonitrile (16u). Compound **16u** was obtained

(13%) as a white solid in a manner similar to that described for the synthesis of **16a**. LC-MS (APCI) *m*/*z* 446.2 $[M + H]^+$. ^{1}H NMR (300 MHz, $CDCl_3$) δ 2.75 (1H, dt, *J* = 15.5, 4.9 Hz), 3.13 (1H, ddd, *J* = 15.5, 10.6, 4.5 Hz), 3.38 (3H, s), 3.50-3.64 (1H, m), 4.24 (1H, dt, *J* = 12.1, 5.3 Hz), 4.42 (1H, dd, *J* = 10.2, 8.3 Hz), 4.64 (1H, dd, *J* = 11.5, 10.0 Hz), 5.44 (2H, s), 5.93 (1H, dd, *J* = 11.5, 8.1 Hz), 7.12-7.27 (5H, m), 7.31 (1H, s), 7.35-7.43 (2H, m). ^{13}C NMR (75 MHz, $CDCl_3$) δ 20.5, 35.6, 45.7, 49.6 (d, *J* = 4.4 Hz), 51.3, 74.8, 113.8 (d, *J* = 9.4 Hz), 117.1 (d, *J* = 3.3 Hz), 119.2 (d, *J* = 24.8 Hz), 121.6, 122.6, 123.3, 125.9, 126.5, 127.2, 128.7 (d, *J* = 4.4 Hz), 129.1 (d, *J* = 14.9 Hz), 131.1 (d, *J* = 4.4 Hz), 136.7, 143.8, 149.9, 159.5 (d, *J* = 251 Hz), 161.0, 169.4. Anal. Calcd for $C_{24}H_{20}FN_5O_3$: C, 64.71; H, 4.53; N, 15.72. Found: C, 64.50; H, 4.53; N, 15.56. Analytical HPLC 99.1% purity.

(3*S*)-3-(2-(4-Methoxybenzyl)-7-oxo-2,4,5,7-tetrahydro-6*H*-pyrazolo[3,4-*c*]pyridin-6-yl)-5-methyl-2,3-dihydro-1,5-benzoxazepin-4(5*H*)-one (16v). Compound **16v** was obtained (65%) as a white solid in a manner similar to that described for the synthesis of **16a**. LC-MS (APCI) *m*/*z* 433.2 $[M + H]^+$. ^{1}H NMR (300 MHz, $CDCl_3$) δ 2.68 (1H, dt, *J* = 15.5, 4.7 Hz), 3.02-3.18 (1H, m), 3.38 (3H, s), 3.46-3.60 (1H, m), 3.79 (3H, s), 4.15-4.28 (1H, m), 4.42 (1H, dd, *J* = 9.8, 8.3 Hz), 4.62 (1H, dd, *J* = 11.7, 10.2 Hz), 5.27 (2H, s), 5.95 (1H, dd, *J* = 11.7, 8.3 Hz), 6.81-7.01 (2H, m), 7.10 (1H, s), 7.12-7.30 (6H, m). ^{13}C NMR (75 MHz, $CDCl_3$) δ 20.5, 35.6, 45.8, 51.2, 55.3, 56.3, 74.8, 114.2, 121.2, 122.6, 123.3, 125.4, 125.8, 127.2, 127.7, 129.6, 136.8, 142.5, 150.0, 159.6, 161.5, 169.6. Analytical HPLC 98.6% purity.

(3*S*)-3-(2-(Cyclopentylmethyl)-7-oxo-2,4,5,7-tetrahydro-6*H*-pyrazolo[3,4-*c*]pyridin-6-yl)-5-meth

yl-2,3-dihydro-1,5-benzoxazepin-4(5*H*)-one (16w). Compound **16w** was obtained (21%) in a manner similar to that described for the synthesis of **16d**. LC-MS (APCI) *m*/*z* 395.1 $[M + H]^+$. Analytical HPLC 100% purity.

(3*S*)-3-(2-(1,4-Dioxan-2-ylmethyl)-7-oxo-2,4,5,7-tetrahydro-6*H*-pyrazolo[3,4-*c*]pyridin-6-yl)-5-methyl-2,3-dihydro-1,5-benzoxazepin-4(5*H*)-one (16x). Compound **16x** was obtained (22%) in a manner similar to that described for the synthesis of **16d**. LC-MS (APCI) *m*/*z* 413.1 $[M + H]^+$. Analytical HPLC 100% purity.

(3*S*)-5-Methyl-3-(7-oxo-2-(tetrahydro-2*H*-pyran-3-ylmethyl)-2,4,5,7-tetrahydro-6*H*-pyrazolo[3,4-*c*]pyridin-6-yl)-2,3-dihydro-1,5-benzoxazepin-4(5*H*)-one (16y). Compound **16y** was obtained (29%) as a white solid in a manner similar to that described for the synthesis of **16a**. LC-MS (APCI) *m*/*z* 411.3 $[M + H]^+$. ^{1}H NMR (300 MHz, $CDCl_3$) δ 1.21-1.38 (1H, m), 1.46-1.80 (3H, m), 2.14-2.36 (1H, m), 2.73 (1H, dt, *J* = 15.49, 4.91 Hz), 3.04-3.28 (2H, m), 3.38 (3H, s), 3.42-3.63 (2H, m), 3.63-3.82 (2H, m), 3.98-4.17 (2H, m), 4.23 (1H, dt, *J* = 11.80, 5.24 Hz), 4.43 (1H, dd, *J* = 9.82, 8.31 Hz), 4.63 (1H, dd, *J* = 11.52, 10.01 Hz), 5.94 (1H, dd, *J* = 11.52, 8.12 Hz), 7.13-7.26 (5H, m). ^{13}C NMR (75 MHz, $CDCl_3$) δ 19.5, 23.3, 25.7, 34.6, 35.6, 44.8, 50.2, 53.5, 67.5, 69.3, 73.8, 119.6, 121.6, 122.2, 124.8, 125.3, 126.1, 135.8, 141.9, 149.0, 160.3, 168.6. Analytical HPLC 98.6% purity.

(3*S*)-5-Methyl-3-(7-oxo-2-(pyrazin-2-ylmethyl)-2,4,5,7-tetrahydro-6*H*-pyrazolo[3,4-*c*]pyridin-6-yl)-2,3-dihydro-1,5-benzoxazepin-4(5*H*)-one (16z). Compound **16z** was obtained (15%) as a white solid in a manner similar to that described for the synthesis of **16a**. LC-MS (APCI) *m*/*z* 405.2 [M +

H]$^+$. ^{1}H NMR (300 MHz, $CDCl_3$) δ 2.76 (1H, dt, *J* = 15.5, 4.5 Hz), 3.15 (1H, ddd, *J* = 15.7, 11.1, 4.9 Hz), 3.38 (3H, s), 3.45-3.64 (1H, m), 4.24 (1H, dt, *J* = 11.9, 5.0 Hz), 4.38-4.48 (1H, m), 4.63 (1H, dd, *J* = 11.7, 10.2 Hz), 5.39-5.58 (2H, m), 5.94 (1H, dd, *J* = 11.5, 8.1 Hz), 7.13-7.25 (4H, m), 7.41 (1H, s), 8.48 (1H, s), 8.53 (2H, s). Analytical HPLC 99.5% purity.

(3*S*)-3-(2-(3-Furylmethyl)-7-oxo-2,4,5,7-tetrahydro-6*H*-pyrazolo[3,4-*c*]pyridin-6-yl)-5-methyl-2, 3-dihydro-1,5-benzoxazepin-4(5*H*)-one (16aa). Compound **16aa** was obtained (11%) in a manner similar to that described for the synthesis of **16d**. LC-MS (APCI) *m*/*z* 393.1 [M + H]$^+$. Analytical HPLC 98.0% purity.

(3*S*)-5-Methyl-3-(2-((3-methyloxetan-3-yl)methyl)-7-oxo-2,4,5,7-tetrahydro-6*H*-pyrazolo[3,4-*c*] pyridin-6-yl)-2,3-dihydro-1,5-benzoxazepin-4(5*H*)-one (16ab). Compound **16ab** was obtained (27%) as a white solid in a manner similar to that described for the synthesis of **16a**. LC-MS (APCI) *m*/*z* 397.3 [M + H]$^+$. ^{1}H NMR (300 MHz, $CDCl_3$) δ 1.24 (3H, s), 2.74 (1H, dt, *J* = 15.49, 4.91 Hz), 3.04-3.20 (1H, m), 3.38 (3H, s), 3.56 (1H, ddd, *J* = 11.90, 10.58, 4.34 Hz), 4.18-4.31 (1H, m), 4.36 (4H, dd, *J* = 6.42, 3.02 Hz), 4.42 (1H, dd, *J* = 9.82, 8.31 Hz), 4.57-4.74 (3H, m), 5.93 (1H, dd, *J* = 11.71, 7.93 Hz), 7.12-7.32 (5H, m). ^{13}C NMR (75 MHz, $CDCl_3$) δ 20.4, 21.8, 35.6, 40.6, 45.7, 51.1, 59.1, 74.8, 80.1, 80.1, 120.7, 122.6, 123.2, 125.9, 126.5, 127.2, 136.8, 143.1, 149.9, 161.3, 169.6. Anal. Calcd for $C_{21}H_{24}N_4O_4$: C, 63.62; H, 6.10; N, 14.13. Found: C, 63.28; H, 6.07; N, 13.89. Analytical HPLC 98.6% purity.

(3*S*)-5-Methyl-3-(2-(1,3-oxazol-2-ylmethyl)-7-oxo-2,4,5,7-tetrahydro-6*H*-pyrazolo[3,4-*c*]pyridin

-6-yl)-2,3-dihydro-1,5-benzoxazepin-4(5*H*)-one (16ac). Compound **16ac** was obtained (37%) in a manner similar to that described for the synthesis of **16d**. LC-MS (APCI) *m*/*z* 394.1 $[M + H]^+$. Analytical HPLC 100% purity.

(3*S*)-5-Methyl-3-(2-((1-methylcyclobutyl)methyl)-7-oxo-2,4,5,7-tetrahydro-6*H*-pyrazolo[3,4-c]pyridin-6-yl)-2,3-dihydro-1,5-benzoxazepin-4(5*H*)-one (16ad). Compound **16ad** was obtained (18%) as a white solid in a manner similar to that described for the synthesis of **16a**. LC-MS (APCI) *m*/*z* 395.3 $[M + H]^+$. ^{1}H NMR (300 MHz, $CDCl_3$) δ 1.07 (3H, s), 1.64-2.12 (6H, m), 2.74 (1H, dt, *J* = 15.5, 4.9 Hz), 3.05-3.21 (1H, m), 3.38 (3H, s), 3.47-3.66 (1H, m), 4.03-4.17 (2H, m), 4.23 (1H, dt, *J* = 12.0, 5.1 Hz), 4.43 (1H, dd, *J* = 10.0, 8.1 Hz), 4.64 (1H, dd, *J* = 11.7, 9.8 Hz), 5.96 (1H, dd, *J* = 11.7, 8.3 Hz), 7.10-7.25 (5H, m). ^{13}C NMR (75 MHz, $CDCl_3$) δ 14.8, 20.5, 24.7, 31.1, 31.1, 35.6, 39.6, 45.8, 51.1, 62.2, 74.9, 120.5, 122.6, 123.2, 125.8, 126.1, 127.1, 136.8, 142.2, 150.0, 161.5, 169.7. Analytical HPLC 99.4% purity.

(3*S*)-5-Methyl-3-(7-oxo-2-(tetrahydrofuran-3-ylmethyl)-2,4,5,7-tetrahydro-6*H*-pyrazolo[3,4-*c*]pyridin-6-yl)-2,3-dihydro-1,5-benzoxazepin-4(5*H*)-one (16ae). Compound **16ae** was obtained (15%) as a white solid in a manner similar to that described for the synthesis of **16a**. LC-MS (APCI) *m*/*z* 397.3 $[M + H]^+$. ^{1}H NMR (300 MHz, $CDCl_3$) δ 1.56-1.71 (1H, m), 1.93-2.09 (1H, m), 2.74 (1H, dt, *J* = 15.39, 4.77 Hz), 2.89 (1H, td, *J* = 7.37, 2.64 Hz), 3.12 (1H, ddd, *J* = 15.49, 10.58, 4.91 Hz), 3.38 (3H, s), 3.50-3.62 (2H, m), 3.69-3.79 (2H, m), 3.84-3.95 (1H, m), 4.08-4.17 (2H, m), 4.24 (1H, dt, *J* = 11.99, 5.15 Hz), 4.42 (1H, dd, *J* = 9.82, 8.31 Hz), 4.64 (1H, dd, *J* = 11.71, 10.20 Hz), 5.94

(1H, dd, *J* = 11.52, 8.12 Hz), 7.13 - 7.26 (5H, m). ^{13}C NMR (75 MHz, $CDCl_3$) δ 20.5, 29.6, 35.6, 40.0, 45.8, 51.2, 55.3, 67.6, 70.8, 74.8, 120.6, 120.7, 122.6, 123.2, 125.9, 126.0, 126.0, 127.2, 136.8, 143.1, 149.9, 161.3, 169.6. Analytical HPLC 98.6% purity.

(3*S*)-3-(2-((3,3-Difluorocyclobutyl)methyl)-7-oxo-2,4,5,7-tetrahydro-6*H*-pyrazolo[3,4-*c*]pyridin-6-yl)-5-methyl-2,3-dihydro-1,5-benzoxazepin-4(5*H*)-one (16af). Compound **16af** was obtained (16%) in a manner similar to that described for the synthesis of **16d**. LC-MS (APCI) *m*/*z* 417.1 [M + H]$^+$. Analytical HPLC 100% purity.

(3*S*)-5-Methyl-3-(7-oxo-2-(pyrimidin-2-ylmethyl)-2,4,5,7-tetrahydro-6*H*-pyrazolo[3,4-*c*]pyridin-6-yl)-2,3-dihydro-1,5-benzoxazepin-4(5*H*)-one (16ag). Compound **16ag** was obtained (4%) in a manner similar to that described for the synthesis of **16d**. LC-MS (APCI) *m*/*z* 405.1 [M + H]$^+$. ^{13}C NMR (75 MHz, $CDCl_3$) δ 20.6, 35.6, 45.8, 51.2, 58.4, 74.8, 120.1, 121.1, 122.6, 123.3, 125.9, 127.2, 127.3, 136.8, 143.3, 150.0, 157.5, 161.3, 164.9, 169.5. Anal. Calcd for $C_{21}H_{20}N_6O_3$ + 0.6 H_2O: C, 60.74; H, 5.15; N, 20.24. Found: C, 60.44; H, 4.93; N, 20.24. Analytical HPLC 96.5% purity.

(3*S*)-3-(2-(3-Methoxybenzyl)-7-oxo-2,4,5,7-tetrahydro-6*H*-pyrazolo[3,4-*c*]pyridin-6-yl)-5-methyl-2,3-dihydro-1,5-benzoxazepin-4(5*H*)-one (16ah). Compound **16ah** was obtained (29%) as a white solid in a manner similar to that described for the synthesis of **16a**. LC-MS (APCI) *m*/*z* 433.2 [M + H]$^+$. ^{1}H NMR (300 MHz, $CDCl_3$) δ 2.70 (1H, dt, *J* = 15.4, 4.8 Hz), 2.99-3.18 (1H, m), 3.38 (3H, s), 3.54 (1H, td, *J* = 11.3, 4.2 Hz), 3.77 (3H, s), 4.22 (1H, dt, *J* = 12.0, 5.1 Hz), 4.42 (1H, dd, *J* = 9.8, 8.3 Hz), 4.63 (1H, dd, *J* = 11.5, 10.0 Hz), 5.31 (2H, s), 5.96 (1H, dd, *J* = 11.7, 8.3 Hz), 6.73-6.88 (3H, m),

7.10-7.31 (6H, m). ^{13}C NMR (75 MHz, $CDCl_3$) δ 20.6, 35.6, 45.8, 51.2, 55.3, 56.7, 74.8, 113.6, 113.9, 120.3, 121.3, 122.6, 123.3, 125.7, 125.9, 127.2, 129.9, 136.8, 137.2, 142.7, 150.0, 160.0, 161.4, 169.6. Anal. Calcd for $C_{24}H_{24}N_4O_4$ + 0.2 H_2O: C, 66.10; H, 5.64; N, 12.85. Found: C, 65.97; H, 5.59; N, 12.55. Analytical HPLC 98.4% purity.

(3*S*)-3-(2-(Cyclopropylmethyl)-7-oxo-2,4,5,7-tetrahydro-6*H*-pyrazolo[3,4-*c*]pyridin-6-yl)-5-methyl-2,3-dihydro-1,5-benzoxazepin-4(5*H*)-one (16ai). Compound **16ai** was obtained (20%) in a manner similar to that described for the synthesis of **16d**. LC-MS (APCI) *m*/*z* 367.1 $[M + H]^+$. Analytical HPLC 100% purity.

(3*S*)-5-Methyl-3-(7-oxo-2-(2-phenylethyl)-2,4,5,7-tetrahydro-6*H*-pyrazolo[3,4-*c*]pyridin-6-yl)-2,3-dihydro-1,5-benzoxazepin-4(5*H*)-one (16aj). Compound **16aj** was obtained (25%) in a manner similar to that described for the synthesis of **16d**. LC-MS (APCI) *m*/*z* 417.1 $[M + H]^+$. Analytical HPLC 100% purity.

(3*S*)-3-(2-Benzyl-3-methyl-7-oxo-2,4,5,7-tetrahydro-6*H*-pyrazolo[3,4-*c*]pyridin-6-yl)-5-methyl-2,3-dihydro-1,5-benzoxazepin-4(5*H*)-one (17). To a solution of **60** (25 mg, 0.05 mmol), $Pd(PPh_3)_4$ (6.00 mg, 5.19 μmol) and 2,4,6-trimethyl-1,3,5,2,4,6-trioxatriborinane (commercially available, 6.52 mg, 0.05 mmol) in THF (5 mL, 0.05 mmol) was added potassium hydroxide (1.039 mL, 0.10 mmol) and at room temperature. The mixture was stirred at 100 °C under Ar for 1 h. The mixture was stirred at room temperature under Ar overnight. The mixture was quenched with water at room temperature and extracted with EtOAc. The organic layer was separated, washed with brine, dried

over Na_2SO_4 and concentrated under reduced pressure. The residue was purified by column chromatography (silica gel, eluted with 50% - 70%EtOAc in hexane). The residue was purified by column chromatography (NH silica gel, eluted with 70% - 90%EtOAc in hexane). The residue was purified by preparative HPLC (L-Column 2 ODS, eluted with H2O in acetonitrile containing 0.1% TFA). The desired fraction was concentrated under reduced pressure. and neutralized with saturated $NaHCO_3$ aq. and extracted with EtOAc. The organic layer was separated, dried over Na_2SO_4 and concentrated under reduced pressure. The residue was purified by column chromatography (NH silica gel, eluted with 50% - 70% EtOAc in hexane). The residue was purified by column chromatography (NH silica gel, eluted with 70% - 90% EtOAc in hexane) to give **17** (2.00 mg, 9 %). LC-MS (APCI) *m*/*z* 417.3 $[M + H]^+$. ^1H NMR (300 MHz, $CDCl_3$) δ 2.10 (3H, s), 2.60 (1H, dt, *J* = 15.3, 4.8 Hz), 3.01 (1H, ddd, *J* = 15.2, 10.4, 4.7 Hz), 3.38 (3H, s), 3.55 (1H, ddd, *J* = 11.8, 10.5, 4.3 Hz), 4.24 (1H, dt, *J* = 11.9, 5.2 Hz), 4.43 (1H, dd, *J* = 9.9, 8.2 Hz), 4.64 (1H, dd, *J* = 11.5, 10.0 Hz), 5.35 (2H, s), 5.97 (1H, dd, *J* = 11.6, 8.2 Hz), 7.07-7.36 (9H, m). Analytical HPLC 99.1% purity.

(3*S*)-3-(2-Benzyl-3-chloro-7-oxo-2,4,5,7-tetrahydro-6*H*-pyrazolo[3,4-*c*]pyridin-6-yl)-5-methyl-2, 3-dihydro-1,5-benzoxazepin-4(5*H*)-one (18). Compound **18** was obtained (23%) as a white solid in a manner similar to that described for the synthesis of **34**. LC-MS (APCI) *m*/*z* 432.7 $[M + H]^+$. ^1H NMR (300 MHz, $CDCl_3$) δ 2.66 (1H, dt, *J* = 15.7, 4.6 Hz), 3.06 (1H, ddd, *J* = 15.5, 10.4, 5.1 Hz), 3.38 (3H, s), 3.56 (1H, ddd, *J* = 12.0, 10.5, 4.3 Hz), 4.25 (1H, dt, *J* = 12.0, 5.1 Hz), 4.42 (1H, dd, *J* = 9.8, 8.3 Hz), 4.62 (1H, dd, *J* = 11.5, 10.0 Hz), 5.39 (2H, s), 5.92 (1H, dd, *J* = 11.7, 8.3 Hz), 7.13-7.38

(9H, m). ^{13}C NMR (75 MHz, $CDCl_3$) δ 19.8, 35.6, 45.4, 51.4, 53.8, 74.7, 118.1, 122.6, 123.2, 123.3, 125.9, 127.2, 127.7, 128.2, 128.7, 135.1, 136.7, 142.3, 149.9, 160.7, 169.4. Anal. Calcd for $C_{23}H_{21}ClN_4O_3$ + 0.5 H_2O: C, 61.95; H, 4.97; N, 12.56. Found: C, 62.36; H, 5.35; N, 12.56. Analytical HPLC 100% purity.

2-Benzyl-6-((3*S*)-5-methyl-4-oxo-2,3,4,5-tetrahydro-1,5-benzoxazepin-3-yl)-7-oxo-4,5,6,7-tetrahydro-2*H*-pyrazolo[3,4-*c*]pyridine-3-carbonitrile (19). To a solution of **60** (15 mg, 0.03 mmol) in *N*,*N*-dimethylformamide (5 mL, 0.03 mmol) was added $Pd(PPh_3)_4$ (3.60 mg, 3.12 μmol) and dicyanozinc (7.32 mg, 0.06 mmol) at room temperature. The mixture was stirred at 100 °C under Ar for 1 h. The mixture was quenched with water at room temperature and extracted with EtOAc. The organic layer was separated, washed with water and brine, dried over Na_2SO_4 and concentrated under reduced pressure. The residue was purified by column chromatography (silica gel, eluted with 50% - 100% EtOAc in hexane). The residue was purified by column chromatography (NH silica gel, eluted with 50% - 75% EtOAc in hexane) to give **19** (12.0 mg, 90%). LC-MS (APCI) *m*/*z* 428.2 $[M + H]^+$. ^{1}H NMR (300 MHz, $CDCl_3$) δ 2.86 (1H, dt, *J* = 16.2, 4.7 Hz), 3.24 (1H, ddd, *J* = 16.1, 10.6, 5.1 Hz), 3.38 (3H, s), 3.57 (1H, ddd, *J* = 12.1, 10.6, 4.2 Hz), 4.29 (1H, dt, *J* = 12.3, 5.0 Hz), 4.41 (1H, dd, *J* = 9.8, 8.3 Hz), 4.62 (1H, dd, *J* = 11.7, 9.8 Hz), 5.50 (2H, s), 5.88 (1H, dd, *J* = 11.5, 8.1 Hz), 7.11-7.42 (9H, m). ^{13}C NMR (75 MHz, $CDCl_3$) δ 20.3, 35.6, 45.0, 51.4, 56.6, 74.6, 109.6, 111.7, 122.6, 123.3, 126.0, 127.3, 128.3, 129.0, 129.1, 129.3, 134.0, 136.6, 142.9, 149.9, 159.6, 169.1. Analytical HPLC 96.3% purity.

2-Benzyl-6-((3*S*)-5-methyl-4-oxo-2,3,4,5-tetrahydro-1,5-benzoxazepin-3-yl)-7-oxo-4,5,6,7-tetrahydro-2*H*-pyrazolo[3,4-*c*]pyridine-3-carboxamide (20). To a solution of **19** (40 mg, 0.09 mmol) and potassium carbonate (15.52 mg, 0.11 mmol) in DMSO (3 mL) was added H_2O_2 (0.041 mL, 0.47 mmol) at room temperature. The mixture was stirred at room temperature under air for 1 h. The mixture was quenched with water at room temperature and extracted with EtOAc. The organic layer was separated, washed with water and brine, dried over Na_2SO_4 and concentrated under reduced pressure. The residue was purified by column chromatography (silica gel, eluted with 80% - 100% EtOAc in hexane). The obtained solids were triturated in EtOAc and collected by filtration to give **20** (25.0 mg, 60%) as a white solid. LC-MS (APCI) *m*/*z* 446.3 $[M + H]^+$. ^{1}H NMR (300 MHz, DMSO-d_6) δ 2.79-2.92 (1H, m), 2.99-3.12 (1H, m), 3.30 (3H, s), 3.52-3.67 (1H, m), 3.94-4.08 (1H, m), 4.34 (1H, dd, *J* = 10.0, 7.7 Hz), 4.85 (1H, dd, *J* = 11.9, 10.4 Hz), 5.55 (1H, dd, *J* = 12.1, 7.9 Hz), 5.63 (2H, s), 7.12-7.20 (2H, m), 7.21-7.37 (6H, m), 7.50 (1H, dd, *J* = 7.6, 1.9 Hz), 7.70 (1H, brs), 7.79 (1H, brs). ^{13}C NMR (75 MHz, $CDCl_3$) δ 21.5, 35.6, 45.1, 51.3, 55.6, 74.7, 121.9, 122.6, 123.2, 126.0, 127.4, 128.0, 128.0, 128.5, 131.0, 136.3, 136.6, 141.6, 149.9, 160.6, 160.8, 169.4. Analytical HPLC 100% purity.

(3*S*)-3-(2-Benzyl-3-chloro-7-oxo-2,4,5,7-tetrahydro-6*H*-pyrazolo[3,4-*c*]pyridin-6-yl)-5-methyl-4-oxo-2,3,4,5-tetrahydro-1,5-benzoxazepine-7-carbonitrile (21). Compound **21** was obtained (29%) as a white solid in a manner similar to that described for the synthesis of **34**. LC-MS (APCI) *m*/*z* 462.2 $[M + H]^+$. ^{1}H NMR (300 MHz, $CDCl_3$) δ 2.68 (1H, dt, *J* = 15.7, 4.8 Hz), 3.05 (1H, ddd, *J* =

15.6, 10.3, 5.1 Hz), 3.39 (3H, s), 3.48-3.61 (1H, m), 4.15-4.28 (1H, m), 4.45 (1H, dd, *J* = 9.8, 7.6 Hz), 4.73 (1H, dd, *J* = 11.7, 10.2 Hz), 5.40 (2H, s), 5.89 (1H, dd, *J* = 11.9, 7.7 Hz), 7.21-7.37 (6H, m), 7.48-7.58 (2H, m). ^{13}C NMR (75 MHz, $CDCl_3$) δ 19.7, 35.8, 45.3, 51.0, 53.9, 75.0, 109.7, 117.7, 118.0, 123.4, 124.1, 127.1, 127.7, 128.2, 128.8, 131.0, 135.0, 137.8, 141.9, 153.3, 160.7, 169.0. Anal. Calcd for $C_{24}H_{20}ClN_5O_3$ + 0.2 H_2O: C, 61.92; H, 4.42; N, 15.04. Found: C, 61.92; H, 4.44; N, 14.79. Analytical HPLC 100% purity.

(3*S*)-3-(2-Benzyl-3-chloro-7-oxo-2,4,5,7-tetrahydro-6*H*-pyrazolo[3,4-*c*]pyridin-6-yl)-5-methyl-4-oxo-2,3,4,5-tetrahydro-1,5-benzoxazepine-8-carbonitrile (22). To a solution of **72a** (1.08 g, 2.09 mmol) and dicyanozinc (0.369 g, 3.14 mmol) in DMF (20 mL) was added $Pd(PPh_3)_4$ (0.484 g, 0.42 mmol) at room temperature. The mixture was stirred at 100 °C under Ar for 2 h. The mixture was quenched with water at room temperature and extracted with EtOAc. The organic layer was separated, washed with water and brine, dried over Na2SO4 and concentrated under reduced pressure. The residue was purified by column chromatography (silica gel, eluted with 40% - 55%EtOAc in hexane). The obtained oil was triturated in Et2O-IPE-EtOAc and the formed solid was collected by filtration to give **22** (0.600 g, 1.299 mmol, 62.0 %) as a white solid. LC-MS (APCI) *m*/*z* 462.2 $[M + H]^+$. ^{1}H NMR (300 MHz, $CDCl_3$) δ 2.69 (1H, dt, *J* = 15.7, 4.8 Hz), 3.05 (1H, ddd, *J* = 15.6, 10.3, 5.1 Hz), 3.39 (3H, s), 3.51-3.61 (1H, m), 4.15-4.27 (1H, m), 4.45 (1H, dd, *J* = 10.2, 7.9 Hz), 4.69 (1H, dd, *J* = 11.9, 10.0 Hz), 5.40 (2H, s), 5.89 (1H, dd, *J* = 11.7, 7.9 Hz), 7.20-7.38 (6H, m), 7.48 (1H, d, *J* = 1.9 Hz), 7.57 (1H, dd, *J* = 8.3, 1.9 Hz). ^{13}C NMR (75 MHz, $CDCl_3$) δ 19.7, 35.6,

45.3, 51.2, 53.9, 74.9, 110.2, 117.6, 118.0, 123.4, 123.8, 126.7, 127.7, 128.2, 128.7, 129.8, 135.0, 141.5, 141.9, 149.9, 160.7, 169.1. Anal. Calcd for $C_{24}H_{20}ClN_5O_3$ + 0.2 H_2O: C, 61.92; H, 4.42; N, 15.04. Found: C, 61.78; H, 4.69; N, 14.78. Analytical HPLC 99.4% purity.

(3*S*)-3-(2-Benzyl-3-chloro-7-oxo-2,4,5,7-tetrahydro-6*H*-pyrazolo[3,4-*c*]pyridin-6-yl)-*N*,5-dimethyl-4-oxo-2,3,4,5-tetrahydro-1,5-benzoxazepine-8-carboxamide (23). Compound **23** was obtained (55%) as a white solid in a manner similar to that described for the synthesis of **34**. LC-MS (APCI) *m*/*z* 494.2 $[M + H]^+$. ^1H NMR (300 MHz, $CDCl_3$) δ 2.66 (1H, dt, *J* = 15.8, 4.8 Hz), 2.91-3.12 (4H, m), 3.38 (3H, s), 3.53 (1H, td, *J* = 11.1, 4.5 Hz), 4.17-4.28 (1H, m), 4.34 (1H, dd, *J* = 10.0, 8.1 Hz), 4.62 (1H, dd, *J* = 11.7, 10.2 Hz), 5.39 (2H, s), 5.86 (1H, dd, *J* = 11.9, 8.1 Hz), 6.41 (1H, d, *J* = 4.5 Hz), 7.19-7.37 (6H, m), 7.54-7.69 (2H, m). Analytical HPLC 99.0% purity.

(3*S*)-3-(2-Benzyl-3-chloro-7-oxo-2,4,5,7-tetrahydro-6*H*-pyrazolo[3,4-*c*]pyridin-6-yl)-*N*,*N*,5-trimethyl-4-oxo-2,3,4,5-tetrahydro-1,5-benzoxazepine-8-carboxamide (24). Compound **24** was obtained (42%) as a white solid in a manner similar to that described for the synthesis of **34**. LC-MS (APCI) *m*/*z* 508.2 $[M + H]^+$. ^1H NMR (300 MHz, $CDCl_3$) δ 2.67 (1H, dt, *J* = 15.7, 4.8 Hz), 2.96-3.19 (7H, m), 3.38 (3H, s), 3.56 (1H, ddd, *J* = 11.9, 10.4, 4.5 Hz), 4.23 (1H, dt, *J* = 11.9, 5.2 Hz), 4.44 (1H, dd, *J* = 10.0, 8.1 Hz), 4.66 (1H, dd, *J* = 11.7, 9.8 Hz), 5.39 (2H, s), 5.93 (1H, dd, *J* = 11.7, 7.9 Hz), 7.21-7.38 (8H, m). Analytical HPLC 99.7% purity.

(3*S*)-3-(2-(2-Fluorobenzyl)-7-oxo-2,4,5,7-tetrahydro-6*H*-pyrazolo[3,4-*c*]pyridin-6-yl)-5-methyl-4-oxo-2,3,4,5-tetrahydro-1,5-benzoxazepine-8-carbonitrile (25). To a mixture of **71e** (3.51 g, 7.03

mmol) and dicyanozinc (1.238 g, 10.54 mmol) in DMF (dry) (35 mL) was added $Pd(PPh_3)_4$ (2.031 g, 1.76 mmol) at room temperature. The mixture was stirred at 100 °C under Ar for 2.5 h. The mixture was quenched with diluted saturated $NaHCO_3$ aq. at 0 °C and extracted with EtOAc. The organic layer was washed with brine, dried over Na_2SO_4 and concentrated under reduced pressure. The residue was purified by column chromatography (silica gel, eluted with 80% - 100% EtOAc in hexane) to give target compound (2.85 g) with triphenylphosphine oxide. To remove triphenylphosphine oxide, the residue were added magnesium chloride (0.669 g, 7.03 mmol) and toluene (10 mL). The mixture was stirred at 50 °C for 30 min. The mixture was purified directly by column chromatography (silica gel, eluted with 80% - 100% EtOAc in hexane) to give **25** (2.57 g, 82 %) as a white amorphous powder. LC-MS (APCI) *m*/*z* 446.3 $[M + H]^+$. ^1H NMR (300 MHz, $CDCl_3$) δ 2.73 (1H, dt, *J* = 15.5, 4.9 Hz), 3.10 (1H, ddd, *J* = 15.2, 10.3, 4.7 Hz), 3.39 (3H, s), 3.54 (1H, ddd, *J* = 11.8, 10.5, 4.2 Hz), 4.14-4.22 (1H, m), 4.44 (1H, dd, *J* = 10.2, 7.9 Hz), 4.68 (1H, dd, *J* = 11.7, 10.2 Hz), 5.40 (2H, s), 5.92 (1H, dd, *J* = 11.9, 8.1 Hz), 7.04-7.14 (2H, m), 7.21-7.36 (4H, m), 7.47 (1H, d, *J* = 1.9 Hz), 7.56 (1H, dd, *J* = 8.3, 1.9 Hz). ^{13}C NMR (75 MHz, $CDCl_3$) δ 20.4, 35.5, 45.7, 50.2 (d, *J* = 4.4 Hz), 51.1, 75.0, 110.1, 115.6 (d, *J* = 21.4 Hz), 117.6, 121.2, 122.8 (d, *J* = 14.3 Hz), 123.8, 124.6 (d, *J* = 3.8 Hz), 126.1, 126.7, 129.7, 130.4 (d, *J* = 8.2 Hz), 130.6 (d, *J* = 3.3 Hz), 141.6, 142.6, 149.9, 160.4 (d, *J* = 248 Hz), 161.4, 169.3. Anal. Calcd for $C_{24}H_{20}FN_5O_3$ + 0.2 H_2O: C, 64.19; H, 4.58; N, 15.60. Found: C, 63.91; H, 4.67; N, 15.39. Analytical HPLC 98.9% purity.

(3*S*)-3-(2-(2,6-Difluorobenzyl)-7-oxo-2,4,5,7-tetrahydro-6*H*-pyrazolo[3,4-*c*]pyridin-6-yl)-5-meth

yl-4-oxo-2,3,4,5-tetrahydro-1,5-benzoxazepine-8-carbonitrile (26). Compound **26** was obtained (85%) as a pale yellow amorphous solid in a manner similar to that described for the synthesis of **22**. LC-MS (APCI) *m/z* 464.2 $[M + H]^+$. ^{1}H NMR (300 MHz, $CDCl_3$) δ 2.71 (1H, dt, *J* = 15.4, 4.8 Hz), 2.99-3.16 (1H, m), 3.38 (3H, s), 3.46-3.59 (1H, m), 4.12-4.21 (1H, m), 4.42 (1H, dd, *J* = 10.0, 8.1 Hz), 4.67 (1H, dd, *J* = 11.9, 10.0 Hz), 5.45 (2H, s), 5.91 (1H, dd, *J* = 11.9, 8.1 Hz), 6.88-7.00 (2H, m), 7.23 (1H, s), 7.28-7.41 (2H, m), 7.46 (1H, d, *J* = 1.9 Hz), 7.56 (1H, dd, *J* = 8.3, 1.9 Hz). ^{13}C NMR (75 MHz, $CDCl_3$) δ 20.5, 35.5, 44.0 (t, *J* = 3.9 Hz), 45.7, 51.1, 75.0, 110.1, 111.5 (m), 111.8 (m), 117.7, 121.1, 123.8, 125.8, 126.7, 129.7, 131.1 (t, *J* = 10.5 Hz), 141.6, 142.5, 149.9, 161.3, 161.5 (dd, *J* = 251, 7.2 Hz), 169.3. Analytical HPLC 97.5% purity.

Methyl 2-benzyl-1*H*-imidazole-5-carboxylate (28). To a solution of (*Z*)-*N*'-hydroxy-2-phenylacetimidamide (**27**) (commercially available, 1.0 g, 6.66 mmol) in MeOH (20 mL) was added methyl propiolate (0.800 mL, 8.99 mmol). The mixture was refluxed for 5 h and concentrated under reduced pressure. The residue was dissolved in diphenyl ether (10 mL) was heated 200 °C for 1 h under microwave irradiation. The mixture was diluted with EtOAc, 1 M HCl aq (10 mL) and water. The aqueous layer was neutralized with saturated $NaHCO_3$ aq and extracted with EtOAc. The organic layer was dried over Na_2SO_4, filtered and concentrated under reduced pressure. The residual solid was washed with EtOAc/hexane to give **28** (0.510 g, 35%) as a pale brown solid. ^{1}H NMR (300 MHz, DMSO-d_6) δ 3.71 (3H x 2/3, s), 3.77 (3H x 1/3, s), 3.98 (2H, s), 7.14-7.36 (5H, m), 7.50 (1H x 1/3, d, *J* = 1.5 Hz), 7.76 (1H x 2/3, d, *J* = 2.3 Hz), 12.46 (1H x 2/3, brs),

13.01 (1H x 1/3, brs). LC-MS (APCI) *m*/*z* 217.3 $[M + H]^+$.

Methyl 2-benzyl-5-bromo-1*H*-imidazole-4-carboxylate (29). To a mixture of **28** (1.37 g, 6.34 mmol) and potassium bicarbonate (0.761 g, 7.60 mmol) in DMF (20 mL) was added bromine (0.390 mL, 7.60 mmol) at rt. After stirring at rt for 2 h, the mixture was diluted with EtOAc , washed with water and brine, dried over Na_2SO_4, filtered and concentrated under reduced pressure. The residue was purified by column chromatography (silica gel, eluted with 5% - 50% EtOAc in hexane) and washed with IPE to give **29** (1.04 g, 56%) as a light brown solid. ^{1}H NMR (300 MHz, $CDCl_3$) δ 3.86 (3H, s), 4.12 (2H, s), 7.23-7.25 (1H, m), 7.27-7.44 (4H, m), 9.25 (1H, brs). LC-MS (APCI) *m*/*z* 295.1 $[M + H]^+$.

Methyl 2-benzyl-5-bromo-1-(4-methoxybenzyl)-1*H*-imidazole-4-carboxylate (30). A mixture of **29** (1.04 g, 3.52 mmol), 4-methoxybenzyl chloride (0.285 mL, 2.10 mmol) and potassium carbonate (0.42 g, 3.04 mmol) in DMF (10 mL) was stirred at rt for 1 day and stirred at 50 °C for 4 h. The mixture was diluted with water and extracted with EtOAc. The organic layer was washed with brine, dried over Na_2SO_4, filtered and concentrated under reduced pressure. The residue was purified by column chromatography (silica gel, eluted with 5% - 70% EtOAc in hexane) to give **30** (0.300 g, 21%) as a colorless oil. ^{1}H NMR (300 MHz, $CDCl_3$) δ 3.79 (3H, s), 3.96 (3H, s), 4.06 (2H, s), 4.93 (2H, s), 6.78-6.89 (4H, m), 7.07-7.15 (2H, m), 7.18-7.32 (3H, m). LC-MS (APCI) *m*/*z* 415.2 $[M + H]^+$.

(*E*)-methyl 2-benzyl-5-(2-ethoxyvinyl)-1-(4-methoxybenzyl)-1*H*-imidazole-4-carboxylate (31). A

mixture of **30** (0.30 g, 0.72 mmol), (*E*)-2-(2-ethoxyvinyl)-4,4,5,5-tetramethyl-1,3,2-dioxaborolane (commercially available, 0.286 g, 1.44 mmol), $Pd(dppf)Cl_2 \cdot CH_2Cl_2$ (0.059 g, 0.07 mmol) and cesium carbonate (0.518 g, 1.59 mmol) in DME (8 mL)-water (1 mL) was stirred at 90 °C overnight under Ar atmosphere. The mixture was diluted with EtOAc, washed with water and brine, dried over Na_2SO_4, filtered and concentrated under reduced pressure. The residue was purified by column chromatography (silica gel, eluted with 20% - 100% EtOAc in hexane) to give **31** (0.220 g, 75%) as a light brown oil. ^{1}H NMR (300 MHz, $CDCl_3$) δ 1.25-1.32 (3H, m), 3.78 (3H, s), 3.87 (2H, q, *J* = 7.2 Hz), 3.93 (3H, s), 4.03 (2H, s), 4.84 (2H, s), 5.71 (1H, d, *J* = 12.8 Hz), 6.70-6.86 (4H, m), 7.07-7.26 (5H, m), 7.31 (1H, d, *J* = 12.8 Hz). LC-MS (APCI) *m*/*z* 407.3 $[M + H]^+$.

Methyl 2-benzyl-1-(4-methoxybenzyl)-5-(2-oxoethyl)-1*H*-imidazole-4-carboxylate (32). To a solution of **31** (110 mg, 0.27 mmol) in THF (5 mL, 0.27 mmol) was added 6 M HCl aq. (1 mL, 6.00 mmol) at room temperature. The mixture was stirred at room temperature for 2 h. To the mixture was added 6 M HCl aq. (2 mL, 12.00 mmol). After stirring at rt for 2 h, the mixture was heated to 60 °C and stirred at 60 °C for 30 min. The mixture was neutralized with saturated $NaHCO_3$ aq, saturated with NaCl and extracted with EtOAc. The organic layer was dried over Na_2SO_4, filtered and concentrated under reduced pressure to give **32** (100 mg, 98%). This product was subjected to the next reaction without further purification. LC-MS (APCI) *m*/*z* 377.1 $[M - H]^+$.

(*S*)-Methyl

2-benzyl-1-(4-methoxybenzyl)-5-(2-((5-methyl-4-oxo-2,3,4,5-tetrahydrobenzo[*b*][1,4]oxazepin-3

-yl)amino)ethyl)-1*H*-imidazole-4-carboxylate (33). To a solution of **32** (100 mg, 0.26 mmol) and (*S*)-3-amino-5-methyl-2,3-dihydrobenzo[*b*][1,4]oxazepin-4(5*H*)-one hydrochloride (60.4 mg, 0.26 mmol) in acetic acid (0.5 mL, 0.26 mmol) and MeOH (5 mL, 0.26 mmol) was added 2-picoline boran (36.7 mg, 0.34 mmol) at room temperature. The mixture was stirred at room temperature under air for 1h. The mixture was quenched with saturated $NaHCO_3$ aq. at room temperature and extracted with EtOAc. The organic layer was dried over Na_2SO_4, filtered and concentrated under reduced pressure. The residue was purified by column chromatography (silica gel, eluted with 30% - 70% EtOAc in hexane) to give **33** (95 mg, 65%) as a colorless oil. LC-MS (APCI) *m*/*z* 555.3 $[M + H]^+$.

(*S*)-3-(2-Benzyl-1-(4-methoxybenzyl)-4-oxo-6,7-dihydro-1*H*-imidazo[4,5-*c*]pyridin-5(4*H*)-yl)-5-methyl-2,3-dihydrobenzo[*b*][1,4]oxazepin-4(5*H*)-one (34). To a solution of **33** (95 mg, 0.17 mmol) in toluene (10 mL) was added trimethylaluminum in toluene (0.285 mL, 0.51 mmol) at room temperature. After stirring at 100 °C for 4 h under Ar atmosphere, the mixture was heated to 120 °C and stirred at 120 °C overnight. The mixture was quenched with water at room temperature and diluted with EtOAc. Saturated Rochelle salt aq was added to the mixture. The organic layer was dried over Na_2SO_4 and concentrated under reduced pressure. The residue was purified by column chromatography (silica gel, eluted with 50% - 100% EtOAc in hexane) to give **34** (45.0 mg, 50%) as an off-white solid. ^{1}H NMR (300 MHz, $CDCl_3$) δ 2.53 (1H, dt, *J* = 16.1, 4.6 Hz), 2.94-3.09 (1H, m), 3.36 (3H, s), 3.58 (1H, td, *J* = 11.6, 4.7 Hz), 3.79 (3H, s), 4.09 (2H, s), 4.18-4.30 (1H, m), 4.36-4.48 (1H, m), 4.51-4.63 (1H, m), 4.69-4.89 (2H, m), 5.93 (1H, dd, *J* = 11.5, 8.1 Hz), 6.70-6.85 (4H, m),

7.10-7.31 (9H, m). LC-MS (APCI) *m*/*z* 523.3 $[M + H]^+$.

Ethyl 4-benzyl-1*H*-imidazole-2-carboxylate (37). To a solution of 1-amino-3-phenylpropan-2-one hydrochloride (**36**) (commercially available, 0.93 g, 5.01 mmol) and ethyl 2-ethoxy-2-iminoacetate (commercially available, 0.727 g, 5.01 mmol) in acetic acid (10 mL, 174.68 mmol) was added sodium acetate (0.740 g, 9.02 mmol) at room temperature, and the mixture was stirred for 6 h at 110 °C in a sealed tube. The reaction mixture was concentrated under reduced pressure. To the residue was added saturated $NaHCO_3$ aq. and extracted with EtOAc. The organic layer was washed with brine, dried over Na_2SO_4, filtered and concentrated under reduced pressure. The residue was purified by column chromatography (silica gel, eluted with 48% - 69% EtOAc in hexane) to give **37** (105 mg, 9.1%) as a brown oil. ^{1}H NMR (300 MHz, DMSO-d_6) δ1.29 (3H, t, *J* = 7.2 Hz), 3.85 (1H, s), 3.94 (1H, s), 4.27 (2H, q, *J* = 7.2 Hz), 7.17-7.35 (6H, m), 12.98-13.34 (1H, m). LC-MS (APCI) *m*/*z* 231.3 $[M + H]^+$.

(*S*)-4-Benzyl-*N*-(5-methyl-4-oxo-2,3,4,5-tetrahydrobenzo[*b*][1,4]oxazepin-3-yl)-1*H*-imidazole-2-carboxamide (38). To a solution of **37** (105 mg, 0.46 mmol) in EtOH (1 mL, 17.04 mmol) was added 2 M sodium hydroxide (0.684 mL, 1.37 mmol) at room temperature, and the mixture was stirred for 30 min at 100 °C. The mixture was concentrated under reduced pressure and dissolved in DMF (2 mL, 25.83 mmol). (*S*)-3-Amino-5-methyl-2,3-dihydrobenzo[*b*][1,4]oxazepin-4(5*H*)-one hydrochloride (136 mg, 0.59 mmol), HATU (225 mg, 0.59 mmol) and DIPEA (0.238 mL, 1.37 mmol) were added to the mixture. After stirring at room temperature for 2h, the mixture was

partitioned between water and EtOAc. The organic layer was washed with water and brine, dried over Na_2SO_4, filtered and concentrated under reduced pressure. The residue was purified by column chromatography (silica gel, eluted with 70% - 90% EtOAc in hexane) to give **38** (101 mg, 59%) as a brown amorphous powder. ^{1}H NMR (300 MHz, $CDCl_3$) δ 3.41 (3H, d, *J* = 5.7 Hz), 3.88 (1H, s), 3.95 (1H, s), 4.29 (1H, dt, *J* = 11.0, 9.4 Hz), 4.64 (1H, dt, *J* = 9.7, 7.4 Hz), 5.00 (1H, tt, *J* = 11.0, 7.6 Hz), 6.63-6.74 (0.5H, m), 6.83-6.88 (0.5H, m), 7.02-7.49 (10H, m), 7.99 (1H, t, *J* = 8.3 Hz), 10.33 (0.5H, brs), 10.54 (0.5H, brs). LC-MS (APCI) *m*/*z* 377.2 $[M + H]^+$.

Ethyl 1-benzyl-1*H*-pyrazole-3-carboxylate (40). To a suspension of ethyl 1*H*-pyrazole-3-carboxylate (commercially available, **39**) (13.4 g, 95.62 mmol) and potassium carbonate (39.6 g, 286.86 mmol) in DMF(dry) (200 mL) was added (bromomethyl)benzene (commercially available, 12.51 mL, 105.18 mmol) at room temperature, and the mixture was stirred for 2 h at room temperature. The mixture was filtered, and then the filtrate was diluted with EtOAc, and washed with water. The aqueous layer was extracted with EtOAc. The combined organic layer was washed with brine, dried over $MgSO_4$, filtered and concentrated under reduced pressure. The residue was purified by column chromatography (silica gel, eluted with 5% - 50% EtOAc in hexane) to give **40** (14.10 g, 64%) as a white solid. ^{1}H NMR (300 MHz, $CDCl_3$) δ 1.40 (3H, t, *J* = 7.0 Hz), 4.42 (2H, q, *J* = 7.2 Hz), 5.40 (2H, s), 6.82 (1H, d, *J* = 2.3 Hz), 7.21-7.26 (2H, m), 7.30-7.41 (4H, m).

Ethyl 1-benzyl-4-bromo-1*H*-pyrazole-3-carboxylate (41). To a solution of **40** (6.68 g, 29.01

mmol) in MeCN (120 mL) was added bromine (2.230 mL, 43.52 mmol) at rt. After stirring at rt overnight, an additional bromine (2.230 mL, 43.52 mmol) was added and the mixture was stirred at rt for 1 day. The mixture was concentrated under reduced pressure, diluted with EtOAc and washed with 10% sodium thiosulfate aq. The aqueous layer was extracted with EtOAc/THF. The combined organic layer was dried over Na_2SO_4, filtered and concentrated under reduced pressure. The residue was purified by column chromatography (silica gel, eluted with 10% - 50% EtOAc in hexane) to give **41** (8.76 g, 98%) as a white solid. ^{1}H NMR (300 MHz, $CDCl_3$) δ 1.43 (3H, t, *J* = 7.0 Hz), 4.44 (2H, q, *J* = 6.9 Hz), 5.35 (2H, s), 7.22-7.44 (6H, m). LC-MS (APCI) *m*/*z* 309.2 $[M + H]^+$.

(*E*)-Ethyl 1-benzyl-4-(2-ethoxyvinyl)-1*H*-pyrazole-3-carboxylate (42). Compound **42** was obtained (94%) as a pale yellow oil in a manner similar to that described for the synthesis of **31**. ^{1}H NMR (300 MHz, $CDCl_3$) δ1.31 (3H, t, *J* = 7.2 Hz), 1.42 (3H, t, *J* = 7.2 Hz), 3.86 (2H, q, *J* = 6.8 Hz), 4.42 (2H, q, *J* = 7.2 Hz), 5.33 (2H, s), 6.19 (1H, d, *J* = 13.2 Hz), 6.81 (1H, d, *J* = 13.6 Hz), 7.20-7.28 (3H, m), 7.31-7.41 (3H, m). LC-MS (ESI) *m*/*z* 301.3 $[M + H]^+$.

Ethyl 1-benzyl-4-(2-oxoethyl)-1*H*-pyrazole-3-carboxylate (43). Compound **43** was obtained (94%) as a brown solid in a manner similar to that described for the synthesis of **32**. ^{1}H NMR (300 MHz, $CDCl_3$) δ1.40 (3H, t, *J* = 7.2 Hz), 3.85 (2H, d, *J* = 0.8 Hz), 4.41 (2H, q, *J* = 7.2 Hz), 5.37 (2H, s), 7.22-7.46 (6H, m), 9.66-9.78 (1H, m).

(*S*)-Ethyl

1-benzyl-4-(2-((5-methyl-4-oxo-2,3,4,5-tetrahydrobenzo[*b*][1,4]oxazepin-3-yl)amino)ethyl)-1*H*-

pyrazole-3-carboxylate (44). Compound **44** was obtained (94%) as a brown solid in a manner similar to that described for the synthesis of **33**.

LC-MS (APCI) *m*/*z* 449.2 $[M + H]^+$. ^{1}H NMR (300 MHz, $CDCl_3$) δ 1.37 (3H, t, *J* = 7.0 Hz), 2.43-2.53 (1H, m), 2.76-2.91 (3H, m), 3.38 (3H, s), 3.52 (1H, dd, *J* = 11.7, 7.6 Hz), 4.06 (1H, dd, *J* = 11.3, 10.2 Hz), 4.30-4.42 (3H, m), 5.32 (2H, s), 7.10-7.24 (7H, m), 7.29-7.38 (3H, m).

(*S*)-5-Methyl-3-(7-oxo-4,5-dihydro-2*H*-pyrazolo[3,4-c]pyridin-6(7*H*)-yl)-2,3-dihydrobenzo[*b*][1, 4]oxazepin-4(5*H*)-one (45). A mixture of **14** (1.29 g, 3.21 mmol), 1 M HCl aq (7 mL, 7.00 mmol) and 10% palladium on carbon (0.341 g, 0.32 mmol) in MeOH (30 mL, 740.59 mmol) was hydrogenated under balloon pressure at room temperature overnight. The catalyst was removed by filtration and the filtrate was concentrated under reduced pressure. The residue was dissolved in MeOH (20 mL, 493.73 mmol) and palladium on carbon (0.682 g, 0.64 mmol) and 1 M HCl aq (5 mL, 5.00 mmol) was added to the solution. The mixture was hydrogenated under balloon pressure for 4 h at room. The catalyst was removed by filtration and the filtrate was concentrated under reduced pressure. The solid was washed with EtOAc/heptane (1/4) to give **45** (0.820 g, 82%) as a white solid. ^{1}H NMR (300 MHz, $CDCl_3$) δ 2.84 (1H, d, *J* = 15.1 Hz), 3.16 (1H, d, *J* = 7.9 Hz), 3.39 (3H, s), 3.62 (1H, brs), 4.19-4.47 (2H, m), 4.68 (1H, t, *J* = 10.4 Hz), 5.81 (1H, dd, *J* = 11.3, 7.6 Hz), 7.11-7.26 (4H, m), 7.78 (1H, s). LC-MS (APCI) *m*/*z* 313.2 $[M + H]^+$.

Ethyl 3-(tert-butoxymethyl)-1*H*-pyrazole-4-carboxylate (47). To a solution of ethyl 4-(tert-butoxy)-3-oxobutanoate (**46**) (commercially available, 12.0 g, 59.3 mmol) in toluene (100

mL) was added DMF-DMA (10.6 g, 89.0 mmol). The mixture was stirred at 65 °C for 16 hr. After cooling to 25 °C, the reaction mixture was concentrated under reduced pressure. To a mixture of the residue and AcOH (20 mL) was added $NH_2NH_2 \cdot H_2O$ (4.55 g, 90.9 mmol). The mixture was stirred at 25-30 °C for 14 hr. The reaction mixture was diluted with EtOAc (300 mL), and it was washed with saturated $NaHCO_3$ aq. (200 mL), brine (200 mL). The organic layer was dried over Na_2SO_4 and concentrated under reduced pressure. The residue was purified by column chromatography (silica gel, eluted with

petroleum ether/EtOAc (3:1) to give **47** (7.00 g, 52%) as a yellow solid. ^{1}H NMR (400 MHz, DMSO-d_6) δ 1.23 (9H, s), 1.27 (3H, t, J = 7.2 Hz), 4.21 (2H, q, J = 7.2 Hz), 4.69 (2H, s), 7.80 (1H, s), 13.27 (1H, brs).

Ethyl 1-benzyl-3-(tert-butoxymethyl)-1*H*-pyrazole-4-carboxylate (48). Two batches of the reaction were conducted and worked up together after the reaction. To a solution of **47** (3.00 g, 13.3 mmol) and benzyl chloride (1.68 g, 13.3 mmol) in MeCN (50 mL) was added potassium carbonate (11.0 g, 79.6mmol). The mixture was stirred at 20-25 °C for 14 h.

To a solution of **47** (7.00 g, 31.0 mmol) and benzyl chloride (2.74 g, 21.7 mmol) in MeCN (50 mL) was added potassium carbonate (18.0g, 130 mmol). The mixture was stirred at 20-25 °C for 14 h. Two reaction mixtures were combined, diluted with water, and extracted with EtOAc (3 times). The combined organic layer was washed with brine, dried over Na_2SO_4, filtered and concentrated under reduced pressure. The residue was purified by column chromatography (silica gel, eluted with 9% -

25% EtOAc in petroleum ether) to give **48** (9.00 g, 64%) as a yellow oil. ^{1}H NMR (400 MHz, $CDCl_3$) δ 1.31 (3H, t, *J* = 6.8 Hz), 1.33 (9H, s), 4.25 (2H, q, *J* = 6.8 Hz), 4.71 (2H, s), 5.28 (2H, s), 7.20-7.30 (2H, m), 7.35-7.45 (3H, m), 7.73 (1H, m).

Ethyl 1-benzyl-3-(hydroxymethyl)-1*H*-pyrazole-4-carboxylate (49). To a solution of **48** (9.00 g, 28. 5 mmol) in DCM (10 mL) was added TFA (5 mL). The mixture was stirred at 20-25 °C for 2 h, quenched with 1 M NaOH aq till pH = 10, diluted with water, and extracted with EtOAc (3 times). The combined organic layer was washed with brine, dried over Na_2SO_4, filtered and concentrated under reduced pressure. The residue was purified by column chromatography (silica gel, eluted with 9% - 25% EtOAc in petroleum ether) to give **49** (6.40 g, 86%) as a yellow oil. ^{1}H NMR (400 MHz, DMSO-d_6) δ 1.26 (3H, t, *J* = 7.2 Hz), 4.19 (2H, q, *J* = 7.2 Hz), 4.58 (2H, d, *J* = 6.0 Hz), 4.84 (1H, t, *J* = 6.0 Hz), 5.32 (2H, s), 7.25-7.40 (5H, m), 8.38 (1H, s).

Ethyl 1-benzyl-3-formyl-1*H*-pyrazole-4-carboxylate (50). To a solution of **49** (4.60 g, 17.7 mmol) in DCM (50 mL) was added MnO_2 (15.0 g, 173 mmol). The reaction was stirred at 40 °C for 14 hr. The reaction was concentrated under reduced pressure. The residue was purified by column chromatography (silica gel, eluted with 9% - 25% EtOAc in petroleum ether) to give **50** (2.70 g, 59%) as an off-white solid. ^{1}H NMR (400 MHz, DMSO-d_6) δ 1.28 (3H, t, *J* = 7.6 Hz), 4.27 (2H, q, *J* = 7.2 Hz), 5.47 (2H, s), 7.25-7.45 (5H, m), 8.63 (1H, s), 10.26 (1H, s).

(*E*)-Ethyl 1-benzyl-3-(2-methoxyvinyl)-1*H*-pyrazole-4-carboxylate (51). To a mixture of (methoxymethyl)triphenylphosphonium chloride (commercially available, 15.8 g, 46.1 mmol) in

THF (50 mL) was added t-BuOK (44.9 mL, 44.9 mmol, 1M in THF) over 1 min at 0 °C. The mixture was stirred at 0 °C for 10 min, and to the mixture was added a solution of **50** (2.70 g, 10.5 mmol) in THF (20 mL) over 20 min. The mixture was stirred at 0 °C for 30 min, and then it was warmed to 20-25 °C for 12 hr. The reaction mixture was diluted with EtOAc (200 mL) and it was washed with water (100 mL) and brine (100 mL). The organic layer was dried over Na_2SO_4 and concentrated under reduced pressure. The residue was purified by column chromatography (silica gel, eluted with 9% - 25% EtOAc in petroleum ether) to give **51** (1.60 g, 53%) as a yellow oil. ^{1}H NMR (400 MHz, DMSO-d_6) δ 1.26 (3H, t, J = 7.2 Hz), 4.19 (2H, q, J = 7.2 Hz), 5.28 (2H, s), 6.16 (1H, d, J = 13.2 Hz), 7.25-7.45 (6H, m), 8.34 (1H, s).

Ethyl 1-benzyl-5-hydroxy-1*H*-pyrazole-3-carboxylate (55). Diethyl but-2-ynedioate (**54**) (commercially available, 20.42 mL, 127.59 mmol) was added to a mixture of benzylhydrazine hydrochloride (commercially available, 20.24 g, 127.59 mmol) and potassium carbonate (26.5 g, 191.39 mmol) in EtOH (600 mL). The mixture was stirred at 90 °C overnight. After stirring at rt for 2 days, the mixture was acidified with 6 M HCl aq (70 mL) at 0 °C and extracted with EtOAc (twice). The combined organic layer was washed with brine, dried over Na_2SO_4, filtered and concentrated under reduced pressure. The residual solid was triturated with MeCN (50 mL), and the collected solid was washed with MeCN (30 mL) to give **55** (11.33 g, 36%) as an off-white solid. ^{1}H NMR (300 MHz, DMSO-d_6) δ1.25 (3H, t, J = 7.0 Hz), 4.21 (2H, q, J = 6.9 Hz), 5.16 (2H, s), 5.81 (1H, s), 7.13-7.21 (2H, m), 7.23-7.40 (3H, m), 11.57 (1H, s). LC-MS (APCI) m/z 247.3 $[M + H]^+$.

Ethyl 1-benzyl-5-bromo-4-formyl-1*H*-pyrazole-3-carboxylate (56a). To a solution of **55** (3.60 g, 14.62 mmol) and phosphoryl tribromide (7.80 g, 27.21 mmol) in 1,2-dichloroethane (60 mL, 14.62 mmol) was added DMF (2.1 mL, 27.29 mmol) at room temperature. The mixture was stirred at 90 °C under air for 3 h. To the mixture was added phosphoryl tribromide (19.6 g, 68.37 mmol) at r.t. The mixture was stirred at 90 °C under air for 19 h. To the mixture was added phosphoryl tribromide (9.64 g, 33.62 mmol) at the same temperature. The mixture was stirred at 90 °C under air for 3 h. The mixture was poured into water with ice. The organic layer was separated. The aqueous layer was extracted with EtOAc. The combined organic layer was dried over anhydrous Na_2SO_4, filtered and concentrated under reduced pressure.The residue was purified by column chromatography (silica gel, eluted with 15% - 30% EtOAc in hexane) to give **56a** (2.340 g, 48 %) as a pale yellow solid. ^{1}H NMR (400 MHz, $CDCl_3$) δ 1.44 (3H, t, J = 7.2 Hz), 4.49 (2H, q, J = 7.2 Hz), 5.51 (2H, s), 7.26-7.39 (5H, m), 10.43 (1H, s). LC-MS (APCI) m/z 337.1 $[M + H]^+$.

Ethyl 1-benzyl-5-chloro-4-formyl-1*H*-pyrazole-3-carboxylate (56b). To a solution of **55** (10.0 g, 40.61 mmol) in DMF (12.50 mL, 162.43 mmol) was dropwisely added phosphoryl trichloride (30.3 mL, 324.86 mmol) at room temperature. The mixture was stirred at 90 °C under air for 7 h. The solvent was removed by rotary evaporation under reduced pressure. To the residue was added saturated $NaHCO_3$ aq. at 0 °C and extracted with EtOAc. The organic layer was separated, washed with brine, dried over Na_2SO_4 and concentrated under reduced pressure. The residue was purified by column chromatography (silica gel, eluted with 20% - 35% EtOAc in hexane) to give **56b** (4.25 g,

36 %) as a pale yellow solid. LC-MS (APCI) *m*/*z* 293.2 $[M + H]^+$. ^1H NMR (300 MHz, $CDCl_3$) δ 1.44 (3H, t, *J* = 7.2 Hz), 4.49 (2H, q, *J* = 7.2 Hz), 5.46 (2H, s), 7.27-7.38 (5H, m), 10.43 (1H, s).

(*E*)-Ethyl 1-benzyl-5-bromo-4-(2-methoxyvinyl)-1*H*-pyrazole-3-carboxylate (57a). Compound **57a** was obtained (30%) as a colorless oil in a manner similar to that described for the synthesis of **51**. LC-MS (APCI) *m*/*z* 365.1 $[M + H]^+$. ^1H NMR (300 MHz, $CDCl_3$) δ 1.41 (3H, t, *J* = 7.2 Hz), 3.69 (3H, s), 4.42 (2H, q, *J* = 7.2 Hz), 5.47 (2H, s), 6.02 (1H, d, *J* = 13.2 Hz), 7.12-7.39 (5H, m).

Ethyl 1-benzyl-5-chloro-4-(2-methoxyvinyl)-1*H*-pyrazole-3-carboxylate (57b). Compound **57b** was obtained (42%) as a colorless oil in a manner similar to that described for the synthesis of **51**. LC-MS (APCI) *m*/*z* 321.2 $[M + H]^+$. ^1H NMR (300 MHz, $CDCl_3$) δ 1.35-1.46 (3H, m), 3.65-3.71 (3H, m), 4.33-4.49 (2H, m), 5.40-5.44 (2H, m), 6.03-6.18 (1H, m), 7.17-7.38 (6H, m).

Ethyl 1-benzyl-5-bromo-4-(2-oxoethyl)-1*H*-pyrazole-3-carboxylate (58a). Compound **58a** was obtained in a manner similar to that described for the synthesis of **32**. This product was subjected to the next reaction without further purification. LC-MS (APCI) *m*/*z* 351.2 $[M + H]^+$.

Ethyl 1-benzyl-5-chloro-4-(2-oxoethyl)-1*H*-pyrazole-3-carboxylate (58b). Compound **58b** was obtained in a manner similar to that described for the synthesis of **32**. This product was subjected to the next reaction without further purification. LC-MS (APCI) *m*/*z* 307.2 $[M + H]^+$.

(*S*)-Ethyl 1-benzyl-5-bromo-4-(2-((5-methyl-4-oxo-2,3,4,5-tetrahydrobenzo[*b*][1,4]oxazepin-3-yl)amino)ethyl)-1*H*-pyrazole-3-carboxylate (59a). Compound **59a** was obtained (67% in 2 steps from **57a**) as a

colorless oil in a manner similar to that described for the synthesis of **33**. LC-MS (APCI) *m*/*z* 527.1 $[M + H]^+$. ^1H NMR (300 MHz, $CDCl_3$) δ 1.36 (3H, t, *J* = 7.0 Hz), 2.36-2.51 (1H, m), 2.66-2.91 (3H, m), 3.38 (3H, s), 3.55 (1H, dd, *J* = 11.7, 7.6 Hz), 4.00-4.17 (1H, m), 4.29-4.41 (3H, m), 5.42 (2H, s), 7.09-7.37 (9H, m).

(*S*)-Ethyl 1-benzyl-5-chloro-4-(2-((5-methyl-4-oxo-2,3,4,5-tetrahydrobenzo[*b*][1,4]oxazepin-3-yl)amino)ethyl)-1*H*-pyrazole-3-carboxylate (59b). Compound **59b** was obtained (94% in 2 steps from **57b**) as a colorless oil in a manner similar to that described for the synthesis of **33**. LC-MS (APCI) *m*/*z* 483.2 $[M + H]^+$. ^1H NMR (300 MHz, $CDCl_3$) δ 1.36 (3H, t, *J* = 7.2 Hz), 2.38-2.53 (1H, m), 2.67-2.92 (3H, m), 3.38 (3H, s), 3.53 (1H, dd, *J* = 11.7, 7.6 Hz), 4.00-4.09 (1H, m), 4.30-4.41 (3H, m), 5.38 (2H, s), 7.09-7.22 (6H, m), 7.27-7.36 (3H, m).

(3*S*)-3-(2-Benzyl-3-bromo-7-oxo-2,4,5,7-tetrahydro-6*H*-pyrazolo[3,4-*c*]pyridin-6-yl)-5-methyl-2,3-dihydro-1,5-benzoxazepin-4(5*H*)-one (60). Compound **60** was obtained (82%) as a white solid in a manner similar to that described for the synthesis of **34**. LC-MS (APCI) *m*/*z* 481.1 $[M + H]^+$. ^1H NMR (300 MHz, $CDCl_3$) δ2.63 (1H, dt, *J* = 15.6, 4.9 Hz), 2.98-3.12 (1H, m), 3.38 (3H, s), 3.49-3.64 (1H, m), 4.20-4.32 (1H, m), 4.42 (1H, dd, *J* = 9.8, 8.3 Hz), 4.63 (1H, dd, *J* = 11.5, 10.0 Hz), 5.43 (2H, s), 5.92 (1H, dd, *J* = 11.5, 8.1 Hz), 7.13-7.35 (9H, m).

Ethyl 4-bromo-1-(2-fluorobenzyl)-1*H*-pyrazole-3-carboxylate (62a). To a solution of ethyl 1*H*-pyrazole-3-carboxylate (commercially available, 13.56 g, 96.76 mmol) in THF (140 mL) was

added 60% NaH in oil (4.64 g, 116.11 mmol) at 0 °C. After being stirred at 0 °C for 20 min, 1-(bromomethyl)-2-fluorobenzene (commercially available, 12.84 mL, 106.44 mmol) was added to the reaction mixture at 0 °C. The mixture was stirred at room temperature overnight. The mixture was quenched with saturated NH_4Cl aq. and extracted with EtOAc. The organic layer was separated, washed with brine, dried over Na_2SO_4 and concentrated under reduced pressure. The residue was purified by column chromatography (silica gel, eluted with 18% - 39% EtOAc in hexane) to give ethyl 1-(2-fluorobenzyl)-1*H*-pyrazole-3-carboxylate (22.77 g, 95%) as a pale yellow oil. LC-MS (APCI) *m*/*z* 249.3 $[M + H]^+$. ^1H NMR (300 MHz, $CDCl_3$) δ 1.40 (3H, t, *J* = 7.2 Hz), 4.41 (2H, q, *J* = 7.2 Hz), 5.46 (2H, s), 6.83 (1H, d, *J* = 2.3 Hz), 7.05-7.15 (2H, m), 7.17-7.24 (1H, m), 7.28-7.37 (1H, m), 7.43 (1H, d, *J* = 1.9 Hz).

A solution of bromine (5.25 mL, 102.37 mmol) in MeCN (30 mL) was added to a solution of ethyl 1-(2-fluorobenzyl)-1*H*-pyrazole-3-carboxylate (commercially available, 22.77 g, 91.72 mmol) in MeCN (200 mL) at room temperature. After being stirred at room temperature overnight, TEA (15.34 mL, 110.07 mmol) was added to the reaction mixture. After being stirred at room temperature for 5 min, bromine (2.87 mL, 56.07 mmol) was added to the reaction mixture. The mixture was quenched with saturated $NaHCO_3$ aq. and extracted with EtOAc. The organic layer was separated, washed with $Na_2S_2O_3$ aq. and brine, dried over Na_2SO_4 and concentrated under reduced pressure. The residue was disolved in MeCN (200 mL) and added a solution of bromine (21.2 g, 132.66 mmol) in MeCN (30 mL) at room temperature. The mixture was stirred at room temperature for 10 min. The

mixture was quenched with $Na_2S_2O_3$ aq. and extracted with EtOAc. The organic layer was separated, washed with saturated $NaHCO_3$ aq. and brine, dried over Na_2SO_4 and concentrated under reduced pressure. The residue was purified by column chromatography (silica gel, eluted with 20% - 40% EtOAc in hexane) to give **62a** (29.5 g, 98%) as a white solid. LC-MS (APCI) *m/z* 327.2 $[M + H]^+$. ^1H NMR (300 MHz, $CDCl_3$) δ 1.42 (3H, t, *J* = 7.2 Hz), 4.43 (2H, q, *J* = 7.2 Hz), 5.42 (2H, s), 7.08-7.18 (2H, m), 7.22-7.29 (1H, m), 7.32-7.41 (1H, m), 7.48 (1H, s)

Ethyl 4-bromo-1-(2,6-difluorobenzyl)-1*H*-pyrazole-3-carboxylate (62b). Bromine (2.194 mL, 42.81 mmol) was added to a solution of ethyl 1*H*-pyrazole-3-carboxylate (**61**) (1.5 g, 10.70 mmol) in AcOH (40 mL) at room temperature. The mixture was stirred at room temperature for 6 h. The mixture was quenched with saturated $Na_2S_2O_3$ aq. anddried up under reduced pressure. The residue was extracted with EtOAc, washed with saturated $NaHCO_3$ aq. and brine, dried over Na_2SO_4 and concentrated under reduced pressure to give ethyl 4-bromo-1*H*-pyrazole-3-carboxylate (2.07 g, 88%) as a white solid. This product was subjected to the next reaction without further purification.

A solution of ethyl 4-bromo-1*H*-pyrazole-3-carboxylate (2.07 g, 9.45 mmol) in THF(dry) (10 mL) was added to a solution of sodium hydride, 60% in oil (0.454 g, 11.34 mmol) in THF(dry) (10 mL) at 0 °C, and then the resulting mixture was stirred for 5 min. To this bright yellow mixture was added 2-(bromomethyl)-1,3-difluorobenzene (2.152 g, 10.40 mmol) dropwise with stirring, and then the resulting mixture was further stirred in an ice bath and was gradually warmed up to rt overnight. The mixture was quenched with saturated NH_4Cl aq. and extracted with EtOAc. The organic layer was

separated, washed with saturated $NaHCO_3$ aq. and brine, dried over Na_2SO_4 and concentrated under reduced pressure. The residue was purified by column chromatography (silica gel, eluted with 15% - 36% EtOAc in hexane) to give **62b** (3.16 g, 97%) as a colorless solid. LC-MS (APCI) *m*/*z* 345.1 $[M + H]^+$. ^1H NMR (300 MHz, $CDCl_3$) δ 1.41 (3H, t, *J* = 7.2 Hz), 4.42 (2H, q, *J* = 7.2 Hz), 5.46 (2H, s), 6.98 (2H, dd, *J* = 8.5, 7.4 Hz), 7.32-7.43 (1H, m), 7.45 (1H, s).

Ethyl 4-(2-ethoxyvinyl)-1-(2-fluorobenzyl)-1*H*-pyrazole-3-carboxylate (63a). Compound **63a** was obtained (84%) as a white solid in a manner similar to that described for the synthesis of **31**. LC-MS (APCI) *m*/*z* 319.2 $[M + H]^+$. ^1H NMR (300 MHz, $CDCl_3$) δ 1.23-1.45 (6H, m), 3.82-4.00 (2H, m), 4.37-4.46 (2H, m), 5.37-5.47 (2H, m), 6.00-6.06 (0.5H, m), 6.14-6.22 (0.5H, m), 6.80-6.88 (0.5H, m), 7.04-7.24 (2.5H, m), 7.27-7.38 (1H, m), 7.93 (0.5H, s).

(*Z*)-ethyl 1-(2,6-difluorobenzyl)-4-(2-ethoxyvinyl)-1*H*-pyrazole-3-carboxylate (63b). A mixture of **62b** (2.80 g, 8.11 mmol), (*Z*)-2-(2-ethoxyvinyl)-4,4,5,5-tetramethyl-1,3,2-dioxaborolane (commercially available, 2.89 g, 14.60 mmol), $PdCl_2$(dppf) (0.594 g, 0.81 mmol) and cesium carbonate (5.82 g, 17.85 mmol) in DME (80 mL)-water (10.00 mL) was stirred at 90 °C overnight under Ar atmosphere. The mixture was diluted with EtOAc, washed with water and brine, dried over Na_2SO_4, filtered and concentrated under reduced pressure. The residue was purified by column chromatography (silica gel, eluted with 5% - 50% EtOAc in hexane) to give **63b** (2.370 g, 87%) as a pale yellow oil. LC-MS (APCI) *m*/*z* 337.2 $[M + H]^+$. ^1H NMR (300 MHz, $CDCl_3$) δ 1.26-1.34 (3H, m), 1.40 (3H, t, *J* = 7.2 Hz), 3.94 (2H, q, *J* = 6.9 Hz), 4.40 (2H, q, *J* = 7.2 Hz), 5.39-5.53 (2H, m),

6.01 (1H, d, *J* = 6.8 Hz), 6.18 (1H, d, *J* = 6.8 Hz), 6.88-7.04 (2H, m), 7.28-7.44 (1H, m), 7.90 (1H, s).

Ethyl 1-(2-fluorobenzyl)-4-(2-oxoethyl)-1*H*-pyrazole-3-carboxylate (64a). To a solution of **63a** (10.33 g, 32.45 mmol) in THF (100 mL) was added 6 M HCl aq in water (50 mL, 300.00 mmol) at room temperature. The mixture was stirred at room temperature under air for 2.5 h. The mixture was quenched with saturated $NaHCO_3$ aq. at room temperature and extracted with EtOAc. The organic layer was separated, washed with brine, dried over Na_2SO_4 and concentrated under reduced pressure. The residue was purified by column chromatography (silica gel, eluted with 29% - 50% EtOAc in hexane) to give **64a** (6.41 g, 68%) as a pale yellow oil. ^{1}H NMR (300 MHz, $CDCl_3$) δ 1.39 (3H, t, *J* = 7.2 Hz), 3.83-3.88 (2H, m), 4.40 (2H, q, *J* = 7.2 Hz), 5.39-5.45 (2H, m), 7.06-7.17 (2H, m), 7.20-7.29 (1H, m), 7.30-7.39 (1H, m), 7.44 (1H, s), 9.72 (1H, t, *J* = 1.3 Hz).

Ethyl 1-(2,6-difluorobenzyl)-4-(2-oxoethyl)-1*H*-pyrazole-3-carboxylate (64b). Compound **64b** was obtained in a manner similar to that described for the synthesis of **32**. This product was subjected to the next reaction without further purification. LC-MS (APCI) *m*/*z* 309.3 $[M + H]^+$.

(*S*)-2-((tert-Butoxycarbonyl)amino)-3-(4-cyano-2-nitrophenoxy)propanoic acid (66a). To the suspendion of 60% NaH in oil (5.12 g, 127.92 mmol) in DMF (95 mL) was added a solution of (*S*)-2-((tert-butoxycarbonyl)amino)-3-hydroxypropanoic acid (commercially available, 12.5 g, 60.91 mmol) in DMF (30 mL) at 0 °C over 20 min. After being stirred at 0 °C for 1 h, 4-fluoro-3-nitrobenzonitrile (**65a**) (commercially available, 10.12 g, 60.91 mmol) was added to the

reaction mixture at 0 °C. The mixture was stirred at 0°C for 2 h, at room temperature for overweekend. The mixture was neutralized with iced water and 1 M HCl aq. (50 mL) at 0 °C and extracted with EtOAc. The organic layer was separated, washed with water and brine, dried over $MgSO_4$ and concentrated under reduced pressure. The residue was purified by column chromatography (silica gel, eluted with 30% - 70% EtOAc in hexane) to give **66a** (4.74 g, 22%) as a yellow gum. ^{1}H NMR (300 MHz, DMSO-d_6) δ 1.35 (9H, s), 4.30-4.60 (3H, m), 7.12-7.21 (1H, m), 7.56 (1H, d, J = 8.7 Hz), 8.10-8.17 (1H, m), 8.46-8.51 (1H, m), 12.99 (1H, brs).

(*S*)-3-(5-Bromo-2-nitrophenoxy)-2-((tert-butoxycarbonyl)amino)propanoic acid (66b). Compound **66b** was obtained (74%) as a yellow gum in a manner similar to that described for the synthesis of **66a**. LC-MS (APCI) *m*/*z* 402.9 $[M - H]^+$. ^{1}H NMR (300 MHz, DMSO-d_6) δ 1.38 (9H, s), 4.33-4.50 (3H, m), 7.09 (1H, d, J = 7.9 Hz), 7.35 (1H, dd, J = 8.7, 1.9 Hz), 7.65 (1H, d, J = 1.9 Hz), 7.84 (1H, d, J = 8.7 Hz), 13.00 (1H, brs).

(*S*)-3-(5-((Benzyloxy)carbonyl)-2-nitrophenoxy)-2-((tert-butoxycarbonyl)amino)propanoic acid (66c). Compound **66c** was obtained in a manner similar to that described for the synthesis of **66a**. This product was subjected to the next reaction without further purification. LC-MS (APCI) *m*/*z* 459.1 $[M - H]^+$.

(*S*)-3-(2-Amino-4-cyanophenoxy)-2-((*tert*-butoxycarbonyl)amino)propanoic acid (67a). A mixture of **66a** (4.2 g, 11.96 mmol), ammonium chloride (2.56 g, 47.82 mmol), and iron (6.68 g, 119.55 mmol) in EtOH (80 mL, 11.96 mmol)/water (16 mL) was stirred at 80 °C for 3 h.To this

mixture was added THF (100 mL) and insoluble material was removed by filtration through celite. The filtrate was evaporated. To the filtrate was added EtOAc and insoluble material was removed by filtration. The filtrate was evaporated to give the crude of **67a** as a brown solid. This product was subjected to the next reaction without further purification. LC-MS (APCI) *m*/*z* 320.1 $[M - H]^+$.

(*S*)-3-(2-Amino-5-bromophenoxy)-2-((*tert*-butoxycarbonyl)amino)propanoic acid (67b). A mixture of **66b** (10.00 g, 24.68 mmol), ammonium chloride (5.28 g, 98.72 mmol), and iron (13.78 g, 246.79 mmol) in EtOH (100 mL, 24.68 mmol)/water (30 mL) was stirred at 80°C for 1.5h. Insoluble material was removed by filtration through celite. The filtrate was evaporated. To the filtrate was added EtOAc and insoluble material was removed by filtration. The filtrate was evaporated to give **67b** (8.40 g, 91%) as a brown solid. LC-MS (APCI) *m*/*z* 372.9 $[M - H]^+$.

(*S*)-3-(2-Amino-5-((benzyloxy)carbonyl)phenoxy)-2-((*tert*-butoxycarbonyl)amino)propanoic acid (67c). To a solution of **66c** (14.98 g, 32.53 mmol) in AcOH (150 mL, 2622.73 mmol) was added zinc powder (21.27 g, 325.35 mmol) at 0 ℃, and the mixture was stirred for 10 min at 0 ℃ and 2 h at rt. The reaction mixture was filtered and the filtrate was concentrated in vauo. AcOH was removed by azeotropic distillation with toluene to give the crude of **67c**. The product was used for next reaction without further purification. LC-MS (APCI) m/z 431.2 [M + H]+.

(*S*)-*tert*-Butyl (7-cyano-4-oxo-2,3,4,5-tetrahydrobenzo[*b*][1,4]oxazepin-3-yl)carbamate (68a). To a mixture of **67a** (3843 mg, 11.96 mmol) and HATU (4775 mg, 12.56 mmol) in DMSO (40 mL) was added TEA (1.834 mL, 13.16 mmol) at room temperature. The mixture was stirred at room

temperature overnight. The mixture was diluted with water and the formed precipitate was collected by filtration and washed with water.

(1) The filtrate was extracted with EtOAc. The organic layer was dried over Na_2SO_4 and concentrated under reduced pressure.

(2) The collected solid was suspended in EtOAc, washed with water, dried over Na_2SO_4 and concentrated under reduced pressure.

(1) and (2) were combined and purified by column chromatography (silica gel, eluted with 10% - 30% EtOAc in hexane) to give **68a** (835 mg, 23% in 2 steps) as a yellow solid. LC-MS (APCI) *m*/*z* 302.1 $[M - H]^+$. ^{1}H NMR (300 MHz, DMSO-d_6) δ 1.37 (9H, s), 4.29-4.45 (3H, m), 7.13-7.20 (1H, m), 7.25 (1H, d, J = 8.3 Hz), 7.48-7.60 (2H, m), 10.21 (1H, s).

(*S*)-*tert*-Butyl (8-bromo-4-oxo-2,3,4,5-tetrahydrobenzo[*b*][1,4]oxazepin-3-yl)carbamate (68b). TEA (3.43 mL, 24.63 mmol) was added to a mixture of **67b** (8.4 g, 22.39 mmol) and HATU (8.94 g, 23.51 mmol) in DMSO (40 mL) at room temperature. The mixture was stirred at room temperature for 1 h. The mixture was diluted with water and precipitate was collected by filtration and washed with water 3 times. The solid was disolved in EtOAc and dried over $MgSO_4$ and concentrated under reduced pressure. The residue was purified by column chromatography (silica gel, eluted with 10% - 30% EtOAc in hexane) to give **68b** (2.290 g, 29%) as a light brown solid. LC-MS (APCI) *m*/*z* 355.0 $[M - H]^+$. ^{1}H NMR (300 MHz, DMSO-d_6) δ 1.36 (9H, s), 4.24-4.40 (3H, m), 7.03 (1H, d, J = 9.1 Hz), 7.11 (1H, d, J = 7.6 Hz), 7.29-7.36 (2H, m), 10.00 (1H, s).

(*S*)-Benzyl 3-((*tert*-butoxycarbonyl)amino)-4-oxo-2,3,4,5-tetrahydrobenzo[*b*][1,4]oxazepine-8-carboxylate (68c). Compound **68c** was obtained (3% in 3 steps from **65c**) as a white solid in a manner similar to that described for the synthesis of **68b**. LC-MS (APCI) *m*/*z* 411.1 $[M - H]^+$.

(*S*)-*tert*-Butyl (7-cyano-5-methyl-4-oxo-2,3,4,5-tetrahydrobenzo[*b*][1,4]oxazepin-3-yl)carbamate (69a). A mixture of **68a** (830 mg, 2.74 mmol), cesium carbonate (1070 mg, 3.28 mmol) and MeI (0.180 mL, 2.87 mmol) in DMF (10 mL) was stirred at room temperature for 3 h. The mixture was quenched with water and extracted with EtOAc. The organic layer was separated, washed with water and brine, dried over $MgSO_4$ and concentrated under reduced pressure. The solid was crystallized from EtOA to give **69a** (389 mg, 45%) as a colorless solid. LC-MS (APCI) *m*/*z* 316.1 $[M - H]^+$. ^1H NMR (300 MHz, DMSO-d_6) δ 1.35 (9H, s), 3.30 (3H, s), 4.34-4.42 (3H, m), 7.21-7.25 (1H, m), 7.37 (1H, d, *J* = 8.3 Hz), 7.75 (1H, dd, *J* = 8.3, 1.9 Hz), 8.08 (1H, d, *J* = 1.9 Hz).

(*S*)-*tert*-Butyl (8-bromo-5-methyl-4-oxo-2,3,4,5-tetrahydrobenzo[*b*][1,4]oxazepin-3-yl)carbamate (69b). A mixture of **68b** (2.2 g, 6.16 mmol), cesium carbonate (3.01 g, 9.24 mmol) and MeI (0.501 mL, 8.01 mmol) in DMF (15 mL) was stirred at room temperature for 3 h. The mixture was diluted with water and extracted with EtOAc. The organic layer was separated, washed with water and brine, dried over $MgSO_4$ and concentrated under reduced pressure. The residue was purified by column chromatography (silica gel, eluted with 10% - 30% EtOAc in hexane) to give **69b** (1.520 g, 67 %) as

a white solid. LC-MS (APCI) *m*/*z* 271.2 [M + H – (Boc)]$^+$. ^{1}H NMR (300 MHz, DMSO-d_6) δ 1.34 (9H, s), 3.26 (3H, s), 4.26-4.43 (3H, m), 7.18 (1H, d, *J* = 7.6 Hz), 7.40-7.53 (3H, m).

(*S*)-Benzyl 3-((*tert*-butoxycarbonyl)amino)-5-methyl-4-oxo-2,3,4,5-tetrahydrobenzo[*b*][1,4]oxazepine-8-carboxylate (69c). Compound **69c** was obtained (75%) as a white solid in a manner similar to that described for the synthesis of **69a**. LC-MS (APCI) *m*/*z* 327.0 [M + H – (Boc)]$^+$. ^{1}H NMR (300 MHz, $CDCl_3$) δ 1.35-1.44 (9H, m), 3.42 (3H, s), 4.16-4.26 (1H, m), 4.53-4.69 (2H, m), 5.30-5.52 (3H, m), 7.22-7.27 (1H, m), 7.32-7.48 (5H, m), 7.82-7.86 (1H, m), 7.93 (1H, dd, *J* = 8.3, 1.9 Hz).

(*S*)-3-((*tert*-Butoxycarbonyl)amino)-5-methyl-4-oxo-2,3,4,5-tetrahydrobenzo[*b*][1,4]oxazepine-8-carboxylic acid (69d). A mixture of **69c** (100 mg, 0.23 mmol) and 10% palladium on carbon (24.95 mg, 0.02 mmol) in THF (3 mL, 36.95 mmol) was hydrogenated under balloon pressure at room temperature for 2 h. The catalyst was removed by filtration and the filtrate was concentrated under reduced pressure to give **69d** (78 mg, 99%) as white solid. LC-MS (APCI) *m*/*z* 335.1 [M - H]$^+$. ^{1}H NMR (300 MHz, DMSO-d_6) δ 1.29-1.43 (9H, m), 3.31 (3H, s), 4.23-4.50 (3H, m), 7.19-7.31 (1H, m), 7.58 (1H, d, *J* = 8.3 Hz), 7.68 (1H, d, *J* = 1.9 Hz), 7.85 (1H, dd, *J* = 8.3, 1.9 Hz), 13.16 (1H, brs).

(*S*)-*tert*-Butyl (5-methyl-8-(methylcarbamoyl)-4-oxo-2,3,4,5-tetrahydrobenzo[*b*][1,4]oxazepin-3-yl)carbamate (69e). Compound **69e** was obtained (100%) as a white solid in a manner similar to that described for the synthesis of **68a**. LC-MS (APCI) *m*/*z* 250.3 [M + H – (Boc)]$^+$. ^{1}H NMR (300 MHz, $CDCl_3$) δ

1.40 (9H, s), 3.02 (3H, d, *J* = 4.9 Hz), 3.41 (3H, s), 4.19 (1H, dd, *J* = 11.0, 9.1 Hz), 4.51-4.71 (2H, m), 5.48 (1H, d, *J* = 6.4 Hz), 6.18 (1H, brs), 7.21-7.27 (1H, m), 7.52 (1H, d, *J* = 1.9 Hz), 7.63 (1H, dd, *J* = 8.3, 1.9 Hz).

(*S*)-*tert*-Butyl (8-(dimethylcarbamoyl)-5-methyl-4-oxo-2,3,4,5-tetrahydrobenzo[*b*][1,4]oxazepin-3-yl)carbamate (69f). Compound **69f** was obtained (85%) as a white solid in a manner similar to that described for the synthesis of **68a**. LC-MS (APCI) *m*/*z* 264.3 $[M + H - (Boc)]^+$. ^{1}H NMR (300 MHz, $CDCl_3$) δ 1.40 (9H, s), 2.91-3.25 (6H, m), 3.41 (3H, s), 4.19 (1H, dd, *J* = 11.0, 9.4 Hz), 4.53-4.74 (2H, m), 5.48 (1H, d, *J* = 6.8 Hz), 7.19-7.33 (3H, m).

(*S*)-3-Amino-5-methyl-4-oxo-2,3,4,5-tetrahydrobenzo[*b*][1,4]oxazepine-7-carbonitrile (70a). A mixture of **69a** (510 mg, 1.61 mmol) and 4 M HCl in EtOAc (6.03 mL, 24.11 mmol) in EtOAc (10 mL)/THF (10 mL) was stirred at room temperature for 3 h. After evaporation of the solvent under reduced pressure, the residue was purified by column chromatography (NH silica gel, eluted with 20% - 100% EtOAc) to give starting material containing mixture (400 mg). The mixture (400 mg) was dissolved in MeOH(10 mL)/THF(12 mL) and to the mixture was added 4 M HCl in EtOAc (8 mL) and the mixture was stirred at rt for 2.5 h. To this mixture was added 4M HCl in EtOAc (6 mL) and the mixture was stirred at rt for 2.5h. After evaporation, the residue was was purified by column chromatography (NH silica gel, eluted with 50% - 100% EtOAc in hexane, 0-10% MeOH in EtOAc) to give **70a** (210 mg, 60%) as a white solid. LC-MS (APCI) m/z 218.4 $[M + H]^+$. ^{1}H NMR (300

MHz, DMSO-d_6) δ 1.83 (2H, s), 3.31 (3H, s), 3.60-3.70 (1H, m), 4.06-4.17 (1H, m), 4.28-4.37 (1H, m), 7.33 (1H, d, J = 8.3 Hz), 7.70 (1H, dd, J = 8.3, 2.3 Hz), 8.01 (1H, d, J = 1.9 Hz).

(*S*)-3-Amino-8-bromo-5-methyl-2,3-dihydrobenzo[*b*][1,4]oxazepin-4(5*H*)-one hydrochloride (70b). A mixture of **69b** (1.2 g, 3.23 mmol) and 4 M HCl in EtOAc (8.08 mL, 32.33 mmol) in EtOAc (10 mL) was stirred at room temperature for 10 h. To this mixture was added 4 M HCl in EtOAc (4 mL) and the mixture was stirred at room temperature for 10 h. The precipitate was collected by filtration and washed with EtOAc to give **70b** (0.970 g, 98%) as a white solid. LC-MS (APCI) m/z 271.2 $[M + H]^+$. ^{1}H NMR (300 MHz, DMSO-d_6) δ 3.33 (3H, s), 4.29-4.68 (3H, m), 7.45-7.59 (3H, m), 8.54 (3H, brs).

(*S*)-3-Amino-*N*,5-dimethyl-4-oxo-2,3,4,5-tetrahydrobenzo[*b*][1,4]oxazepine-8-carboxamide (70c). A solution of **69e** (162 mg, 0.46 mmol) in 4 M hydrogen chloride in EtOAc (2 mL, 8.00 mmol) was stirred for 2 h at rt. MeOH was added to the reaction mixture and filtered through a short pad of NH silica gel eluted with MeOH. The residue was concentrated to give **70c** (85 mg, 74%) as white solid. LC-MS (APCI) m/z 250.3 $[M + H]^+$. ^{1}H NMR (300 MHz, DMSO-d_6) δ 1.75 (2H, brs), 2.78 (3H, d, J = 4.5 Hz), 3.31 (3H, s), 3.60 (1H, dd, J = 11.5, 7.4 Hz), 4.03 (1H, dd, J = 11.5, 10.0 Hz), 4.29 (1H, dd, J = 10.0, 7.4 Hz), 7.48 (1H, d, J = 8.3 Hz), 7.61 (1H, d, J = 1.9 Hz), 7.72 (1H, dd, J = 8.3, 1.9 Hz), 8.48 (1H, d, J = 4.2 Hz).

(*S*)-3-Amino-*N*,*N*,5-trimethyl-4-oxo-2,3,4,5-tetrahydrobenzo[*b*][1,4]oxazepine-8-carboxamide (70d). Compound **70d** was obtained (71%) as a white solid in a manner similar to that described for

the synthesis of **70c**. LC-MS (APCI) *m*/*z* 264.3 $[M + H]^+$. ^1H NMR (300 MHz, DMSO-d_6) δ 1.73 (2H, s), 2.96 (6H, brs), 3.30 (3H, s), 3.63 (1H, dd, *J* = 11.5, 7.4 Hz), 3.94-4.09 (1H, m), 4.29 (1H, dd, *J* = 10.0, 7.4 Hz), 7.18 (1H, d, *J* = 1.9 Hz), 7.28 (1H, dd, *J* = 7.9, 1.9 Hz), 7.45 (1H, d, *J* = 7.9 Hz).

(*S*)-Ethyl 1-benzyl-5-chloro-4-(2-((7-cyano-5-methyl-4-oxo-2,3,4,5-tetrahydrobenzo[*b*][1,4]oxazepin-3-yl) amino)ethyl)-1*H*-pyrazole-3-carboxylate (71a). Compound **71a** was obtained (81%) as a colorless oil in a manner similar to that described for the synthesis of **33**. LC-MS (APCI) *m*/*z* 508.2 $[M + H]^+$. ^1H NMR (300 MHz, $CDCl_3$) δ 1.38 (3H, t, *J* = 7.2 Hz), 2.41-2.54 (1H, m), 2.68-2.91 (3H, m), 3.39 (3H, s), 3.57 (1H, dd, *J* = 11.7, 7.2 Hz), 4.05-4.23 (2H, m), 4.31-4.44 (3H, m), 5.39 (2H, s), 7.15-7.36 (6H, m), 7.45-7.54 (2H, m).

(*S*)-Ethyl 1-benzyl-4-(2-((8-bromo-5-methyl-4-oxo-2,3,4,5-tetrahydrobenzo[*b*][1,4]oxazepin-3-yl)amino)et hyl)-5-chloro-1*H*-pyrazole-3-carboxylate (71b). Compound **71b** was obtained (100%) as a white solid in a manner similar to that described for the synthesis of **33**. LC-MS (APCI) *m*/*z* 561.1 $[M + H]^+$. ^1H NMR (300 MHz, $CDCl_3$) δ 1.37 (3H, t, *J* = 7.2 Hz), 2.37-2.52 (1H, m), 2.71-2.92 (3H, m), 3.35 (3H, s), 3.53 (1H, dd, *J* = 11.5, 7.4 Hz), 3.99-4.09 (1H, m), 4.27-4.42 (3H, m), 5.38 (2H, s), 7.06 (1H, d, *J* = 8.3 Hz), 7.14-7.22 (2H, m), 7.24-7.37 (5H, m).

(*S*)-Ethyl 1-benzyl-5-chloro-4-(2-((5-methyl-8-(methylcarbamoyl)-4-oxo-2,3,4,5-tetrahydrobenzo[*b*][1,4]o

xazepin-3-yl)amino)ethyl)-1*H*-pyrazole-3-carboxylate (71c). Compound **71c** was obtained (48%) as a white solid in a manner similar to that described for the synthesis of **33**. LC-MS (APCI) *m*/*z* 540.3 $[M + H]^+$. ^1H NMR (300 MHz, $CDCl_3$) δ 1.32-1.44 (3H, m), 2.38-2.56 (1H, m), 2.66-2.92 (3H, m), 2.98-3.15 (3H, m), 3.39 (3H, s), 3.45-3.65 (1H, m), 4.07-4.17 (1H, m), 4.27-4.51 (3H, m), 5.38 (2H, s), 6.11 (1H, brs), 7.09-7.38 (6H, m), 7.51 (1H, d, *J* = 1.9 Hz), 7.62 (1H, dd, *J* = 8.3, 1.9 Hz).

(*S*)-Ethyl

1-benzyl-5-chloro-4-(2-((8-(dimethylcarbamoyl)-5-methyl-4-oxo-2,3,4,5-tetrahydrobenzo[*b*][1,4

]oxazepin-3-yl)amino)ethyl)-1*H*-pyrazole-3-carboxylate (71d). Compound **71d** was obtained (49%) as a white solid in a manner similar to that described for the synthesis of **33**. LC-MS (APCI) *m*/*z* 554.2 $[M + H]^+$. ^1H NMR (300 MHz, $CDCl_3$) δ 1.38 (3H, t, *J* = 7.2 Hz), 2.34-2.52 (1H, m), 2.64-2.90 (3H, m), 2.97-3.22 (6H, m), 3.39 (3H, s), 3.54 (1H, dd, *J* = 11.7, 7.6 Hz), 3.98-4.17 (1H, m), 4.28-4.46 (3H, m), 5.36-5.43 (2H, m), 7.10-7.41 (8H, m).

(*S*)-Ethyl

4-(2-((8-bromo-5-methyl-4-oxo-2,3,4,5-tetrahydrobenzo[*b*][1,4]oxazepin-3-yl)amino)ethyl)-1-(2-

fluorobenzyl)-1*H*-pyrazole-3-carboxylate (71e). Compound **71e** was obtained (77%) as a white solid in a manner similar to that described for the synthesis of **33**. LC-MS (APCI) *m*/*z* 545.1 $[M + H]^+$. ^1H NMR (300 MHz, $CDCl_3$) δ 1.37 (3H, t, *J* = 7.2 Hz), 2.44-2.57 (1H, m), 2.75-2.92 (3H, m), 3.36 (3H, s), 3.52 (1H, dd, *J* = 11.7, 7.2 Hz), 4.03-4.09 (1H, m), 4.31-4.40 (3H, m), 5.38 (2H, s), 7.04-7.20 (4H, m), 7.28-7.37 (4H, m). NH proton was not detected.

(*S*)-Ethyl 4-(2-((8-bromo-5-methyl-4-oxo-2,3,4,5-tetrahydrobenzo[*b*][1,4]oxazepin-3-yl)amino)ethyl)-1-(2,6-difluorobenzyl)-1*H*-pyrazole-3-carboxylate (71f). Compound **71f** was obtained (58% in 2 steps from **64b**) as a colorless oil in a manner similar to that described for the synthesis of **33**. LC-MS (APCI) *m*/*z* 563.2 $[M + H]^+$. ^{1}H NMR (300 MHz, $CDCl_3$) δ 1.36 (3H, t, *J* = 7.0 Hz), 2.40-2.54 (1H, m), 2.71-2.92 (3H, m), 3.35 (3H, s), 3.51 (1H, dd, *J* = 11.7, 7.6 Hz), 4.00-4.10 (1H, m), 4.27-4.43 (3H, m), 5.41 (2H, s), 6.90-7.01 (2H, m), 7.07 (1H, d, *J* = 8.3 Hz), 7.27-7.40 (4H, m).

(*S*)-3-(2-Benzyl-3-chloro-7-oxo-4,5-dihydro-2*H*-pyrazolo[3,4-*c*]pyridin-6(7*H*)-yl)-8-bromo-5-methyl-2,3-dihydrobenzo[*b*][1,4]oxazepin-4(5*H*)-one (72a). Compound **72a** was obtained (83%) as a white solid in a manner similar to that described for the synthesis of **34**. LC-MS (APCI) *m*/*z* 515.1 $[M + H]^+$. ^{1}H NMR (300 MHz, $CDCl_3$) δ 2.67 (1H, dt, *J* = 15.9, 4.7 Hz), 3.05 (1H, ddd, *J* = 15.5, 10.4, 5.1 Hz), 3.35 (3H, s), 3.54 (1H, ddd, *J* = 12.0, 10.5, 4.3 Hz), 4.23 (1H, dt, *J* = 12.1, 5.3 Hz), 4.41 (1H, dd, *J* = 10.0, 8.1 Hz), 4.64 (1H, dd, *J* = 11.7, 10.2 Hz), 5.39 (2H, s), 5.90 (1H, dd, *J* = 11.7, 8.3 Hz), 7.11 (1H, d, *J* = 8.3 Hz), 7.23-7.42 (7H, m).

(*S*)-8-Bromo-3-(2-(2-fluorobenzyl)-7-oxo-4,5-dihydro-2*H*-pyrazolo[3,4-*c*]pyridin-6(7*H*)-yl)-5-methyl-2,3-dihydrobenzo[*b*][1,4]oxazepin-4(5*H*)-one (72b). Compound **72b** was obtained (89%) as a white solid in a manner similar to that described for the synthesis of **34**. LC-MS (APCI) *m*/*z* 499.1 $[M + H]^+$. ^{1}H NMR (300 MHz, $CDCl_3$) δ 2.72 (1H, dt, *J* = 15.5, 4.7 Hz), 3.10 (1H, ddd, *J* = 15.1, 10.6, 4.5 Hz), 3.35 (3H, s), 3.53 (1H, ddd, *J* = 11.8, 10.7, 4.3 Hz), 4.16-4.24 (1H, m), 4.41 (1H, dd, *J*

= 10.0, 8.1 Hz), 4.63 (1H, dd, *J* = 11.7, 10.2 Hz), 5.40 (2H, s), 5.93 (1H, dd, *J* = 11.7, 8.3 Hz), 7.04-7.14 (3H, m), 7.20-7.26 (2H, m), 7.27-7.41 (3H, m).

(*S*)-8-Bromo-3-(2-(2,6-difluorobenzyl)-7-oxo-4,5-dihydro-2*H*-pyrazolo[3,4-*c*]pyridin-6(7*H*)-yl)-5-methyl-2,3-dihydrobenzo[*b*][1,4]oxazepin-4(5*H*)-one (72c). Compound **72c** was obtained (59%) as an off-white solid in a manner similar to that described for the synthesis of **34**. LC-MS (APCI) *m*/*z* 517.1 $[M + H]^+$. ^{1}H NMR (300 MHz, $CDCl_3$) δ 2.69 (1H, dt, *J* = 15.5, 4.7 Hz), 2.99-3.15 (1H, m), 3.34 (3H, s), 3.43-3.58 (1H, m), 4.06-4.25 (1H, m), 4.39 (1H, dd, *J* = 10.0, 8.1 Hz), 4.61 (1H, dd, *J* = 11.9, 10.0 Hz), 5.45 (2H, s), 5.92 (1H, dd, *J* = 11.7, 7.9 Hz), 6.89-6.99 (2H, m), 7.10 (1H, d, *J* = 8.3 Hz), 7.22 (1H, s), 7.27-7.42 (3H, m).

TR-FRET binding assay. TR-FRET binding assays were conducted using human GST-His-RIPK1(1-375)[33] and a fluorescent labeled probe **9** (supporting information). The human RIPK1 cDNA (NM_003804) coding 1-375 aa was cloned to have an N-terminal GST-His tag. Human GST-His-RipK1(1-375) has two protease recognition sites and results in GST-(PreScission)-His-(TEV)-human RIPK1 (1-375). GST-His-human RIPK1 (1-375) baculovirus was generated using the BaculoDirect Baculovirus Expression System (Invitrogen) according to manufacturer's specifications.[33]

Data analysis. The obtained data at 10 min and 6 h reactions were globally fitted to the following equation described by Motulsky and Mahan[39] to estimate association rates (k_3), dissociation rates (k_4), and dissociation constants (K_I):

$$Y = \frac{B_{max} k_1 [L]}{K_F - K_S}\left(\frac{k_4(K_F - K_S)}{K_F K_S} + \frac{(k_4 - K_F)}{K_F}\exp(-K_F t) - \frac{(k_4 - K_S)}{K_S}\exp(-K_S t)\right)$$

$$K_F = 0.5(K_A + K_B + S)$$

$$K_S = 0.5(K_A + K_B - S)$$

$$K_A = k_1[L] + k_2$$

$$K_B = k_3[I] + k_4$$

$$S = \sqrt{(K_A - K_B)^2 + 4k_1 k_3 [L][I]}$$

where t is the reaction time, B_{max} is the total amount of enzyme ,Y is the specific binding of the probe, [L] is the concentration of the probe, [I] is the concentration of test compound, k_1 and k_2 are the association rate and dissociation rate of the probe, respectively, k_3 and k_4 are the association rate and dissociation rate of the test compound. The dissociation half-life ($t_{1/2}$) was determined as $t_{1/2} = \ln(2)/k_4$, and the kinetic equilibrium dissociation constant of unlabeled compound (K_I) was determined as $K_I = k_4/k_3$.

Docking study. Molecular docking study was performed using Glide 7.2 (Schrodinger Inc., USA) for better understanding of the interaction of **14** with RIP1 kinase. Crystal structure of RIP1 kinase (PDB ID: 5TX5) was obtained from the Protein Data Bank and prepared by a multistep process through protein preparation wizard in Maestro 2016-3 by using OPLS3 force field. The grid for molecular docking was generated with the bound co-crystallized ligand. The ligand was submitted to the LigPrep module to generate a range of ionization states, and docked into the binding site of the RIP1 kinase structure using Glide.

Pharmacokinetic analysis in mouse cassette dosing. Compound **22** was administered intravenously (0.1 mg/kg) or orally (1 mg/kg, suspended in 0.5% methylcellulose aqueous solution)

to non-fasted mice by cassette dosing. After administration, blood samples (10 μL) were collected and then centrifuged to obtain plasma fraction. The plasma samples were deproteinized with CH_3CN containing an internal standard. After centrifugation, the compound concentrations in the supernatant were measured by LC/MS/MS.

Brain and plasma concentration in mice. Compound **22** was administered orally to non-fasted mice (n = 3) at 10 mg/kg. After sacrifice, blood and brain samples were collected at 1 h after oral administration. The blood samples were centrifuged to obtain the plasma fraction. The brain samples were homogenized in saline to obtain the brain homogenate. Plasma and brain protein binding of compound **22** was determined using the equilibrium dialysis method.[40] The plasma and brain homogenate samples were deproteinized with CH_3CN containing an internal standard. After centrifugation, the compound concentrations in the supernatant were measured by LC/MS/MS.

Biological *in vitro* cell assay.

Reagents. Z-VAD-FMK as a 20 mM stock solution in neat DMSO purchased from Promega (cat. no. G7232). Smac mimetic (AT-406) was purchased from AdooQ BioScience (cat. no. A11163-10). Recombinant human, mouse and rat TNFα were purchased from Wako and R&D systems (cat. no. 210-TA-100, 410-MT-050 and 510-RT-050, respectively). The following antibodies were used for simple Western (WES system): human phospho-MLKL/Ser358 (Abcam, cat. no. ab187091). The following antibodies were used for ELISA: mouse MLKL (Millipore, MABC604), mouse phosphor-MLKL/S345 (Abcam, cat. no. ab196436), rabbit IgG HRP(Jackson ImmunoResearch,

711-035-152). TMB was purchased from KPL (cat. no.52-00-02).

Protocol. The efficacies of RIP1 kinase inhibitors were tested in vitro using human colorectal adenocarcinoma HT-29 cells and mouse L-cells NCTC 929 (L929) cells in a necroptosis assay.[32] HT-29 and L929 cells were acquired from ATCC (cat. no. HTB-38 and CCL-1, respectively) and banked in liquid nitrogen. For HT-29 necroptosis assay, frozen HT-29 cells were thawed and diluted to 1.5 $\times 10^5$ cells/mL in McCoy's 5A Medium (Invitrogen, cat. no. 16600108) supplemented with 10% fetal bovine serum, 100 units/mL penicillin, and 100 μg/mL streptomycin. A 20 μL aliquot of cell suspension (3,000 cells) was added to each well of a 384-assay plate and were incubated for 16–20 hr at 37 °C with 5% CO_2. After overnight incubation, each well was added with 2.5 μL of inhibitor-containing medium, and then treated with 2.5 μL of necroptosis inducer containing rat TNFα, AT-406, and zVAD-FMK to achieve a final concentration of 20 ng/mL, 1 μM, and 20 μM, respectively. After the incubation at 37 °C with 5% CO_2 for 16–20 h, the LDH quantity in supernatant of culture medium in each well was measured by CytoTox 96 Non-Radioactive Cytotoxicity Assay (Promega, cat. no. G1780) according to the manufacturer's instructions. The Absorbance of test plate was measured by 2103 EnVision Multilabel plate reader. Percentage inhibition was calculated from the signal intensity of CytoTox assay by using the following formula; % inhibition = 100 - (A - X) x 100 / (A - B); A: No necroptosis inducer, B: Necroptosis inducer, X: Necroptosis inducer plus Test inhibitor. IC_{50} values were estimated using a four-parameter logistic curve using XLfit software (IDBS, London, UK). All of the data are shown as

mean ± standard error of the mean. For mouse L929 necroptosis assay, 3×10^4 of L929 cells in 120 µl of RPMI1640 medium supplemented with 10%FBS, 100 units/mL penicillin, and 100 µg/mL streptomycin were added to each well of a 96-well assay plates and cultured overnight. The next day, the cells were treated with 15 µl of compound in the growth medium for 30 min and then stimulated with 15 µl of necroptosis stimulation mixture containing mouse TNFα and Z-VAD-FMK (final concentration was 20 ng/mL and 20 µM, respectively). After incubation for 4 h at 37 °C with 5% CO_2, supernatant LDH was measured in the same way as HT-29. The IC_{50} values were calculated from sigmoidal-dose response curves utilizing Prism 5.0 (Graphpad, San Diego, CA).

Human pMLKL WES assay. For the detection of phospho-MLKL, 3×10^5 cells were seeded in 12-well dishes and cultured overnight. The next day,cells were treated with compounds for 30 min and then stimulated with TNFα/AT-406/Z-VAD-FMK mixture as descrived above. After 6-hour incubation, cells were washed in ice cold PBS, lysed in 1x Cell Lysis Buffer (Cell signaling Technology, cat. no.#9803) containing 1 mM PMSF. After harvesting cells with cell scrapers, cell lysates were snap-frozen in liquid nitrogen and stored at -80 °C until following WES. For WES experiments, the cell lysates were allowed to thaw, and centrifuged at 20,000 x g for 15 minutes at 4 °C to remove insoluble cellular debris, and resulting cell lysates were assayed for protein content. Protein content was normalized to 1 mg/mL using the same lysis buffer, and analyzed in duplicate with the anti-pMLKL/S358 antibodies using a WES Simple Western system (Protein Simple) according to the manufacturer's instructions.

Mouse pMLKL ELISA assay. Phospho-MLKL in L929 cells were detected by general sandwich ELISA. L929 cell lysates stimulated with necroptotosis inducer were prepared in the same manner as the case of HT29. The protein content of each cell lysates were adjusted to 200–300 μg/mL to be normalized. Then 100 μl of normalized samples were added onto 96-well ELISA plates (Nunc, cat. no. 442404) which had been coated with 100 μl of anti-mouse MLKL Ab (1 μg/mL in PBS) for O/N at 4 °C, and incubated for 1 h at RT. Next, plates were incubated with 100 μl of anti-phospho-MLKL Ab (1 μg/mL in PBS supplemented with 1% BSA and 0.05% Tween20) for 1 h at RT. Then, plates were reacted with 100 μl of anti-rabbit IgG HRP followed by detecting with 100 μl of TMB. After stopping reaction by adding 100 μl of 0.5M H_2SO_4, plates were read on a spectrophotometer, Viento® (DS Pharma Biomedical) at A450.

Mice. C57BL/6J (female, 10-week-old, Charles River Japan) were used for EAE model. The mice were bred on white chip. All procedures were performed in accordance with the standards for humane care, and treatment of research animal was approved by the Takeda Institutional Animal Ethics Committee (Approval No. 10111).

Induction of experimental autoimmune encephalomyelitis (EAE). EAE induction was performed as previously described.[20] Briefly, C57BL/6 mice were immunized subcutaneously in back with an emulsion containing of 200 μg of MOG35-55 peptide and 500 μg of killed Mycobacterium tuberculosis H37Ra suspended in Freund's incomplete adjuvant on day 0, followed by intraperitoneal injection with 200 ng of pertussis toxin on day 0 and day 2. Clinical signs of EAE in individual mice

were assessed using the following score: 0, no clinical signs; 0.5, Partially limp tail; 1, Paralyzed tail; 2, Partially paralysis of hind limb; 3, Complete paralysis of both hind limbs: 4, Partially paralysis of forelimbs; 5, Complete paralysis of forelimbs, death or humane endpoint. The clinical score was daily observed under blind fashion except holiday after the onset.

Prophylactic efficacy of RIP1 kinase inibitor 22 in murine EAE model. RIP1 kinase inhibitor **22** was suspended in 0.5% methyl cellulose (0.5% MC) and administered twice a day to the mice by oral gavage from day 0 to day 26 after MOG-immunization. Vehicle-treated control mice were administered with 0.5% MC solution. Clinical symptoms of EAE were daily scored as mentioned above. The cumulative score was calculated by adding the individual score obtained from day 0 to day 26.

Statistical Analysis. Data are presented as mean± SEM of nine to twelve mice/group. A statistical comparison of data was analyzed by Dunns and p values lower than 0.05 were considered significant. Statistical analyses were performed using GraphPad Prism 6.01 software (GraphPad Software Inc., La Jolla, CA, USA).

Transcellular transport study using transporter-expression system. Human MDR1-expressing LLC-PK1 cells were cultured with minor modification as reported previously.[41] The transcellular transport study was performed as reported previously.[42] In brief, the cells were grown for 7 days in HTS Transwell® 96 well permeable support (pore size 0.4 μm, 0.143 cm^2 surface area) with polyethylene terephthalate membrane (Corning Life Sciences, Lowell, MA, USA) at a density of

1.125 × 10^5 cells/well. The cells were preincubated with M199 at 37 °C for 30 min. Subsequently, transcellular transport was initiated by the addition of M199 either to apical compartments or to the basolateral compartments containing 1 μM test compounds and terminated by the removal of each assay plate after 1 h. The aliquots in the opposite compartments were measured in a LC-MS/MS analysis. The apparent permeability (P_{app}) of test compounds in the receiver wells was determined and the *ER* for MDR1 membrane permeability test was calculated using the following equation:

$$ER = P_{app,\,\mathrm{BtoA}}/P_{app,\,\mathrm{AtoB}}$$

where $P_{app,\,\mathrm{AtoB}}$ is the apical-to-basal passive permeability-surface area product and $P_{app,\,\mathrm{BtoA}}$ is the basal-to-apical passive permeability-surface area product.

ASSOCIATED CONTENT

Supporting Information. Synthesis of fluorescent probe **9**, the detailed kinetic parameters of compounds **16a**–**aj**, metabolic stabilities of compounds **16a** and **16d**, PK graph of **22**, experimental methods for cloning, expression and purification of RIP1 kinase, as well as crystallization, data collection and structure solution of RIP1 kinase are provided in supporting information. The results of Reaction Biology Corp kinase panel and Eurofins Panlabs panel are listed in supporting information. Molecular formula strings are also available. This material is available free of charge via the Internet at http://pubs.acs.org."

AUTHOR INFORMATION

Corresponding Author

* E-mail: takatoshi.yogo@takeda.com. Phone: (+81)-466-32-1076. FAX: (+81)-466-29-4454.

Present Addresses

†If an author's address is different than the one given in the affiliation line, this information may be included here.

Morihisa Saitoh; Boehringer Ingelheim Japan, Inc., Osaka, Japan

Etsuro Watanabe; UCB Japan Co., Ltd., Tokyo, Japan

Yoshihisa Nakada; ICHIMARU PHARCOS Co., Ltd., Gifu, Japan

Author Contributions

The manuscript was written through contributions of all authors. All authors have given approval to the final version of the manuscript.

ACKNOWLEDGEMENT

We thank Dr. Ikuo Miyahisa for fruitful discussions and valuable suggestions to develop TR-FRET assay for kinetic analysis, Dr. Jeong-ho Oak for fruitful discussion about biology, Dr. Shigekazu Sasaki for kind supports to manage CRO, Dr. Kimio Tohyama for data checking of PK profiles in plasma and brain, Dr. Masato Yoshida for fruitful discussions and valuable suggestions about synthetic strategy and research plans, and Dr. Takashi Ichikawa for valuable suggestions and substantial supports to progress the project.

ABBREVIATIONS

ADMET, absorption, distribution, metabolism, excretion, and toxicity; ALS, amyotrophic lateral sclerosis; AUC, area under the plasma concentration-time curve; CL, total clearance; C_{max}, maximum plasma concentration; Cb, total brain concentration; Cb,u, unbound brain concentration; Cp, total plasma concentration; Cp,u, unbound plasma concentration; DP1, deep pocket 1; DP2, deep pocket 2; EAE, experimental autoimmune encephalomyelitis; ER, efflux ratio; *F*, bioavailability; Kp, brain-to-plasma ratio; Kp,uu, unbound brain-to-plasma ratio; HBAs, hydrogen-bonding acceptors; HBDs, hydrogen-bonding donors; HTS, high-throughput screening; MRT, mean residence time; MS, multiple sclerosis; Parkinson's disease, PD; P-gp, P-glycoprotein; PK, pharmacokinetics; pMLKL, phosphorylation of MLKL; RIP1, receptor interacting protein 1; SBDD, structure-based drug design; SKRs, structure−kinetic relationships; TPSA, topological polar surface area; TR-FRET, time-resolved fluorescence resonance energy transfer

Accession Codes

The coordinates of the crystal structures of RIP1 kinase in complex with compounds **10** (6C3E) and **22** (6C4D) have been deposited in the Protein Data Bank. Authors will release the atomic coordinates and experimental data upon article publication.

REFERENCES

1. Weinlich, R.; Oberst, A.; Beere, H. M.; Green, D. R. Necroptosis in development, inflammation and disease. *Nat. Rev. Mol. Cell Biol.* **2017,** *18*, 127–136.
2. Wegner, K. W.; Saleh, D.; Degterev, A. Complex pathologic roles of RIPK1 and RIPK3: moving beyond necroptosis. *Trends Pharmacol. Sci.* **2017,** *38*, 202–225.
3. Shao, L.; Yu, S.; Ji, W.; Li, H.; Gao, Y. The contribution of necroptosis in neurodegenerative diseases. *Neurochem. Res.* **2017**, *42*, 2117–2126.
4. Ofengeim, D.; Ito, Y.; Najafov, A.; Zhang, Y.; Shan, B.; DeWitt, J. P.; Ye, J.; Zhang, X.; Chang, A.; Vakifahmetoglu-Norberg, H.; Geng, J.; Py, B.; Zhou, W.; Amin, P.; Berlink Lima, J.; Qi, C.; Yu, Q.; Trapp, B.; Yuan, J. Activation of necroptosis in multiple sclerosis. *Cell Rep.* **2015,** *10*, 1836–1849.
5. Wu, J. R.; Wang, J.; Zhou, S. K.; Yang, L.; Yin, J. L.; Cao, J. P.; Cheng, Y. B. Necrostatin-1 protection of dopaminergic neurons. *Neural Regen. Res.* **2015,** *10*, 1120–1124.
6. Politi, K.; Przedborski, S. Axonal degeneration: RIPK1 multitasking in ALS. *Curr. Biol.* **2016,**

26, 932–934.

7. Ito, Y.; Ofengeim, D.; Najafov, A.; Das, S.; Saberi, S.; Li, Y.; Hitomi, J.; Zhu, H.; Chen, H.; Mayo, L.; Geng, J.; Amin, P.; DeWitt, J. P.; Mookhtiar, A. K.; Florez, M.; Ouchida, A. T.; Fan, J. B.; Pasparakis, M.; Kelliher, M. A.; Ravits, J.; Yuan, J. RIPK1 mediates axonal degeneration by promoting inflammation and necroptosis in ALS. *Science* **2016,** *353*, 603–608.
8. Degterev, A.; Huang, Z.; Boyce, M.; Li, Y.; Jagtap, P.; Mizushima, N.; Cuny, G. D.; Mitchison, T. J.; Moskowitz, M. A.; Yuan, J. Chemical inhibitor of nonapoptotic cell death with therapeutic potential for ischemic brain injury. *Nat. Chem. Biol.* **2005,** *1*, 112–119.
9. Degterev, A.; Hitomi, J.; Germscheid, M.; Ch'en, I. L.; Korkina, O.; Teng, X.; Abbott, D.; Cuny, G. D.; Yuan, C.; Wagner, G.; Hedrick, S. M.; Gerber, S. A.; Lugovskoy, A.; Yuan, J. Identification of RIP1 kinase as a specific cellular target of necrostatins. *Nat. Chem. Biol.* **2008,** *4*, 313–321.
10. Takahashi, N.; Duprez, L.; Grootjans, S.; Cauwels, A.; Nerinckx, W.; DuHadaway, J. B.; Goossens, V.; Roelandt, R.; Van Hauwermeiren, F.; Libert, C.; Declercq, W.; Callewaert, N.; Prendergast, G. C.; Degterev, A.; Yuan, J.; Vandenabeele, P. Necrostatin-1 analogues: critical issues on the specificity, activity and in vivo use in experimental disease models. *Cell Death Dis.* **2012,** *3*, e437.
11. Roskoski, R. Jr. Classification of small molecule protein kinase inhibitors based upon the structures of their drug-enzyme complexes. *Pharmacol. Res.* **2016**, *103*, 26–48.

12. Harris, P. A.; Bandyopadhyay, D.; Berger, S. B.; Campobasso, N.; Capriotti, C. A.; Cox, J. A.; Dare, L.; Finger, J. N.; Hoffman, S. J.; Kahler, K. M.; Lehr, R.; Lich, J. D.; Nagilla, R.; Nolte, R. T.; Ouellette, M. T.; Pao, C. S.; Schaeffer, M. C.; Smallwood, A.; Sun, H. H.; Swift, B. A.; Totoritis, R. D.; Ward, P.; Marquis, R. W.; Bertin, J.; Gough, P. J. Discovery of small molecule RIP1 kinase inhibitors for the treatment of pathologies associated with necroptosis. *ACS Med. Chem. Lett.* **2013,** *4*, 1238–1243.

13. Najjar, M.; Suebsuwong, C.; Ray, S. S.; Thapa, R. J.; Maki, J. L.; Nogusa, S.; Shah, S.; Saleh, D.; Gough, P. J.; Bertin, J.; Yuan, J.; Balachandran, S.; Cuny, G. D.; Degterev, A. Structure guided design of potent and selective ponatinib-based hybrid inhibitors for RIPK1. *Cell Rep.* **2015,** *10*, 1850–1860.

14. Huang, W. S.; Metcalf, C. A.; Sundaramoorthi, R.; Wang, Y.; Zou, D.; Thomas, R. M.; Zhu, X.; Cai, L.; Wen, D.; Liu, S.; Romero, J.; Qi, J.; Chen, I.; Banda, G.; Lentini, S. P.; Das, S.; Xu, Q.; Keats, J.; Wang, F.; Wardwell, S.; Ning, Y.; Snodgrass, J. T.; Broudy, M. I.; Russian, K.; Zhou, T.; Commodore, L.; Narasimhan, N. I.; Mohemmad, Q. K.; Iuliucci, J.; Rivera, V. M.; Dalgarno, D. C.; Sawyer, T. K.; Clackson, T.; Shakespeare, W. C. Discovery of 3-[2-(imidazo[1,2-*b*]pyridazin-3-yl)ethynyl]-4-methyl-*N*-{4-[(4-methylpiperazin-1-yl)-methyl]-3-(trifluoromethyl)phenyl}benzamide (AP24534), a potent, orally active pan-inhibitor of breakpoint cluster region-abelson (BCR-ABL) kinase including the T315I gatekeeper mutant. *J. Med. Chem.* **2010,** *53*, 4701–4719.

15. Harris, P. A.; King, B. W.; Bandyopadhyay, D.; Berger, S. B.; Campobasso, N.; Capriotti, C. A.; Cox, J. A.; Dare, L.; Dong, X.; Finger, J. N.; Grady, L. C.; Hoffman, S. J.; Jeong, J. U.; Kang, J.; Kasparcova, V.; Lakdawala, A. S.; Lehr, R.; McNulty, D. E.; Nagilla, R.; Ouellette, M. T.; Pao, C. S.; Rendina, A. R.; Schaeffer, M. C.; Summerfield, J. D.; Swift, B. A.; Totoritis, R. D.; Ward, P.; Zhang, A.; Zhang, D.; Marquis, R. W.; Bertin, J.; Gough, P. J. DNA-encoded library screening identifies benzo[b][1,4]oxazepin-4-ones as highly potent and monoselective receptor interacting protein 1 kinase inhibitors. *J. Med. Chem.* **2016,** *59*, 2163–2178.

16. Harris, P. A.; Berger, S. B.; Jeong, J. U.; Nagilla, R.; Bandyopadhyay, D.; Campobasso, N.; Capriotti, C. A.; Cox, J. A.; Dare, L.; Dong, X.; Eidam, P. M.; Finger, J. N.; Hoffman, S. J.; Kang, J.; Kasparcova, V.; King, B. W.; Lehr, R.; Lan, Y.; Leister, L. K.; Lich, J. D.; MacDonald, T. T.; Miller, N. A.; Ouellette, M. T.; Pao, C. S.; Rahman, A.; Reilly, M. A.; Rendina, A. R.; Rivera, E. J.; Schaeffer, M. C.; Sehon, C. A.; Singhaus, R. R.; Sun, H. H.; Swift, B. A.; Totoritis, R. D.; Vossenkamper, A.; Ward, P.; Wisnoski, D. D.; Zhang, D.; Marquis, R. W.; Gough, P. J.; Bertin, J. Discovery of a first-in-class receptor interacting protein 1 (RIP1) kinase specific clinical candidate (GSK2982772) for the treatment of inflammatory diseases. *J. Med. Chem.* **2017,** *60*, 1247–1261.

17. Ren, Y.; Su, Y.; Sun, L.; He, S.; Meng, L.; Liao, D.; Liu, X.; Ma, Y.; Liu, C.; Li, S.; Ruan, H.; Lei, X.; Wang, X.; Zhang, Z. Discovery of a highly potent, selective, and metabolically stable inhibitor of receptor-interacting protein 1 (RIP1) for the treatment of systemic inflammatory

response syndrome. *J. Med. Chem.* **2017,** *60*, 972–986.

18. Berger, S. B.; Harris, P.; Nagilla, R.; Kasparcova, V.; Hoffman, S.; Swift, B.; Dare, L.; Schaeffer, M.; Capriotti, C.; Ouellette, M.; King, B. W.; Wisnoski, D.; Cox, J.; Reilly, M.; Marquis, R. W.; Bertin, J.; Gough, P. J. Characterization of GSK'963: a structurally distinct, potent and selective inhibitor of RIP1 kinase. *Cell Death Dis.* **2015,** *1*, 15009.
19. Ertl, P.; Rohde, B.; Selzer, P. Fast calculation of molecular polar surface area as a sum of fragment-based contributions and its application to the prediction of drug transport properties. *J. Med. Chem.* **2000,** *43*, 3714–3717.
20. Stromnes, I. M.; Goverman, J. M. Passive induction of experimental allergic encephalomyelitis. *Nat. Protoc.* **2006,** *1*, 1952–1960.
21. Copeland, R. A.; Pompliano, D. L.; Meek, T. D. Drug-target residence time and its implications for lead optimization. *Nat. Rev. Drug Discov.* **2006,** *5*, 730–739.
22. Copeland, R. A. The drug-target residence time model: a 10-year retrospective. *Nat. Rev. Drug Discov.* **2016,** *15*, 87–95.
23. Copeland, R. A. The dynamics of drug-target interactions: drug-target residence time and its impact on efficacy and safety. *Expert Opin. Drug Discov.* **2010,** *5*, 305–310.
24. Copeland, R. A. Evaluation of enzyme inhibitors in drug discovery. A guide for medicinal chemists and pharmacologists. *Methods Biochem. Anal.* **2005,** *46*, 1–469.
25. Tummino, P. J.; Copeland, R. A. Residence time of receptor-ligand complexes and its effect on

biological function. *Biochemistry* **2008,** *47*, 5481-92.

26. Wager, T. T.; Chandrasekaran, R. Y.; Hou, X.; Troutman, M. D.; Verhoest, P. R.; Villalobos, A.; Will, Y. Defining desirable central nervous system drug space through the alignment of molecular properties, in vitro ADME, and safety attributes. *ACS Chem. Neurosci.* **2010,** *1*, 420–434.

27. Kelder, J.; Grootenhuis, P. D.; Bayada, D. M.; Delbressine, L. P.; Ploemen, J. P. Polar molecular surface as a dominating determinant for oral absorption and brain penetration of drugs. *Pharm. Res.* **1999,** *16*, 1514–1519.

28. Pajouhesh, H.; Lenz, G. R. Medicinal chemical properties of successful central nervous system drugs. *NeuroRx* **2005,** *2*, 541–553.

29. Wager, T. T.; Hou, X.; Verhoest, P. R.; Villalobos, A. Moving beyond rules: the development of a central nervous system multiparameter optimization (CNS MPO) approach to enable alignment of druglike properties. *ACS Chem. Neurosci.* **2010,** *1*, 435–549.

30. Sirimulla, S.; Bailey, J. B.; Vegesna, R.; Narayan, M. Halogen interactions in protein-ligand complexes: implications of halogen bonding for rational drug design. *J. Chem. Inf. Model* **2013,** *53*, 2781–2791.

31. Bissantz, C.; Kuhn, B.; Stahl, M. A medicinal chemist's guide to molecular interactions. *J. Med. Chem.* **2010,** *53*, 5061–5084.

32. He, S.; Wang, L.; Miao, L.; Wang, T.; Du, F.; Zhao, L.; Wang, X. Receptor interacting protein

kinase-3 determines cellular necrotic response to TNF-alpha. *Cell* **2009,** *137*, 1100–1011.

33. Ishii, T. Okai, T. Yoshihara, M.; Mochizuki, M. Unno, S.; Kuno, M.; Yoshikawa, M.; Shibata, S.; Nakakariya, M.; Yogo, T.; Kawamoto, T. CETSA quantitatively verifies in vivo target engagement of novel RIPK1 inhibitors in various biospecimens. *Sci. Rep.* **2017** Oct 12;7(1):13000.

34. Berger, S. B.; Kasparcova, V.; Hoffman, S.; Swift, B.; Dare, L.; Schaeffer, M.; Capriotti, C.; Cook, M.; Finger, J.; Earle, A. H.; Harris, P. A.; Kaiser, W. J.; Mocarski, E. S.; Bertin, J.; Gough, P. J. RIP1 kinase activity is dispensable for normal development but is a key regulator of inflammation in SHARPIN-deficient mice. *J. Immunol.* **2014**, *192*, 5476–5480.

35. Polykratis, A.; Hermance, N.; Zelic, M.; Roderick, J.; Kim, C.; Van, T. M.; Lee, T. H.; Chan, F. K. M.; Pasparakis, M.; Kelliher, M. A. RIPK1 Kinase inactive mice are viable and protected from TNF-induced necroptosis in vivo. *J. Immunol.* **2014**, *193*, 1539–1543.

36. Rodriguez, D. A.; Weinlich, R.; Brown, S.; Guy, C.; Fitzqerald, P.; Dillon, C. P.; Oberst, A.; Quarato, G.; Low, J.; Cripps, J. G.; Chen, T.; Green, D. R. Characterization of RIPK3-mediated phosphorylation of the activation loop of MLKL during necroptosis. *Cell Death Differ.* **2016**, *23*, 76–88.

37. Chan, F. K.; Shisler, J.; Bixby, J. G.; Felices, M.; Zheng, L.; Appel, M.; Orenstein, J.; Moss, B.; Lenardo, M. J. A role for tumor necrosis factor receptor-2 and receptor-interacting protein in programmed necrosis and antiviral responses. *J. Biol. Chem.* **2003**, *278*, 51613–51621.

38. Schoop, A.; Dey, F. On-rate based optimization of structure-kinetic relationship - surfing the kinetic map. *Drug Discov. Today Technol.* **2015,** *17*, 9–15.

39. Motulsky, H. J.; Mahan, L. C. The kinetics of competitive radioligand binding predicted by the law of mass action. *Mol. Pharmacol.* **1984,** *25*, 1–9.

40. Nakakariya, M.; Ono, M.; Amano, N.; Moriwaki, T.; Maeda, K.; Sugiyama, Y. In vivo biliary clearance should be predicted by intrinsic biliary clearance in sandwich-cultured hepatocytes. *Drug Metab. Dispos.* **2012,** *40*, 602–609.

41. Sugimoto, H.; Hirabayashi, H.; Kimura, Y.; Furuta, A.; Amano, N.; Moriwaki, T. Quantitative investigation of the impact of P-glycoprotein inhibition on drug transport across blood-brain barrier in rats. *Drug Metab. Dispos.* **2011,** *39*, 8–14.

42. Takeuchi, T.; Yoshitomi, S.; Higuchi, T.; Ikemoto, K.; Niwa, S.-I.; Ebihara, T.; Katoh, M.; Yokoi, T.; Asahi, S. Establishment and characterization of the transformants stably-expressing MDR1 derived from various Animal species in LLC-PK1. *Pharm. Res.* **2006,** *23*, 1460–1472.

Table of Contents Graphic